Proton-Transfer Reaction Mass Spectrometry

Robert S. Blake, Paul S. Monks, and Andrew M. Ellis*

Department of Chemistry, University of Leicester, University Road, Leicester LE1 7RH, United Kingdom

Received June 4, 2008

Contents

* Corresponding author. E-mail: andrew.ellis@le.ac.uk. Tel.: +44 (0)116 252 2138. Fax: +44 (0)116 252 3789.

1. Introduction

Proton-transfer reaction mass spectrometry (PTR-MS) is a technique developed almost exclusively for the detection of gaseous organic compounds in air. Volatile organic compounds (VOCs) in air have both natural and anthropogenic sources. Natural sources include the emission of organic gases by living objects, both plants and animals. A well-known example, which is discussed later in this review, is the emission of a variety of gaseous organic compounds in the breath of animals, which are released from both the digestive system and the lungs. Plants are major sources of organic gases, as is the decay of dead animal and plant matter. Subsequent photochemistry can add further compounds to the mixture. Consequently, even without contributions from humans, ambient air from the Earth's atmosphere would consist of a complex mixture of VOCs.

Anthropogenic sources of VOCs include emissions from the extraction and refining of fossil fuels, the incomplete burning of fossil fuels by motorized transport and by heat and electrical power generators, the evaporation of solvents employed in industrial and domestic operations, and the leakage of gases from landfill sites. VOCs from these and other man-made sources are of concern for a number of reasons, particularly with regard to pollution and the health impacts that may accrue when potentially toxic compounds reach unacceptably high levels. The sources and inventories of VOCs in air have been comprehensively reviewed, e.g., by Hewitt[1] and Hester.[2]

Although VOCs in air are ubiquitous, they actually constitute only a small proportion of everyday air. By far the most common organic compound found in the Earth's atmosphere is methane, but even this compound is only present at an average level of around 2 parts per million by volume (2 ppmV). After methane, the most abundant VOCs include ethane, propane, isoprene, acetone, and methanol, but typical mixing ratios for these compounds are in the region of a few parts per billion (ppbV). Many other VOCs have been identified with concentrations in the parts per trillion (pptV) range, some of which will be discussed later in this review. Although such levels seem extremely small, the health effects of many VOCs have not been fully established and it is possible that the presence of some compounds at ppbV or even high pptV levels may have harmful effects on human health. Beyond the issue of human health, the organic composition of air has implications for our understanding of the natural environment and the impact human activities have on the local and global ecosystem. For these and other reasons, techniques capable of detecting the trace levels of organic constituents found in air are important.

10.1021/cr800364q CCC: $71.50 © 2009 American Chemical Society
Published on Web 02/12/2009

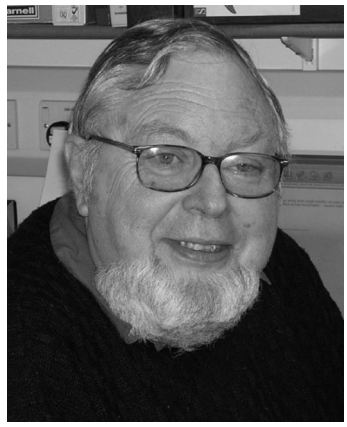

Robert Blake studied for B.Sc. and M.Sc. degrees in South Africa before obtaining a Ph.D. in experimental nuclear physics from the University of Manchester in the U.K. in 1964. He continued his work on Gamma Ray Spectrometry at Rice University, Texas, and at the Institut de Physique Nucleaire at Orsay, France. He then changed fields to IT, where he worked in Software and Systems Support, Project Management, and CADD applications in South Africa, Namibia, and the U.K. In 2002 he enrolled at the University of Leicester working with Paul Monks and Andrew Ellis, where he was awarded a Ph.D. in atmospheric science in 2006. His work involved the incorporation of time-of-flight mass spectrometry into the PTR-MS technique, with the primary purpose of monitoring VOCs in the atmosphere and, subsequently, in health and forensic applications. Along with this current line of research, he is exploring variations of the PTR-MS technique with collaborators in Japan.

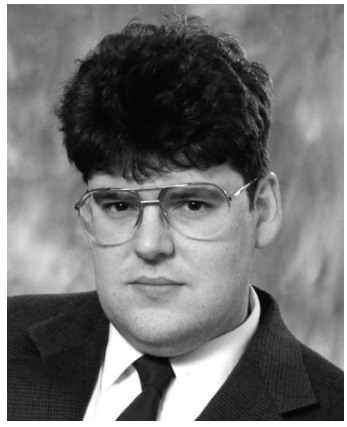

Paul Monks was born in St. Helens in 1968. He received his B.Sc. degree from the University of Warwick and his D.Phil. from the University of Oxford in 1991 with Richard Wayne. In 1992 he took up a NAS/NRC fellowship in Astrochemistry at NASA/Goddard with Lou Stief before returning to the U.K. in 1994 to a postdoctoral position with Stuart Penkett at UEA. In 1996 he was appointed to a lectureship in Earth Observation Science in the Department of Chemistry at the University of Leicester and promoted to the current position of a Professor in Atmospheric Chemistry in 2006. His primary research interests are the scientific questions underlying the role of photochemistry in the control of atmospheric composition; chemistry and transport, particularly the impact of long-range transport on chemical composition; the feedback between climate and atmospheric chemistry; the organic complexity and the control of regional pollution and the measurement of the chemical composition of the troposphere from space.

The most widely used tool for detecting and quantifying gaseous VOCs is gas chromatography−mass spectrometry, or GC-MS. This excellent technique has been in use for many years and is capable of achieving sensitivities as low as 0.1 pptV. However, although it is a highly sensitive and reliable technique, it suffers from several shortcomings, the most notable of which is its temporal resolution. It takes considerable time, at least minutes if not tens of minutes, to separate fully the constituents of a gas mixture on a capillary column.

Andrew Ellis obtained his first degree in chemistry at the University of Southampton. He remained in Southampton to carry out his Ph.D. studies with John Dyke, focusing on the photoelectron and chemielectron spectroscopy of metals and metal oxides in the gas phase. In 1989 he joined Terry A. Miller's research group at Ohio State University as a NATO/SERC postdoctoral fellow, investigating new types of free radicals using laser spectroscopy. He returned to the U.K. in 1991, taking up an academic post in the Department of Chemistry at the University of Leicester. His research interests include the spectroscopy and reaction dynamics of small molecules and molecular clusters, the study of clusters in helium nanodroplets, the growth of nanoparticles using gas-phase techniques, and the development and application of techniques based on proton-transfer reaction mass spectrometry for the analysis of trace organic compounds.

Furthermore, it is also necessary to preconcentrate the analyte sample when the gases of interest are at the low levels found for organic compounds in air. Typically this preconcentration process, which is essential to attain an adequate detection sensitivity, is achieved by adsorbing the VOCs onto a suitable adsorbant, with the most widely used being Tenax. After collection for a few minutes, the adsorbed gases are then released thermally and are injected into the column. This preconcentration process further limits the time resolution, and as a result, GC-MS is a relatively slow technique for detecting VOCs in air. Preconcentration can also introduce problems for oxygenated VOCs, which may not be fully released into the column injector.

If speed is not important, then GC-MS is probably the best technique available for measuring trace levels of gaseous VOCs. However, faster techniques are required if it is necessary to monitor a variety of specific gases on a time scale of 1 min or less. This almost invariably means utilizing mass spectrometric techniques without chromatographic separation. Electron impact ionization mass spectrometry is of little use in this regard for three reasons. First, the common inorganic constituents of the Earth's atmosphere, such as N_2, O_2, and CO_2, tend to overwhelm the instrument response at the low mass end of the spectrum. Second, many ions show extensive fragmentation following electron impact, and this can make identification difficult, and frequently impossible, in multicomponent analytes. Finally, the quantification of individual species is complicated by the choice of inlet conditions and by the variation in the ionization cross section from one molecule to another. Alternative ionization sources, such as chemical ionization,[3] are more selective and softer in their ionization processes and can be chosen to both eliminate contributions from the abundant inorganic gases and yield less ion fragmentation. However, the problem of determining the concentrations of specific gases remains, and thus, an alternative solution based on mass spectrometry is desirable.

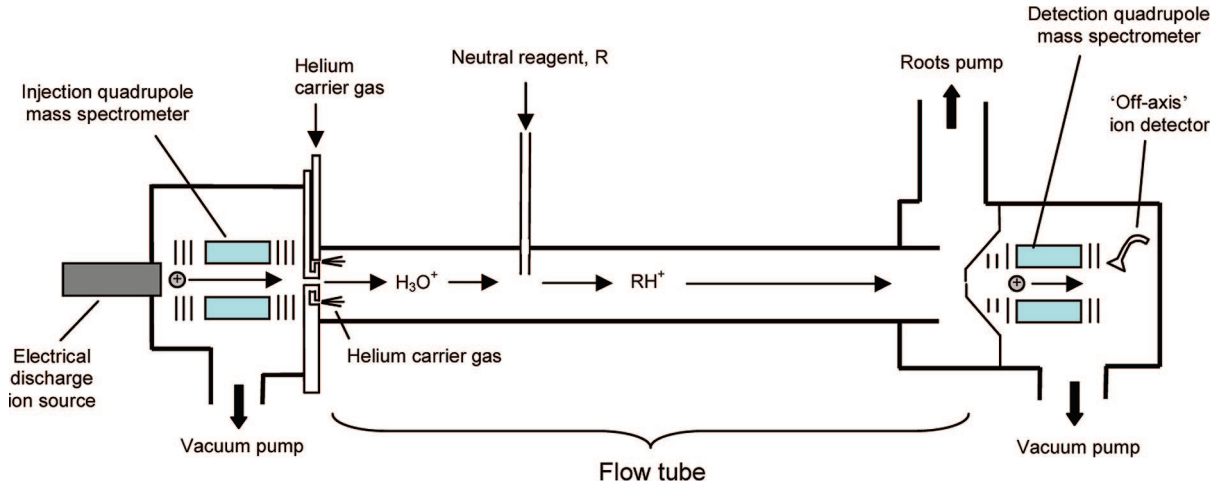

Figure 1. Schematic illustration of a selected ion flow tube (SIFT) instrument.

In recent decades, several mass spectrometric techniques have become established for the quantitative detection of VOCs in air. These methods combine chemical ionization with reaction kinetics to determine concentrations of specific compounds. There has been much work with negative ion sources, and these are particularly good for detecting inorganic nitrogen-containing species, such as nitric acid. These anion-based techniques, which are sometimes known simply as chemical ionization mass spectrometry (CIMS), have been described in two excellent reviews.[4,5] The subject of the current review, PTR-MS, makes use of positive ions and, in particular, a proton donor to transfer protons to gaseous organic compounds.

PTR-MS was first introduced in the mid-1990s and has seen an enormous growth in use in the past decade. The *modus operandi* of PTR-MS is the chemical ionization, by proton transfer, of a gas sample inside a drift tube. The proton source is normally H_3O^+. The fixed length of the drift tube provides a fixed reaction time for the ions as they pass along the tube: the ion residence (and, thus, reaction) time can be measured or it can be calculated from ion transport properties. If the proton donor concentration is largely unchanged by the addition of an analyte sample, then measurement of the (proton donor)/(protonated acceptor) ion signal ratio allows the absolute concentration of the acceptor molecules to be calculated from a simple kinetic analysis, as shown later. Consequently, by combining reaction kinetics with mass spectrometry, it is possible to both identify and quantify individual organic gases on a relatively short time scale and with a sensitivity that can reach well into the pptV mixing regime.

There have been several previous reviews of PTR-MS. The technique originated in the laboratory of Werner Lindinger in Innsbruck, and the Lindinger group authored several of the early reviews.[6−8] More recently, Hewitt et al.[9] and de Gouw and Warneke[10] have reviewed aspects of PTR-MS as it relates specifically to atmospheric monitoring. Here we provide a review that not only summarizes key experimental developments over the past decade but also attempts to reflect the many and diverse applications of the technique by providing a comprehensive account of its application in areas such as atmospheric science, aerosol formation chemistry, breath analysis, flavor chemistry, food diagnostics, and the study of biochemical pathways in plants and small animals. The literature coverage included here extends from the inception of the PTR-MS technique through to the end of 2007.

2. Historical Development

Proton-transfer reaction mass spectrometry has its origins in the development of the flowing afterglow method for the study of ion−molecule reaction kinetics. This so-called swarm technique was introduced in the 1960s by Ferguson and co-workers and involves the injection of ions into an inert buffer gas containing a small amount of neutral reactant to achieve reactions at thermal or near-thermal collision energies.[11,12] The term "afterglow" refers to the means used to produce the ions, which was typically a discharge that created a bright glow due to light emitted by electronically excited constituents of the gas. This glow would extend from the source region into the buffer gas region, hence the name afterglow. The study of ion-molecule reaction kinetics and thermodynamics was revolutionized by the flowing afterglow approach.

A weakness of the original afterglow experiments was that no ion selection was attempted prior to reaction. For reactions of relatively simple ions, such as N_2^+, this caused little difficulty, but for more complex molecular ions, the possibility of producing a variety of secondary ions in the discharge source causes excessive complications in the product analysis and necessitates some means of ion selection prior to reaction. This key step was tackled by Adams and Smith in a groundbreaking piece of work that led to the introduction of the selected ion flow tube (SIFT) technique.[13] The basic components of a SIFT instrument are illustrated in Figure 1. As in the flowing afterglow method, ions are produced by an electrical discharge, but now a quadrupole filter allows ions of only a specific mass/charge ratio, m/z, to pass into the next part of the instrument, the flow tube. The selected ions enter the flow tube through a Venturi inlet, which is an aperture shaped to minimize ingress of gases from the flow tube into the ion source. The ions are mixed with flowing helium (the thermalizing buffer gas) as they enter the flow tube and are then carried along toward a second quadrupole mass spectrometer at the far end of the instrument. The neutral reagent is added downstream of the Venturi inlet to allow adequate thermalization of the reagent ions. The resulting ion products and unreacted ions are detected by the mass spectrometer at the end of the flow

tube. Since the reaction time is determined by the distance traveled by the reacting mixture prior to detection and by the flow rate of the carrier gas, a kinetic analysis of the ion-molecule chemistry is possible if the flow rate is varied.

Early work with SIFT concentrated on fundamental studies of ion-molecule reaction kinetics, and this technique has produced most of the kinetic data that guides PTR-MS, as well as being of enormous value in other fields where ion-molecule reactions are important, such as atmospheric and interstellar chemistry. SIFT is still used today for the investigation of ion-molecule reaction kinetics, but it has also been developed as a means of detecting and quantifying trace gases in air. In its analytical guise, the technique is more commonly known as SIFT-MS, and the use of SIFT-MS for VOC detection has been pioneered by Smith and Španěl.[14,15] The apparatus employed is essentially the same as that shown in Figure 1, but at the point where neutral reagent R is shown to be injected, the analyte sample (e.g., air) is continuously added instead. The focus on organic gases is achieved by careful selection of the reagent ions. For gas-analysis applications, the most commonly used ion in SIFT-MS is H_3O^+, but other ions, such as NO^+ and O_2^+, have also received considerable attention. Taking H_3O^+ for illustration and assuming reaction with only a single organic gas, designated R, proton transfer to R can yield RH^+. If RH^+ is assumed to be the only product and, furthermore, conditions are chosen such that $[H_3O^+] \gg [RH^+]$, then a simple kinetic analysis shows that

$$[RH^+]/[H_3O^+] = kt[R] \qquad \text{(E1)}$$

where k is the proton-transfer rate coefficient and t is the reaction time. If both k and t are known, and if the measured ion signals are proportional to the ion concentrations, then measurement of the RH^+/H_3O^+ signal ratio seen by the mass spectrometer will allow the absolute concentration of gas R to be determined. Note that this is essentially the converse of the original use of SIFT, where the aim was normally to determine k for a specific reaction. However, once k has been measured for the reaction of a particular analyte gas, the rate constant can then be used in the quantification of that gas via SIFT-MS.

Variations of the SIFT-MS technique have been carried out. In terms of the historical development of PTR-MS in its current guise, Werner Lindinger and co-workers coupled a mass-selected H_3O^+ source with a flow drift tube in 1994 and showed that this was an effective means of analyzing trace organic gases in air.[16] In a flow tube, ions are transported by added carrier gas, whereas in a drift tube an electric field is the primary means to transport ions: a flow drift tube clearly combines the two. The effect of the electric field in the selected ion flow drift tube mass spectrometry (SIFDT-MS) experiment is to increase the average collision velocity of an ion with the buffer gas. This results in the declustering of hydrated hydronium ions of the type $H_3O^+(H_2O)_n$, which tend to form in humid air and which would otherwise complicate the kinetic analysis.

PTR-MS as it is known today was introduced in 1995 and involved two further important changes.[17] First, the mass filter that is employed in SIFT to select specific ions prior to reaction with an analyte was dispensed with and replaced with a hollow-cathode discharge source that could generate H_3O^+ with high efficiency (>99.5%) without any need for a mass filter. A second innovation was to replace the flow tube with a relatively short drift tube. Instead of employing a carrier gas to transport ions along the tube, the analyte air sample was directly injected into the drift tube and the unreactive components of the air (N_2, O_2, etc.) served as thermalizing agents. In SIFT-MS, the dilution of the analyte gas flow in excess helium is essential to minimize ion−molecule cluster formation, particularly those derived from residual water vapor. However, in PTR-MS, the substantially higher ion−molecule collision energies when a drift tube is employed mean that the formation of $H_3O^+(H_2O)_n$ and other cluster ions can be reduced to negligible levels without sample dilution. This can come at the expense of a shorter reaction time and some additional product ion fragmentation when compared to SIFT-MS, but the net result is a detection sensitivity for PTR-MS that is some two orders of magnitude better than that for SIFT-MS. Furthermore, the resulting instrument can be made more compact and can be put together more cheaply than SIFT-MS devices. These two facets of PTR-MS, the high detection sensitivity (approaching 10 pptV) and the relatively compact size and, therefore, the affordability of the instrument, have led to the explosion of interest in the technique over the past decade.

3. Proton-Transfer Reactions

3.1. Thermodynamics of Proton Transfer

Proton transfer from donor ion XH^+ to some gas R is defined by the reaction

$$XH^+(g) + R(g) \rightarrow RH^+(g) + X(g) \qquad \text{(R1)}$$

Reaction R1 will be thermodynamically spontaneous if the standard Gibbs energy change at temperature T, ΔG_T^0, is negative. This quantity can be derived from the difference in the gas-phase basicities of X and R, where the gas-phase basicity is the negative of the Gibbs energy change for a substance accepting an isolated proton, $H^+(g)$. Tabulated values of this quantity for a wide range of molecules have been compiled by Hunter and Lias.[18] The same authors have also tabulated proton affinities, which are defined as the negative of the enthalpy change for reaction R1.

Proton affinities are commonly used to assess whether or not a proton-transfer reaction is likely to be spontaneous. For example, the accepted value for the proton affinity of H_2O is 691 ± 3 kJ mol^{-1}, whereas the alkenes ethene and propene have the values 681 ± 2 and 752 ± 3 kJ mol^{-1}, respectively. Since propene has a much larger proton affinity than H_2O, the proton-transfer process

$$H_3O^+ + CH_3CH{=}CH_2 \rightarrow H_2O + [CH_3CHCH_3]^+ \qquad \text{(R2)}$$

is strongly exothermic and is expected to be spontaneous. In contrast, the proton affinity of H_2O exceeds that of ethene and so reaction R3 below will be endothermic and should not occur.

$$H_3O^+ + CH_2{=}CH_2 \rightarrow H_2O + [CH_3CH_2]^+ \qquad \text{(R3)}$$

Of course, in the strictest sense, the Gibbs energy changes for proton-transfer reactions should be used to determine spontaneity rather than the difference in proton affinities (enthalpies) of the substrate molecules. However, the entropic contributions in proton-transfer reactions are often small and show little difference from reaction to reaction.[18] Consequently, relative proton affinities can be justifiably used as

Table 1. Some Illustrative Proton Affinities[a]

classification	molecule	proton affinity/kJ mol^{-1}
inorganic gases	O_2	421
	N_2	494
	CO_2	541
	O_3	626
	H_2O	691
	NH_3	854
alkanes	methane	544
	ethane	596
	propane	626
	i-butane	678
alkenes	ethene	641
	propene	752
alkynes	acetylene	641
	propyne	748
aromatics	benzene	750
	toluene	784
	phenol	817
	aniline	883
other organics	chloromethane	647
	formaldehyde	713
	acetaldehyde	769
	ethanol	776
	acetone	812
	acetonitrile	779

[a] Taken from compilation by Hunter and Lias.[18]

a quick and reasonably reliable means for assessing the spontaneity of proton-transfer reactions.

There are two important features of proton-transfer reactions that emerge from the proton-transfer thermodynamics. Assuming H_3O^+ as the proton source, most of the common inorganic constituents of air possess proton affinities lower than that of H_2O, whereas for most non-alkane organic gases, the opposite is true, as can be seen from inspection of Table 1. As a result, H_3O^+ will transfer a proton to most organic molecules but not to the common inorganic constituents of air, making PTR-MS "transparent" to all but trace organic gases. A second important characteristic concerns the excess energy resulting from proton transfer. Some organic molecules possess proton affinities in excess of 1000 kJ mol^{-1}, but most have values significantly smaller than this, and many small- and medium-sized organic molecules have proton affinities < 900 kJ mol^{-1}. Consequently, the excess energy released on proton transfer is usually small enough to avoid extensive fragmentation of ions, and thus proton transfer is frequently regarded as a soft ionization method.

Nevertheless, there are a number of well-known cases where other reactions compete with, or even dominate over, reaction R1. For example, all C_3 and higher alcohols give mainly dehydration products,[19] viz.

$$H_3O^+ + C_nH_{2n+1}OH \rightarrow 2H_2O + C_nH_{2n+1}^+ \quad \text{(R4)}$$

Dehydration products are also known for other carbonyl-containing molecules, such as some of the heavier aldehydes and carboxylic acids.[20,21]

Light alkanes, as already mentioned above for ethane, undergo endothermic proton-transfer reactions with H_3O^+. However, as the molecular mass increases, the proton affinity of the alkane increases, and therefore, for larger alkanes, reaction R1 should eventually become exothermic. Arnold and co-workers have estimated that the endothermic/exothermic crossover point occurs at hexane, such that all heavier alkanes should have clear exothermic proton-transfer reactions with H_3O^+.[22] For heptane and higher alkanes, fast reaction with H_3O^+ is seen, but the rate coefficient falls short of that predicted from collision-limiting models (see next section). Furthermore, the reaction is dominated not by proton transfer but instead by association, i.e.,

$$H_3O^+ + C_nH_{2n+2} + M \rightarrow H_3O^+C_nH_{2n+2} + M \quad \text{(R5)}$$

where M is a third body. The same conclusion was reached independently by Španěl and Smith.[23]

The above examples of fragmentation processes were all established by SIFT-MS, where the ion-molecule collision energies are essentially thermal, and in most cases, the experiments are carried out at room temperature. Under these conditions some, ion-molecule complexes, such as the hydronium−alkane cluster ions on the right-hand side of reaction R5, have a chance of surviving. The elevated collision energies in PTR-MS mean that the branching ratio for fragmentation can be larger than that found in SIFT-MS; also, new fragmentation channels can arise. It is important to be aware of this limitation when using SIFT-MS data to predict the ion-molecule chemistry in PTR-MS. Some examples of systematic studies of fragmentation processes in PTR-MS for specific classes of compounds are given in section 5.3.

3.2. Kinetics of Proton Transfer

Extensive early work by Bohme and co-workers using the flowing afterglow method has shown that those proton-transfer reactions that are distinctly exothermic are almost always fast.[24] Fast ion-molecule reactions are substantially faster than the barrierless neutral−neutral reactions limit because of long-range attractive forces that increase the reaction cross section beyond the notional hard sphere maximum. Thus, a fast ion-molecule reaction implies rate coefficients $\geq 10^{-9}$ cm^3 s^{-1}. A compilation of the early kinetic data for proton-transfer reactions can be found in the book by Ikezoe and co-workers.[25] Our knowledge of rate coefficients for proton transfer from H_3O^+ is now comprehensive thanks to a large number of more recent studies using SIFT-MS, particularly by Smith and Španěl (see, for example, a recent summary in ref 14) but also by other groups such as Viggiano and co-workers[22,26−28] and Arijs and co-workers.[29−31] A summary of all the relevant kinetic data, valid through to the end of 2003, can be found in a report by Anicich.[32] Rate coefficients for proton transfer from H_3O^+ to many different classes of organic molecules are now available, but the conclusion remains the same as from the earlier flowing afterglow work, namely, that the exothermic proton-transfer reactions are invariably fast and, in most cases, agree very closely with theoretical rate coefficient predictions based on barrierless ion-molecule capture processes. Consequently, the absence of an experimental value for the rate coefficient of a particular proton-transfer reaction of importance in a PTR-MS study is not necessarily an impediment, since a theoretical value can be derived that is likely to possess an error margin comparable to that in any experimental determination.

There are a number of theoretical prescriptions for estimating rate coefficients of exothermic ion-molecule reactions. If the reaction involves a non-polar neutral molecule, a satisfactory expression for calculating the rate coefficient is

$$k_L = \sqrt{\frac{\pi\alpha e^2}{\mu\varepsilon_0}} \quad \text{(E2)}$$

where α is the polarizability of the neutral reactant molecule, μ is the reduced mass of the colliding partners, e is the fundamental unit charge, and ε_0 is the permittivity of free space. [The expression for k_L in eq E2 assumes that all quantities are expressed in SI units and, therefore, gives the rate coefficient in $m^3\ s^{-1}$. Note that this use of SI units differs from the expressions in the older literature.] The expression above is said to give the Langevin-limiting rate coefficient, k_L, since it is derived from the Langevin model of the long-range interaction between a point charge and a polarizable molecule.[33]

Equation E2 is found to be unsatisfactory for reactions involving polar neutral molecules because its derivation neglects the interaction between the positive charge and the permanent electric dipole moment of the neutral molecule. The net effect is for the Langevin model to underestimate the rate coefficient. A possible solution is to introduce the effect of a dipole moment in the neutral molecule through the "locked-dipole" model, in which the dipole moment is assumed to be fixed at the most energetically favorable orientation with respect to the reactant ion.[34] However, the locked-dipole model tends to overestimate rate coefficients because it unrealistically discounts a range of thermally accessible dipole orientations. A more realistic description was provided by Su and Bowers and is known as the average dipole orientation (ADO) theory.[35,36] The ADO rate coefficient is given by

$$k_{ADO} = \sqrt{\frac{\pi\alpha e^2}{\mu\varepsilon_0}} + \frac{C\mu_D e}{\varepsilon_0}\sqrt{\frac{1}{2\pi\mu kT}} \quad \text{(E3)}$$

where μ_D is the dipole moment of the neutral molecule and C is a "locking" parameter that accounts for the average orientation of the neutral molecule's dipole moment, such that, when $C = 1$, eq E3 is equivalent to the locked-dipole theory. C turns out to be a function of μ_D and α, specifically the ratio $\mu_D/\alpha^{1/2}$. Su and Bowers have parametrized and tabulated C as a function of $\mu_D/\alpha^{1/2}$, and thus, provided μ_D and α are known for the neutral molecule of interest, it is then a simple matter to extract the value of C.[37]

A comparison of the rate coefficients predicted from the ADO procedure with experimental values shows that the ADO values tend to underestimate the rate constants, typically by 10−20%.[37,38] This is attributable in large part to the neglect of the dipole moment of the charged reagent, which is treated as a point charge in the standard ADO treatment. Nevertheless, the ADO theory provides a means of obtaining decent estimates of rate coefficients for proton-transfer reactions where the experimental value is unknown.

Su and Chesnavich have carried out detailed trajectory studies to refine the ADO parametrization process.[39] The resulting rate coefficient, termed the capture coefficient, k_{cap}, is given by $k_{cap}(T) = k_L \times K_{cap}(T)$. Here, $K_{cap}(T)$ incorporates the dipole-locking effects, and as with the second term on the right-hand side of the expression for k_{ADO}, it can be expressed as a function of μ_D and α and, thus, can be readily calculated provided these two quantities are known. In the past 25 years, various improvements have been made to the capture theory, including parametrization over a wide temperature range[40] and the extension to reactions between ions and quadrupolar linear molecules.[41,42]

If experimental values of the polarizability and/or the dipole moment of the neutral molecule are unavailable, these quantities can be calculated from ab initio quantum chemical calculations. Zhao and Zhang have provided a comprehensive evaluation of this approach by carrying out calculations on 78 hydrocarbons and 58 non-hydrocarbons.[43] It was shown that a quite modest level of theory (density functional theory (B3LYP) with a 6−31G(d,p) Gaussian basis set) can yield good estimates of proton-transfer rate coefficients for use in PTR-MS. In particular, where experimental rate coefficients for reactions of H_3O^+ are available for comparison, the agreement between theory and experiment was better than 25% in most cases.

We close this section with an important caveat. It is commonly assumed that room-temperature rate coefficients can be employed for quantitative analysis in PTR-MS. This is not strictly true since ion-molecule collisions in the drift tube are normally far more energetic than room-temperature collisions. In other words, there is a higher effective temperature for ion-molecule collisions in PTR-MS when compared to SIFT-MS, as already mentioned in section 3.1. Experimental studies by McFarland et al.[44] have shown that the following expression, which follows from original work by Wannier,[45,46] can be used to estimate the effective ion translational temperature, T_{eff}:

$$T_{eff} = T + \frac{m_b v_d^2}{3k_B} \quad \text{(E4)}$$

In the above equation, T is the drift tube temperature, m_b is the mass of the buffer molecules (equivalent to the weighted mass of N_2 and O_2 when the buffer is air), v_d is the ion drift velocity, and k_B is Boltzmann's constant. It is possible to estimate the ion drift velocity from mobility calculations, or it can be measured, as carried out by McFarland and co-workers. Equation E4 leads to effective ion temperatures in excess of 1000 K at E/N values exceeding 100 Td (for a definition of E/N, see later), which suggests that the use of room-temperature rate coefficients in the PTR-MS analysis is likely to be, at the very least, a questionable assumption.

3.3. Proton Transfer from Hydrated Hydronium Cluster Ions

H_3O^+ is the proton donor most commonly employed in PTR-MS. Ideally, pure H_3O^+ would be generated in the ion source (see later), and therefore, one need only consider the reactions of this ion with the organic gases in the analyte gas. Unfortunately, the presence of unreacted water vapor in the ion source inevitably leads to some formation of cluster ions of the type $H_3O^+(H_2O)_n$ via the process

$$H_3O^+(H_2O)_{n-1} + H_2O + M \rightarrow H_3O^+(H_2O)_n + M \quad \text{(R6)}$$

where M is a third body. Water vapor in the analyte gas can also lead to the formation of $H_3O^+(H_2O)_n$. In PTR-MS, attempts are made to minimize the proportion of $H_3O^+(H_2O)_n$ ions ($n \geq 1$) relative to H_3O^+ in the drift tube through the use of collision-induced dissociation (see later). Nevertheless, despite these efforts, hydrated hydronium ions are still frequently observed in mass spectra from PTR-MS, and so it is important to be aware of the impact they may have on the ion chemistry.

The key point to note is that water clusters possess higher proton affinities than the bare water molecule (691 ± 3 kJ

mol^{-1}).[18] For example, the water dimer, $(H_2O)_2$, has a proton affinity of 808 ± 6 kJ mol^{-1}.[47] The higher proton affinity is the result of the added stability of the H_3O^+ brought about by sharing the positive charge with an additional water molecule. As more water molecules are added, the proton affinity of the water cluster increases but the incremental effect declines in magnitude as the cluster grows.

There are two important consequences of water cluster ion formation. First of all, the increased proton affinity means that some reactions that occur with H_3O^+ do not occur with $H_3O^+(H_2O)_n$. A good example would be acetaldehyde, whose proton affinity (see Table 1) lies between those of H_2O and $(H_2O)_2$ and should, therefore, accept a proton from H_3O^+ but not from $H_3O^+(H_2O)$. This brings us to the second important point about water cluster ions, which is that proton transfer is not the only possible reaction channel. In the case of acetaldehyde, it is known that reaction with H_3O^+ does indeed proceed by proton transfer and occurs at the collision-limiting rate. However, as shown by flowing afterglow[48] and SIFT[27] studies, reaction of $H_3O^+(H_2O)$ with acetaldehyde also occurs at the collision-limiting rate, but in this case proceeds via so-called ligand switching:

$$H_3O^+(H_2O) + CH_3CHO \rightarrow H_3O^+(CH_3CHO) + H_2O \quad \text{(R7)}$$

Toluene is another molecule that possesses a lower proton affinity than water dimer, and therefore, if any reaction with $H_3O^+(H_2O)$ occurs, then it would be expected to be dominated by a ligand-switching process analogous to reaction R7 above. In fact, SIFT studies show that proton transfer is the dominant process and occurs at roughly one-half the expected capture rate at room temperature, even though the reaction is endothermic.[49] The explanation of this initially surprising finding lies in the average thermal energy possessed by a toluene molecule at room temperature, which is just about sufficient to counterbalance the reaction endothermicity. This example illustrates that some caution is warranted in using the proton affinity tables to determine whether or not proton transfer occurs.

If the ligand-switching reaction proceeds at the collision-limited rate, the presence of $H_3O^+(H_2O)_n$ ions in PTR-MS is not necessarily a problem, since product ions containing the analyte molecule will still be formed. However, the presence of additional product channels from hydrated hydronium ions increases the complexity of data analysis and is best avoided if possible. Fortunately, as already mentioned earlier and discussed again later, collision-induced dissociation in the drift tube can be used to reduce the quantity of ionic clusters, in both the reactant and product channels.

3.4. Other Proton-Transfer Reagents

Alternative proton donors to H_3O^+ were known in standard chemical ionization mass spectrometry and its atmospheric pressure variant long before the advent of PTR-MS.[3,50] Alternative proton sources have been considered in PTR-MS, most notably NH_4^+.[7] Proton donation from NH_4^+ is less exothermic than from H_3O^+ because the proton affinity of NH_3 lies 163 kJ mol^{-1} above that of H_2O (see Table 1). There are two benefits that this might offer. First, for those analyte molecules that possess higher proton affinities than NH_3, the much lower energy release when using NH_4^+ compared to H_3O^+ might reduce any ion fragmentation, perhaps simplifying mass spectral interpretation. Furthermore, in particularly fortuitous cases, it is possible that two different analyte species with the same molecular mass might have very different proton affinities such that only one of the gases will accept a proton from NH_4^+. An example where this has been employed has been highlighted by Lindinger and co-workers, namely, for a mixture of pinene and 2-ethyl-3,5-dimethylpyrazene, both of which have molecular masses of 136.[7] Whereas H_3O^+ will donate a proton to both molecules, only 2-ethyl-3,5-dimethylpyrazene has a proton affinity suitable for accepting a proton from NH_4^+. Consequently, separate PTR-MS experiments using H_3O^+ followed by NH_4^+ could potentially allow absolute quantification of both pinene and 2-ethyl-3,5-dimethylpyrazene.

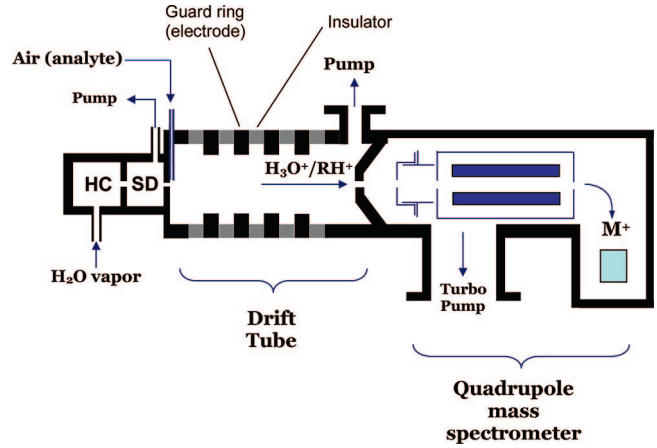

Figure 2. Simplified representation of a proton-transfer reaction mass spectrometer utilizing a quadrupole mass filter: HC = hollow-cathode discharge source and SD = source drift region.

In our own laboratory, we have also explored applications of NH_4^+ in PTR-MS. In practice, it was found that, where reaction occurred, ion association products of the type $R.NH_4^+$ tended to dominate, which are formed either by direct three-body ion−molecule association reactions or by ligand-switching processes.[51] We have also attempted to employ CH_5^+, a commonly used ion in standard chemical ionization mass spectrometry, in PTR-MS work. However, this ion gave poor yields and resulted in a much reduced ion signal in the mass spectrum.[52] In practice, the potential benefits of using alternatives to H_3O^+ as proton sources are usually minimal, and thus, H_3O^+ is overwhelmingly the reagent of choice in PTR-MS work to date.

4. Experimental Techniques

The experimental realization of proton-transfer reaction mass spectrometry was first achieved by Hansel et al.[17] Figure 2 shows the typical experimental arrangement for a PTR-MS instrument based on quadrupole mass spectrometry. An in-depth description of the components of such an instrument along with operational details can be found in the original publication. Here we provide only a brief outline of "standard" PTR-MS instruments and concentrate primarily on new experimental developments.

As discussed earlier, there are two key differences between SIFT-MS and PTR-MS: in PTR-MS, there is (i) no initial mass selection of reagent ions and (ii) no dilution of the analyte sample in a carrier gas. To realize (i), the ion source must be carefully chosen to avoid contamination with "impurity" ions. Hansel et al. employed a hollow-cathode discharge through water vapor to generate H_3O^+ with high

purity, and today this remains the most commonly employed ion source in PTR-MS. From an experimental point of view, H_3O^+ is a good reagent to choose because all the potential contaminant ions generated in the discharge process, such as O^+, OH^+, and H_2O^+, undergo fast reactions with H_2O that ultimately lead to the formation of H_3O^+. This conversion process begins in the hollow-cathode source and is facilitated further in the source drift region shown in Figure 2 immediately downstream of the hollow-cathode source. The nominal purity achieved in this type of ion source has been shown to be >99.5% for H_3O^+. It should be noted, however, that small quantities of analyte air can diffuse into the source region of the instrument, which usually leads to a small percentage of contaminant ions, with O_2^+ and NO^+ being the main culprits.

The ions from the source drift region are drawn by an electric field into a drift tube. It is here that the analyte sample is injected. In an attempt to confine the reaction between H_3O^+ and the analyte gases to the drift tube, some research groups have employed a Venturi-type inlet to minimize backstreaming of gases into the source drift region, as mentioned in the case of SIFT in section 2. However, the hypersonic flow rates needed to achieve a true Venturi effect[53] are far higher than those employed in PTR-MS and so some backstreaming is inevitable, particularly when the pressure in the drift tube exceeds that in the ion source. The drift tube is normally 5−15 cm long and provides an electric field to drag positive ions through the gas mixture toward an aperture at the downstream end of the drift tube. The electric field is provided by a series of ring electrodes interspersed with insulating material, usually Teflon, to provide electrical isolation. The typical operating pressure in the tube is in the region of 2 mbar, and the electric field strength (E) is generally near 60 V cm^{-1}. These operating parameters, which are extremely important, are more commonly combined and expressed in terms of the E/N value of the drift tube, where N is the gas number density (in units of cm^{-3}). For the aforementioned conditions, the E/N is 123 Td, where 1 Td = 1 Townsend = 10^{-17} cm^2 V^{-1}.

The electric field serves to accelerate the ions, but collisions with the gas tend to slow them down. The net effect is that the ions quickly adopt a steady-state velocity as they progress down the drift tube that is determined by the value of E/N. Increasing the E/N ratio results in more energetic collisions, which reduces the proportion of cluster ions such as $H_3O^+(H_2O)_n$ in the drift tube (see section 2). However, at the same time, this increased average collision energy may increase the fragmentation of ions produced by the reaction between H_3O^+ and analyte gases, which is often undesirable because of the complications it causes in the mass spectral analysis. As a result, the choice of operating E/N is a compromise and typical values fall in the range 100−140 Td. This gives a center-of-mass collision energy in the region of 0.2 eV, which is nearly one order of magnitude larger than the thermal ion-molecule collision energies met in SIFT-MS.

Entrance of the analyte gas into the drift tube can be controlled by a mass flow controller (MFC), with most of the gas being ultimately pumped away through a pumping port located near the end of the drift tube. A potential disadvantage of MFCs is that some VOCs can linger on the stainless steel surfaces in the MFC interior, causing memory effects in time-resolved measurements. A way of avoiding this has been described by de Gouw et al.[54] Their solution

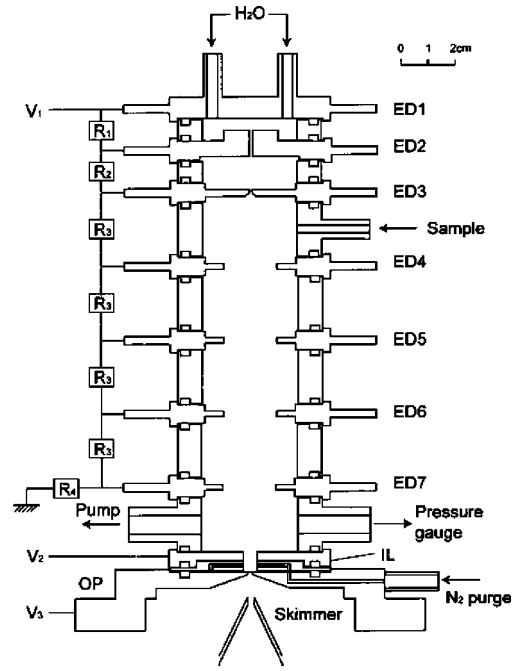

Figure 3. Discharge source and drift tube assembly used by Inomata and co-workers. The primary discharge region consists of elements ED1−ED2 and is followed by a source drift region (ED2−ED3). The drift tube runs from ED3 through to the interface plate (shown as IL). Voltages are maintained along the electrode network via a potential divider using the resistors shown along the left side of the electrode chain. Reprinted with permission from ref 55. Copyright 2006 Wiley.

employs a gas line constructed of materials that are much less "sticky" than stainless steel, namely, Teflon and perfluoroalkoxy (PFA) polymer. The inlet to the PTR-MS is split off from this main inlet line, and the flow rate is controlled through a combination of an upstream needle valve and a downstream pressure controller. An alternative to an MFC or a pressure-controlled inlet is simply to employ a critical orifice to deliver analyte gas into the drift tube. The latter delivers gas into the system at a constant rate determined by the aperture size and is the preferred option for high temporal resolution.

The positive ions, both unreacted H_3O^+ and the proton-transfer products from reaction with the analyte, are drawn toward the plate at the end of the drift tube, and an aperture in this plate allows a small proportion of the ions into the final part of the instrument, the mass spectrometer chamber. The instrument illustrated in Figure 2 shows a quadrupole mass spectrometer, which is currently by far the most widely used type of mass analyzer in PTR-MS. Typical H_3O^+ ion count rates at the detector are $\geq 10^6$ s^{-1}. A commercial version of the instrument represented in Figure 2 has been available for several years and is produced by Ionicon Analytik (http://www.ptrms.com/).

4.1. Alternative Ion Sources

A hollow-cathode discharge is the staple ion source for the majority of PTR-MS instruments. However, an alternative plane electrode dc discharge source has recently been reported by Inomata and co-workers.[55] As in the hollow-cathode source of Hansel et al.,[17] there is both a primary discharge region (E1−E2) and a source drift region (E2−E3) prior to the drift tube (see Figure 3). The discharge is initiated by the entrance of water vapor between anode and cathode

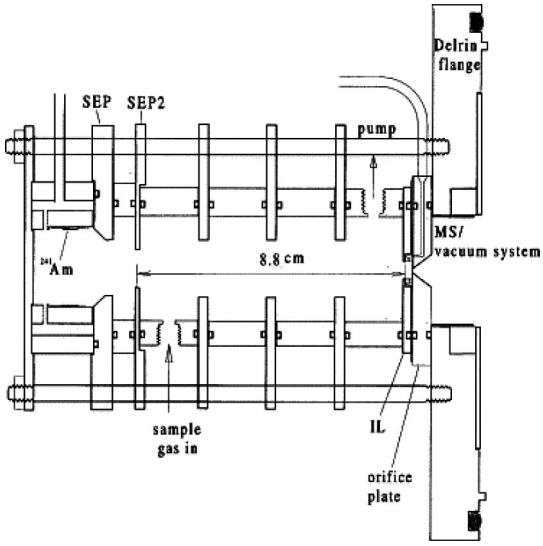

Figure 4. Radioactive ion source and drift tube developed by Hanson et al. The radioactive source is an alpha source consisting of a sealed strip of ^{241}Am located on the inside surface of a stainless steel cylinder. SEP refers to "source exit plate", and the drift tube part of the apparatus extends from SEP2 to the mass spectrometer inlet plate, IL. Reprinted with permission from ref 56. Copyright 2003 Elsevier.

plates located ~5 mm apart with a potential difference of 500 V. To help confine the discharge to this primary region, the primary and source drift regions are separated by a capillary of length 12 mm and diameter 1 mm in the cathode. This source has been tested on a PTR-MS instrument equipped with a time-of-flight mass spectrometer (see later) and provides a stable source of H_3O^+. The level of contamination by O_2^+ and NO^+ is small (~0.5%) because the capillary prevents most analyte backstreaming. However, the H_3O^+ current level at the mass spectrometer is ~ one order of magnitude less than that typically found for hollow-cathode ion sources, and thus a disadvantage of the planar discharge source is reduced detection sensitivity.

A more radical departure from the hollow-cathode discharge is the radioactive ion source reported by Hanson et al.[56] This exploits a low-level α particle emitter, ^{241}Am, to ionize water vapor and generate H_3O^+. As illustrated in Figure 4, the α source is deposited on a metal strip located on the inside wall of a protective stainless steel cylinder, which replaces the discharge region in a hollow-cathode source. The energetic (5 MeV) α particles are able to cause multiple ionization events, and the H_3O^+ current injected into the drift tube is in the region of 300 pA, or 2×10^9 ions/s. With this type of ion source, there is no external current driver and the long-term stability of the ion current is excellent. Contamination from stray analyte gas entering the ion source region was found to be minimal, as judged by the low level of contaminant ions such as NO^+. This was attributed to the high operating flow of gas into the ion source (up to 20 sccm of an N_2/H_2O mixture), which minimizes backstreaming. The drift tube could be operated at substantially higher pressures (up to 13 mbar) than normally used in PTR-MS, which in turn can confer higher VOC detection sensitivity. Count sensitivities of several hundred Hz per ppbV were achieved for common VOCs such as acetone and isoprene, which means that detection sensitivities of a few tens of pptV for individual VOCs are possible in well under 1 s.

A version of the Hanson radioactive source has been built in our own laboratory and has been shown to successfully generate clean sources of chemical ionization reagents other than H_3O^+.[51,57] In particular, both NO^+ and O_2^+ ion streams have been generated by this means and offer useful alternatives to H_3O^+ in a few specific cases, as discussed later in section 5.1.

Although a radioactive source would appear to be an excellent alternative to the discharge sources mentioned above, there are also some disadvantages. One important disadvantage is that, in some circumstances, the inclusion of a radioactive component is undesirable from the point of view of safety, or perceived safety. Second, the use of a relatively high drift pressure implies higher water vapor number densities, which in turn can lead to unwanted reverse proton-transfer reactions for compounds with relatively low proton affinities.

To close this section, we note that a clean O_2^+ source has also recently been demonstrated in a conventional PTR-MS instrument with a hollow-cathode discharge source.[58] This was employed as a means of detecting NH_3, which is difficult to quantify when using H_3O^+ as the CI reagent because of large quantities of residual NH_4^+ formed by reactions from N_2 leaking into the ion source. O_2^+ reacts with NH_3 (and almost all VOCs) by charge transfer, since O_2 possesses a significantly higher ionization energy than NH_3.

4.2. Alternative Mass Analyzers

Although linear quadrupole filters dominate as the mass analyzers in most current PTR-MS instruments, the possibility of utilizing other types of mass analyzers has begun to be explored.

4.2.1. Ion Trap Systems

The first ion trap (IT) system in PTR-MS was reported by Prazeller and co-workers in 2003.[59] This consisted of a standard hollow-cathode discharge/drift tube arrangement that was interfaced to a commercial quadrupole ion trap via an einzel lens. The authors identified two important potential advantages of ion traps over linear quadrupole filters for PTR-MS. The first advantage derives from the way ion trap mass spectrometry works. The ion trap consists of two end caps, one with an aperture to allow entry of ions from the drift tube, and a ring electrode lying between the two end-cap electrodes. These are shown in cross section in the bottom part of Figure 5. To obtain a mass spectrum, ions are injected into the ion trap and stored for a sufficient length of time by applying a radiofrequency (rf) electrical field to the ring electrode. Trapping times up to several seconds are possible. The mass spectrum is then accumulated by progressively ramping up the rf amplitude such that ions of increasing mass are ejected from the trap, where they are then detected by an external detector. Because the ramp time can be very short relative to the accumulation time, a high duty cycle, in excess of 90%, is potentially possible. This high duty cycle is achieved for all of the ions in the trap, whereas a linear quadrupole is only able to provide a signal for an ion with a single m/z at any instant in time. Thus, real sensitivity benefits could potentially accrue when investigating complex mixtures that give rise to many different mass peaks. A second important advantage of ion traps is that they provide a means to carry out tandem mass spectrometry (MS/MS) studies. By application of tailored

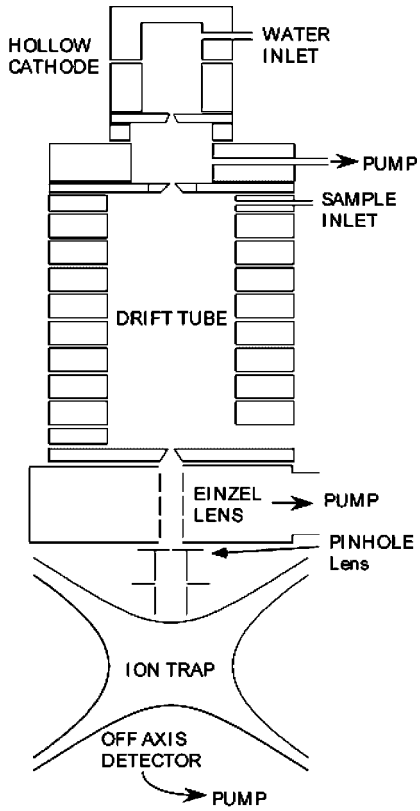

Figure 5. Cross-sectional view of a PTR-MS system based on an ion trap mass spectrometer. The ion trap consists of three electrodes shown at the bottom of the diagram: two end electrodes located along the axis of initial ion injection and a ring electrode (shown in cross section) lying between the two end electrodes. Reprinted with permission from ref 59. Copyright 2003 Wiley.

waveforms to the electrodes, all ions can be ejected from the trap except those of one particular mass. It is then possible to perform collision-induced dissociation (CID) studies on the selected ion(s) inside the ion trap to assist with additional species identification. This procedure, which is not available in a PTR-MS system employing a linear quadrupole analyzer, has the potential to distinguish between isobaric molecules.

Prazeller et al. were able to demonstrate the value of MS/MS by successfully distinguishing between methyl vinyl ketone and methacrolein with their new ion trap system. However, the sensitivity advantages were not achieved, and the detection sensitivity for individual species was limited to ~100 pbbV. This relatively poor detection sensitivity was largely due to the location of the ion detector, part of which was in line with the exit hole from the drift tube. This produced a noisy background signal, making it difficult to detect low levels of VOCs.

The best detection sensitivity so far achieved with PTR-IT-MS has been reported by Warneke and co-workers.[60] This research team constructed a new, purpose-built instrument with improved differential pumping and a carefully designed four-lens system to focus, transmit, and gate the passage of ions into the IT. A difficulty arises from the dominance of H_3O^+, which quickly fills the trap to the point where space charge effects become a problem *before* significant numbers of less abundant ions have been accumulated. As a result, a two-stage data accumulation procedure was employed: (i) accumulation for a short (50 ms) period to measure the H_3O^+ signal and (ii) ejection of all ions followed by a second and longer (~2 s) accumulation period with an rf amplitude on the ring electrode set to reject H_3O^+ ions. Although this adds a little complexity, this procedure was shown to be effective and the value of the new instrument was demonstrated through ambient air measurements in the Boulder (Colorado) area for a period of several days. A detection sensitivity in the region of 500 pptV was achieved for one-minute data accumulation, which is not quite as good as with linear quadrupole instruments but which shows that PTR-IT-MS is beginning to approach the performance levels of standard PTR-MS. This performance level is achieved in multiple mass channels simultaneously. The clear utility of CID in an IT-MS was demonstrated by using the different CID patterns of acetone and propanal to show unambiguously that the *m*/*z* 59 signal in air sampling experiments was predominantly due to acetone.

Warneke and co-workers have also suggested additional potential advantages of PTR-IT-MS, such as the possibility of operating the drift tube at higher pressures than normal to improve sensitivity and the use of ion−molecule reactions inside the ion trap to selectively remove particular types of molecules.[61] Ordinarily the former might cause a problem, since a higher drift tube pressure lowers the *E*/*N* in the drift tube and can lead to increased levels of hydrated hydronium ions. However, with an ion trap, this is not a significant problem since the ion clusters can easily be broken up in the trapping process. A practical demonstration of this has recently been provided by Steeghs and co-workers, who constructed a new PTR-IT-MS system based on a commercially available ion trap.[62] For standard PTR-MS, the normal *E*/*N* used is in the region of 120 Td. For their PTR-IT-MS, Steeghs et al. found that the *E*/*N* for best sensitivity was compound-specific, but analysis of the data from a simple calibrated VOC mixture suggested that the optimal value was ~95 Td. Moving from 120 Td to the lower value of 95 Td improved the overall detection sensitivity by ~25%. It is also worth adding that the lower *E*/*N* has the additional advantage of reducing fragmentation in the drift tube, which can simplify any subsequent CID analysis. As a further investigation of the instrumental conditions on CID analysis, Steeghs et al. chose a series of monoterpenes to determine the role of *E*/*N* in the drift tube and the CID conditions (helium pressure and rf excitation amplitude on the end electrodes) in the ion trap.[63] Sufficient differences were found in the CID responses to distinguish all 10 terpenes investigated, although such an analysis would prove more troublesome in any complex VOC mixture, such as might be the case for terpenes originating from biogenic sources (see later).

4.2.2. Time-of-Flight Systems

Another alternative to quadrupole filter analyzers is the time-of-flight (TOF) mass analyzer. In its most commonly used form, time-of-flight mass spectrometry works by deflecting a batch of ions into a flight tube by an electric field and then separating them according to their flight times to a detector. Since the heavier ions travel more slowly than lighter ones, the time-of-flight spectrum can be converted into a mass spectrum. A TOF-MS is a multichannel instrument that collects the whole mass spectrum at once and thus, in this regard, is similar to the case of IT-MS. Consequently, like PTR-IT-MS, PTR-TOF-MS offers exciting potential for analyzing complex mixtures in real-time.

The first published description of a PTR-TOF-MS instrument was given by Blake et al. in 2004, and the experimental arrangement is shown in Figure 6.[64] The instrument coupled

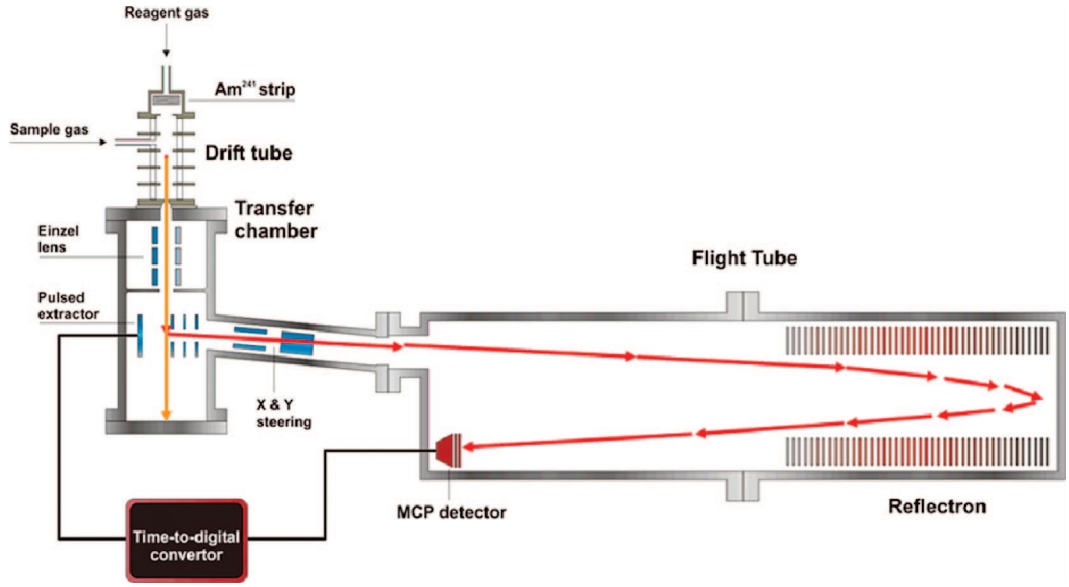

Figure 6. Schematic representation of the University of Leicester PTR-TOF-MS system equipped with a radioactive ion source. Reprinted with permission from ref 64. Copyright 2007 European Geophysical Union.

a radioactive ion source of the Hanson-type, which was described earlier in section 4.1, with a commercial reflectron TOF-MS. This instrument has been tested against gas standards and against other analytical techniques, and the limit of detection was estimated to be 10 ppbV for one-minute data accumulation.[65] This is a respectable sensitivity, but there is considerable room for improvement. Improved ion transmission between the drift tube and the mass spectrometer inlet is expected to improve the signal considerably. Furthermore, there are limitations due to the poor duty cycle of the standard TOF-MS technique. The source of the low duty cycle is the orthogonal injection of a single bunch of ions into the flight tube from a continuous stream of incoming ions. Once these ions are in the flight tube, no further ions can be injected until the slowest ion has reached the detector. As a result, typically 1 or 2% of the ions entering the source region of the TOF-MS are deflected into the flight tube. Consequently, 98−99% of the potential ion signal available is, in effect, thrown away. Nevertheless, as will be seen in examples presented later, PTR-TOF-MS holds considerable promise as a means of monitoring complex VOC mixtures, such as in urban air. Another notable feature of PTR-TOF-MS is the good mass resolution achievable with a reflectron analyzer, which can be comfortably in excess of 1000 ($m/\Delta m$). In particular, a resolution better than 2000 opens up the possibility of distinguishing nominally isobaric compounds on the basis of accurate masses. For example, protonated methacrolein ($m/z = 71.0898$) and 1-pentene ($m/z = 71.1329$) can readily be distinguished with this resolution.

Two other groups have also recently described purpose-built PTR-TOF-MS instruments. Ennis et al. were the first to couple a hollow-cathode ion source with a commercial reflectron TOF-MS, achieving limits of detection close to 1 ppbV in less than one minute.[66] Even more recently, Tanimoto and co-workers have constructed an instrument with a hollow-cathode ion source and a linear TOF-MS and have achieved impressive detection sensitivities of <100 pptV for individual VOC components in a one-minute integration time.[67] This improvement in performance when compared with that of Ennis et al. is attributable to the higher operating pressure in the drift tube, which was in the region of 6 mbar versus 1 mbar in the case of Ennis et al.

Two companies now produce commercial versions of PTR-TOF-MS systems, namely, Ionicon Analytik and Kore Technology. The claim for the Ionicon system is a sensitivity to benzene as good as 10 pptV with one-minute data averaging.

4.3. Combination of Gas Chromatography with PTR-MS

The principal weakness of PTR-MS is its reliance solely on mass spectrometry to provide compound discrimination. In complex VOC mixtures, it is almost inevitable that some molecules will have the same mass (are isobaric) and/or there will be some fragment ions that coincide with parent ion masses. In such circumstances, it can be difficult, if not impossible, to identify all the species present, let alone determine their individual concentrations. A solution to this predicament is to add some further means of separation, and one possibility is to combine gas chromatography (GC) with PTR-MS.

This combination was first carried out by Fall and co-workers, who were motivated by the need to distinguish between the possible contributions of several C5 alcohols and aldehydes to a single mass peak arising from leaf wounding (see also section 5.2).[68] There have been several subsequent studies that have combined GC with PTR-MS.[69−71] Of course, the combination of GC with PTR-MS is no panacea, since it will inevitably result in a major loss of time resolution due to the relatively slow transit times of compounds through a GC column. A degradation in detection sensitivity is also expected.

A different solution to the mass complexity problem has been demonstrated by Lindingder and co-workers.[72] Instead of coupling a GC unit and a PTR-MS instrument in series, the effluent from the GC is fed into both a PTR-MS and an electron impact mass spectrometer (EI-MS) simultaneously. The fragmentation of ions in EI-MS is actually an advantage when coupled with GC, since the fragmentation patterns can allow for unambiguous identification of compounds. The coupling of GC to two separate mass spectrometry systems is nontrivial, requiring careful matching of gas flows through the two parts of the instrument via the judicious use of flow

controllers, "Y" connectors, and a pressure-controlled bypass. In order to minimize the loss of time resolution, Lindinger et al. employed a wide-bore capillary column in their GC system, and the effluent from this could be passed either into a standard electron impact MS or could be fed into the inlet port of a PTR-MS instrument. The initial application of the technique was to identify the volatiles above coffee solutions, where the complex array of VOCs poses severe challenges for PTR-MS when employed on its own.

4.4. Membrane Inlet PTR-MS

Polymer membranes have been used for several decades for the selective introduction of molecules into the ion source region of a mass spectrometer. The membrane is employed as a barrier between the vacuum conditions of the mass spectrometer and the sample under investigation, which may be a gas or a liquid. By choosing an appropriate membrane material, some molecules may permeate readily through the membrane whereas others may show little or no permeation. A classic example is the use of a hydrophobic polymeric membrane to sample VOCs dissolved in aqueous solutions.

Alexander and co-workers were the first to combine a membrane inlet with PTR-MS.[73,74] Employing a polydimethylsiloxane (PDMS) membrane, this group was able to use PTR-MS to determine the diffusion coefficient of various organic molecules in the membrane material. This investigation of the transport of VOCs across a membrane was facilitated by both the rapid detection capability of PTR-MS and the ability to measure absolute concentrations of a variety of compounds almost simultaneously. The same research team was also able to exploit the lack of water penetration through a PDMS membrane, which in PTR-MS would cause major problems through the excessive formation of hydrated hydronium cluster ions. This was demonstrated through the ability to measure VOCs in the vapor above hot water[73] and the detection of specific VOCs present in both fresh and salty liquid water.[74] For the liquid water measurements, detection limits in the region of several parts per billion were achieved for compounds such as methanol and benzene, and for dimethylsulfide, an even better detection limit of 100 pptV was attained. On the downside, the slow permeability of compounds through the membrane limits the response time of the membrane inlet PTR-MS technique to several minutes.

4.5. Calibration and the Effect of Humidity

An important aim of many applications of PTR-MS is to determine the absolute concentrations of a variety of trace VOCs. In principle, eq E1 can be employed for this purpose with a generic, estimated rate coefficient for protonation or through use of a specific experimentally determined rate coefficient. However, there are a number of approximations incurred in this approach that may seriously curtail the accuracy of any concentration determination.

Sources of error originate from the rate coefficient itself, which, even if it has been determined experimentally, may have a reported error margin of up to 50% of the mean value. Futhermore, as first pointed out in section 3.2, PTR-MS measurements are made at an elevated effective temperature for ion−molecule collisions. This temperature can be estimated, but it is not clear that this derived temperature is precisely applicable to the proton-transfer chemistry taking place in the drift tube, which introduces further uncertainty in the effective rate coefficient. There are other potential sources of error, including uncertainty in the transit time of ions across the drift tube and variation in ion transmission as a function of m/z. Furthermore, the quantification of PTR-MS using eq E1 is predicated on equal mobilities for H_3O^+ and the protonated VOC in the drift tube. However, Keck et al. have recently demonstrated that such mobilities can vary substantially, and this factor alone can introduce an error in excess of 20% in the determination of a given compound concentration.[75]

The bottom line is that, for truly accurate concentration determinations, calibration of the instrument against specific gas standards is essential. An excellent demonstration of this has been provided by de Gouw and co-workers, who have made a detailed comparison of PTR-MS versus GC-MS for a range of VOCs to assess the accuracy and precision of PTR-MS determinations.[54] The overall conclusion is that PTR-MS can achieve accuracies in the region of 25% with the aid of suitable calibration. Improvements beyond this are difficult to achieve because of background signals from various impurities in the ion source and drift tube. The precision improves as the concentration increases but is rarely better than 10−15%.

The determination of compound concentrations can also be affected by humidity. The humidity effect derives from the increase in the amount of hydrated hydronium clusters, $H_3O^+(H_2O)_n$, within the drift tube as the humidity of the analyte gas increases. Many compounds will have a different reactivity with hydrated hydronium clusters when compared to reaction with H_3O^+, while some will not react at all (as already discussed in section 3.3). Raising the E/N of the drift tube can reduce the proportion of hydrated hydronium clusters, but there are limits as to how far this can be elevated before other, unwanted, fragmentation effects occur.

Interestingly, under certain circumstances, the sample humidity can have an effect on concentration determinations even for those compounds that do not react with $H_3O^+(H_2O)$. An excellent demonstration of this has been provided by Warneke et al., who used benzene and toluene as the illustrative compounds.[76] Both benzene and toluene will accept a proton from H_3O^+, but their reaction with $H_3O^+(H_2O)$ is thermodynamically forbidden (but note that some net reaction, albeit at a rate lower than the collisional limit, has been reported for toluene by Midey et al.[28] and was discussed in section 3.3). The sensitivity toward these compounds was found to decline quite markedly at a fixed E/N (106 Td in this specific case) as the relative humidity was increased from 20% to 100%. Application of eq E1 would suggest that this should not happen; since the ion count rates of H_3O^+ and RH^+ can still be measured by the mass spectrometer and since there is little or no reaction with hydrated hydronium ions, their presence should not be an issue. However, many PTR-MS instruments, such as the one employed by Warneke et al., include a collision-induced dissociation (CID) region at the downstream end of the drift tube, the purpose of which is to raise the E/N over a short distance and thus help to simplify the mass spectrum by removing cluster ions. Warneke and co-workers demonstrated that an elevated E/N in the CID region relative to the rest of the drift tube leads to an overestimate of the amount of H_3O^+ since it includes contributions from fragmented $H_3O^+(H_2O)_n$ ions. The net effect is an underestimation of VOC concentrations at increasing humidity.

Variation in sample humidity can also be a problem for those compounds whose proton affinities are only marginally above that of water. It is tempting to think of proton-transfer reactions as one-way reactions, but in reality, reaction R1 is reversible and, thus, deprotonation of a VOC is also possible by reaction with water. For most VOCs, the high endothermicity means that the reverse reaction is extremely slow, and thus, equilibrium overwhelmingly favors the protonated VOC. However, there are examples where this is not the case, the best known of which is formaldehyde, whose proton affinity is only 22 kJ mol^{-1} above that of H_2O (see Table 1). The proton-transfer reaction between H_3O^+ and formaldehyde is fast with a rate coefficient of 3×10^{-9} cm^3 s^{-1} at 300 K.[48] At the same temperature, the rate coefficient for the reverse reaction is some two orders of magnitude slower, so the reversibility of the reaction might be thought to be unimportant. However, the rate coefficient for the reverse reaction is strongly temperature-dependent and increases as the temperature is raised.[77] Since the effective ion temperature is elevated in PTR-MS by the applied electric field (see eq E4 in section 3.2), the rate coefficient of the reverse reaction will increase while the rate of the forward (proton-donation) reaction will decrease (as would be expected, for example, from the average dipole orientation prediction in eq E3). Furthermore, increased humidity will also enhance the rate of the reverse reaction since it increases the concentration of water vapor. Consequently, it is vital to consider the effect of humidity when attempting a determination of formaldehyde via PTR-MS.[78]

The examples above show that the effect of humidity on concentration determinations will vary from compound to compound. However, any accurate determination requires a calibration procedure that includes the effect of humidity. A convenient procedure has been described by de Gouw et al.,[54] who employed the ion signal ratio

$$\frac{i(RH^+)}{i(H_3O^+) + X_R \times i(H_3O^+(H_2O))}$$

in place of the $i(RH^+)/i(H_3O^+)$ ratio in eq E1. The quantity X_R is a compound-specific parameter whose value can be determined empirically from measurements with gas standards at high and low humidities such that the ion signal ratio above becomes humidity-independent. Many compounds show a value of X_R of ~0.5, but aromatics such as benzene, toluene, and ethylbenzene have values near zero because of their low or negligible reaction with $H_3O^+(H_2O)$.

5. Applications

5.1. Atmospheric Chemistry

A major application of PTR-MS technology has been in the area of atmospheric science. The importance of PTR-MS stems from its capability as a rapid, online, and highly sensitive monitoring tool for a whole range of VOCs. VOCs are emitted from both natural (biogenic) and man-made (anthropogenic) sources and show large spatial and temporal variations.[1] In the atmosphere, VOCs are important because they may impact on photochemical ozone formation, particulate formation, stratospheric ozone depletion, and climate.[79] Many VOCs are also toxic and/or carcinogenic, and in establishing their effect on human health, it is vital to be able to monitor their concentrations in a wide range of environments.

5.1.1. General Atmospheric Performance

For many atmospheric applications, there is a requirement for a well-characterized performance of PTR-MS with respect to sensitivity, selectivity, and quantification. The earliest applications of PTR-MS as an atmospheric-measurement technique have been described by the Innsbruck group,[7,80] while Hayward et al. and Steinbacher et al. have described some of the general performance features required for atmospheric measurements.[81,82] Because PTR-MS is inherently a real-time direct mass spectrometric technique, much work has focused on the calibration, validation, and comparison of atmospheric measurements.[54,69,76,78,82−92] The atmospheric PTR-MS measurements have been compared to online techniques such as GC-FID,[84,85,88] GC-MS,[54] AP-CIMS,[90] DOAS,[92] and off-line sampling methods coupled to GC analysis.[76,81,87,89,91] The capabilities of PTR-MS as an atmospheric sensor have been reviewed by Hewitt et al.[9] and, more recently, by de Gouw and Warneke.[10]

As a relatively compact and robust instrumental technique, PTR-MS has been deployed on a range of atmospheric-measurement platforms including ground-based measurement stations,[93] vehicles,[94] ships,[54] research aircraft,[95] and operational aircraft.[96]

One of the strengths of PTR-MS for atmospheric VOC analysis is the wide range of VOCs that can be detected. This is illustrated by Table 2, which lists the masses and likely assignments of compounds detected by the technique in ambient air measurements. As already noted in section 3.1, many light hydrocarbons cannot be detected by PTR-MS because of their unfavorable proton affinities. However, heavier hydrocarbons, particularly unsaturated compounds such as aromatics, are amenable to detection. Furthermore, the ability to detect the following classes of compounds is worthy of note.

(a) *Nitrogen-Containing Compounds.* The chemical interactions of odd nitrogen constituents with other trace species are important in a range of oxidation processes in the atmosphere.[79] The sum of total reactive nitrogen or total odd nitrogen is often referred to as NOy and can be defined as NOy = NOx + NO_3 + $2N_2O_5$ + HNO_3 + HNO_4 + HONO + PAN + MPAN + nitrate + alkyl nitrate, where NOx = NO + NO_2.[97] PTR-MS has the ability (see Table 2) to measure key components of this budget such as PAN[98] and more recently C_1-C_5 alkyl nitrates,[99] as well as reduced nitrogen compounds such as HCN,[78] acetonitrile,[54,87,90] and acrylonitrile.[78]

(b) *Oxygenated VOCs.* Oxygenated volatile organic compounds (OVOCs), such as alcohols, aldehydes, ketones, and carboxylic acids, are ubiquitous in the troposphere.[100] They have both primary and secondary sources, being emitted by anthropogenic and biogenic processes, as well as being formed from the gas-phase oxidation of parent hydrocarbons. They represent a particular analytical challenge for conventional GC-based techniques. A number of groups have demonstrated the utility of PTR-MS based measurements for the determination of a wide-range of OVOCs (see also Table 2).[65,83,92,101−104] Northway et al. have shown that caution must be exercised with airborne sampling of OVOCs, ascribing unusually large measurements of acetaldehyde from PTR-MS to a sampling artifact that apparently arises from the heterogeneous ozonolysis of alkenes to form acetaldehyde.[105] The performance

Table 2. Compounds Identified by PTR-MS in Ambient Air (Table Adapted from de Gouw and Warneke[10])

m/z^a	compound	references
28	HCN	78
31	HCHO	82, 92
33	methanol	54, 87, 101
42	acetonitrile	54, 87, 90
45	acetaldehyde	54, 85
47	formic acid	113, 115
54	acrylonitrile	78
57	butenes, methyl *tert*-butyl ether, butanol	78
59	acetone	54, 85, 87, 88, 90
61	acetic acid	54, 89
63	dimethylsulfide	10, 81
69	isoprene, furan	54, 81, 84, 85, 88
71	methyl vinyl ketone, methacrolein	10, 54, 88
73	methyl ethyl ketone	54, 89
75	hydroxy acetone	115, 121
77	peroxy acetyl nitrate (PAN)	54, 98
79	benzene	54, 76, 84, 85, 87−89
81	monoterpenes hexenal	10, 54, 84, 91, 71, 136, 217
83	hexenol, hexanal, hexenylacetate methylfuran, isoprene hydroxyl carbonyls	70, 71, 122, 217, 115
85	ethyl vinyl ketone	122
87	2-methyl-3-buten-2-ol c_5 carbonyls, methacrylic acid	102, 115
91	peroxypropionyl nitrate (PPN)	98
93	toluene	54, 76, 84, 85, 87, 89
95	2-vinylfuran phenol	115, 119
99	hexanal	71, 122, 136
101	isoprene hydroperoxides	114−116, 121
103	peroxymethacrylic nitric anhydride (MPAN)	98
105	styrene, peroxyisobutyric nitric anhydride (PiBN)	85
107	C_8 aromatics	54, 82, 84, 85, 89
115	heptanal	122
121	C_9 aromatics	54, 84, 85, 89
129	octanal naphthalene	122, 78
135	C_{10} aromatics	70, 145
137	monoterpenes	10, 54, 84, 91
139	nopinone	102
143	nonanal	122
149	C_{11} aromatics methylchavicol	78, 102
151	pinonaldeyde	102
163	C_{12} aromatics	78

[a] m/z used for compound identification. For many of the compounds, the dominant peak in the mass spectrum is the protonated parent species. However, fragmentation is significant for some compounds, such as some of the alcohols and aldehydes, and in these cases, fragment ions may have been used for identification. For further information, the reader is directed to the original publications.

of PTR-MS for measuring acetone was compared as part of an aircraft-based intercomparison with atmospheric-pressure chemical ionization mass spectrometry.[90] A comprehensive multi-instrument OVOC intercomparison exercise has recently been reported, and PTR-MS has been shown to perform reliably in the quantification of OVOCs.[65] This study by Wyche et al. utilized a large atmospheric chamber, and participants in the exercise were not informed of the constituent concentrations prior to completion of the experimental work. Figure 7 illustrates the performance by showing the concentration of acetaldehyde versus time measured by PTR-MS (circle points) with the estimated injected chamber concentrations (blue line). Calibration against gas standards was found to be essential in this intercomparison exercise to obtain compound concentrations with satisfactory accuracy.

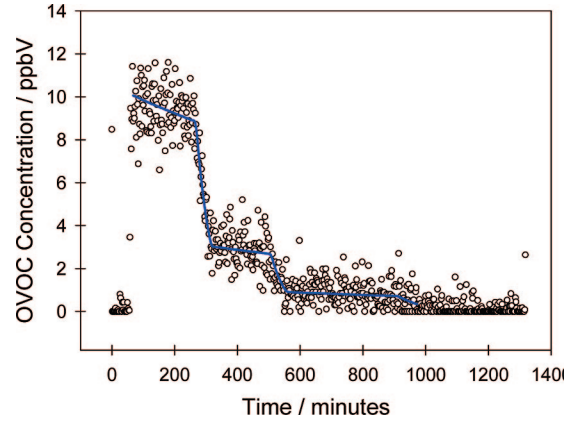

Figure 7. Time profile from an atmospheric simulation chamber experiment showing a comparison of the concentration of acetaldehyde (circle points) measured by PTR-TOF-MS with the estimated chamber concentration (blue line). Reprinted with permission from ref 65. Copyright 2007 European Geophysical Union.

One of the recurrent problems in the application of PTR-MS is distinguishing between isobaric compounds. As already mentioned in section 4.1, Wyche et al. have demonstrated a variant on PTR-MS that utilizes alternatives to H_3O^+ as the ionization reagent.[57] In particular, switching to the charge-transfer agent, NO^+, has shown the potential to distinguish isobaric aldehydes and ketones. For example, proton transfer from H_3O^+ to the molecules methyl vinyl ketone and methacrolein, which are both oxidation products of isoprene, results in protonated ions with the same mass, i.e., the protonated parent species are isobaric. On the other hand, proton transfer is not available to NO^+, and it tends to ionize molecules either by charge transfer or by

hydride anion transfer. For the reactions of methyl vinyl ketone and methacrolein with NO^+, the end result is that more than one product ion is generated in each case but the ion distribution patterns differ. This difference in mass spectra conferred by the switch from H_3O^+ to NO^+ as the reagent ion may be used to distinguish the contributions from isobaric molecules in cases where the mass spectrum is not too complex. Since proton transfer is no longer the only means for generating ions, we refer to this approach as chemical ionization reaction mass spectrometry, or CIR-MS for short.

Knighton et al. have demonstrated an aldehyde scrubber system that can be used to resolve isobaric aldehyde/alkene interferences in PTR-MS.[106] As mentioned earlier in section 4.2, the ability to utilize collision-induced dissociation in an ion trap in PTR-IT-MS also offers good prospects for distinguishing isobaric species in atmospheric trace gas measurements.[86]

5.1.2. Biogenic VOCs

A major class of atmospheric VOCs are those with a natural biological source, which are known as biogenic VOCs. The annual global natural VOC flux (excluding methane) is estimated to be 1150 Tg of carbon, which is composed of 44% isoprene, 11% monoterpenes, 22.5% other reactive VOCs, and 22.5% other (relatively unreactive) VOCs.[107,108] Biogenic VOCs are thought to have a substantial impact on atmospheric composition and climate. PTR-MS has been used to make measurements of biogenic VOC emissions in the immediate environment of individual plants, and these are dealt with in detail later. Here we focus on biogenic VOC measurements on larger scales.

Atmospheric determinations of biogenic VOCs have tended to focus on isoprene, methanol, and the monoterpenes (see also Table 2).[88,91,101,102,109−112] Tropical forests are thought to be major emitters of VOCs. For example, tropical broadleaf trees contribute almost half of the estimated global annual isoprene emission because of their relatively high emission factors and because they are often exposed to conditions (higher temperatures, higher levels of photoactive radiation, and a longer growing season) that are conducive for isoprene emission.[107,113] Measurements have been made from airborne platforms in the tropical forest of Surinam, showing large emissions of isoprene and its oxidation products.[114−116] A signal attributed to dimethylsulfide has also been observed, which is interesting since this is a compound normally associated with marine environments. Crutzen et al. postulated that this compound emanates from the coast and is transported deep into the tropical forest.[114] Normally, the dimethylsulfide would be lost through reactions of OH, but in the tropical forest there is strong competition from OH reactions with hydrocarbons, which prolongs the lifetime of dimethylsulfide.

PTR-MS measurements of isoprene and its oxidation products in Venezuela have been used to estimate the global emission of isoprene to the atmosphere from tropical savannas as being between 53 and 79 Tg C/yr.[117] Mueller et al. investigated biogenic carbonyl compounds within and above a coniferous forest showing that the concentrations of carbonyl compounds above the canopy are typically higher than those within the crown region of the Norway spruce stand.[118] There were major differences between daytime and nighttime concentrations of acetaldehyde and acetone, which have not been fully explained.

PTR-MS measurements in a boreal forest showed that the observed mass peaks could be divided into three classes by factor analysis.[119] The first class was correlated with the ambient air temperature and light and included reactive compounds with local biological, anthropogenic, or chemical sources. The compounds in this class, such as methanol, acetone, methyl vinyl ketone, methacrolein, butanol, and hexanal, generally had the highest concentrations in the late afternoon and minima during the night. The class 2 compounds included monoterpenes and were correlated with the mixing timescale, having the highest concentrations at night and the lowest during the day. Class 3 was not correlated with local meteorology and included rather long-lived compounds such as benzene.[119]

From multivariate analysis of PTR-MS measurements in Crete, Salisbury et al. showed that missing methanol and acetone sources apparent in a chemical transport model are, at least to a large extent, biogenic emissions and also that biogenic sources of acetone are considerably more important than anthropogenic sources.[112] From roadside measurements, Holzinger et al. were able to separate biogenic methanol signals from those of vehicle emissions, with the biogenic component showing a strong seasonal variation.[101] PTR-MS measurements of the vertical concentration gradients of VOCs and their oxidation products in a Ponderosa pine forest in central California have revealed large quantities of previously unreported oxidation products of short-lived biogenic precursors.[102]

A combination of long-term PTR-MS analysis of VOCs with the procedure known as the variability-lifetime method has been used to assess the dominant cause of the variability in VOC concentrations.[120] This methodology was used to understand and identify VOC sources and VOC photochemical processing, i.e., source-receptor relationships of VOCs detected in ambient air at field measurement sites.[121−123] For example, Williams et al. used aircraft-measurement data from over Surinam to estimate an OH concentration of 2×10^5 molecules cm^{-3}.[121]

The fast response of PTR-MS makes it suitable for measurement of biogenic VOC fluxes using techniques such as eddy covariance (EC).[88,91,95,113,124−128,71] The EC method directly determines the vertical flux of a trace component by measuring the covariance between fluctuations in vertical wind velocity and the mixing ratios of the trace components. Other methods include relaxed eddy accumulation[91,129] and disjunct eddy covariance[124] as well as more conventional enclosure methods.[130] The experimental validation of the EC methods has been tackled by Ammann et al. using water vapor detection by both PTR-MS and an IR gas analyzer.[131] The successful validation for the H_2O flux suggested that eddy flux meaurements of VOCs will be similarly well-described by PTR-MS. Table 3 gives a summary of the environments in which such PTR-MS based flux measurements have been made.

Ammann et al. have measured a range of biogenic VOCs in a mixed deciduous forest.[88] A thorough description of the calibration procedures necessary to obtain reliable quantitative information was described. The ability to measure vertical gradients in the canopy was also demonstrated, as illustrated in Figure 8 for monoterpenes. Spirig et al. have worked in similar forests in N.W. Germany, looking at the application of EC methodology and PTR-MS measurements for the derivation of biogenic VOC fluxes.[125]

Table 3. Summary of Measurement Methodologies for Determining Biogenic VOC Fluxes using PTR-MS

ecosystem type	method[a]	reference
mixed deciduous forest	gradient	88
mixed deciduous forest	EC	125
Ponderosa pine	EC, REA	91, 134
subalpine forest	DEC	127
norway spruce	DEC, REA, EM	129, 130, 194
alfalfa	DEC	124, 136
Scot's pine	DEC, EM	132, 133, 320
agricultural soil	REA	135
tropical rain forest	DEC	113, 321

[a] EC = Eddy covariance; DEC = disjunct eddy correlation; REA = relaxed eddy accumulation; EM = enclosure method.

Emission fluxes of methanol, acetaldehyde, acetone, and monoterpenes have been measured by PTR-MS above a Scot's pine forest in Finland.[132] Chemical modeling showed that there was little loss owing to reaction and the fluxes followed the traditional exponential temperature-dependent emission algorithm. Daily patterns of monoterpene emissions have also been measured in the same forest using a PTR-MS instrument coupled to an in situ sampling chamber in the canopy.[133] Holzinger et al. have measured long-term monoterpene fluxes over a *ponderosa* pine plantation.[134] Seasonal flux measurements revealed that the total annual monoterpene emission may be underestimated by ~50% when using a model optimized to reproduce monoterpene emissions in summer. Analysis of the long-term data set also revealed an indirect connection between non-stomatal ozone flux and monoterpene emissions beyond the dependence on temperature that has been shown for both fluxes, indicative of emissions of unobserved highly reactive biogenic species.[102]

PTR-MS has been combined with eddy covariance to measure the fluxes of methanol and acetone from an agricultural field in Europe during one of the hottest weeks of the heat wave of the summer of 2003.[135] Significant positive fluxes from the bare, plowed soil were found for both methanol and acetone. Furthermore, there were significant increases at night, consistent with a soil emission source for both compounds. Methanol emissions correlated well with heat flux, peaking at around noon. Assuming abiological production from organic matter in the topsoil, an activation energy of 48 kJ mol^{-1} was required to liberate the methanol from the topsoil.[135]

Karl et al. observed significant fluxes of 2-methyl-3-buten-2-ol, methanol, acetone, and acetaldehyde at a subalpine forest site governed by a short growing season and cool temperatures.[127] Flux measurements have been made over an alfalfa field before, during, and after cutting, using a combination of disjunct eddy covariance[124] and PTR-MS.[136] Significant methanol fluxes as well as hexenals, acetaldehyde, and acetone were observed throughout the day. After the alfalfa was cut, the emissions of methanol, acetaldehyde, acetone, and hexenals were significantly enhanced and remained high for three days, during which the alfalfa was drying. The authors suggest that the global source of OVOCs from the production of hay is of minor importance, but the emission flux of methanol from vegetation during the growing season may be very large on a global basis.[136]

Karl et al. have investigated the use of PTR-MS over deciduous temperate, tropical rain, and evergreen needle forests in order to assess atmospheric variability, lifetimes, and fluxes of biogenic VOCs.[126] The tropical forests showed particularly large emissions of VOCs.[113] The key conclusion from this work was that the dynamic response of PTR-MS can be successfully used for assessing the magnitude and homogeneity of surface fluxes. It can also be used to characterize atmospheric lifetimes in remote locations, with the lifetime being dominated by chemical losses due to reactions with OH, O_3, and NO_3.[126] Lee et al. have compared total monoterpene flux measurements from PTR-MS with GC-based results, showing that apparent discrepancies in the daytime findings could be removed by identification of β-pinene peaks in the chromatograms, leaving nighttime discrepancies that were attributed to shorter-lived terpenes not present during the day.[91]

The emission of biogenic compounds over the Amazon basin has been investigated using eddy covariance measurements (so-called mixed-layer variance (MLV)) from both the aircraft and ground and compared to the emission model MEGAN (see Figure 9).[95] Isoprene and monoterpenes accounted for ~75% of the total OH reactivity in this region and are important volatile organic compounds (VOCs) for modeling atmospheric chemistry in Amazonia. The presence of fair-weather clouds (*cumulus humilis*) has an important impact on the vertical distribution and chemistry of VOCs through the planetary boundary layer, the cloud layer, and the free troposphere.

PTR-MS has been used in a phytoplankton mesocosm enclosure experiment in a Norwegian Fjord to explore at the ocean emissions/uptake of methanol, acetone, acetaldehyde, isoprene, and dimethylsulfide.[137] The experiments showed that the net flux of methanol was always into the ocean and was stronger at night. Isoprene and acetaldehyde were emitted from the ocean, correlating with light intensity and phytoplankton abundance, whereas dimethylsulfide was also emitted to the air but did not correlate significantly with light.

Although much of the focus of the biogenic VOC work has been on compounds such as isoprene, methanol, and

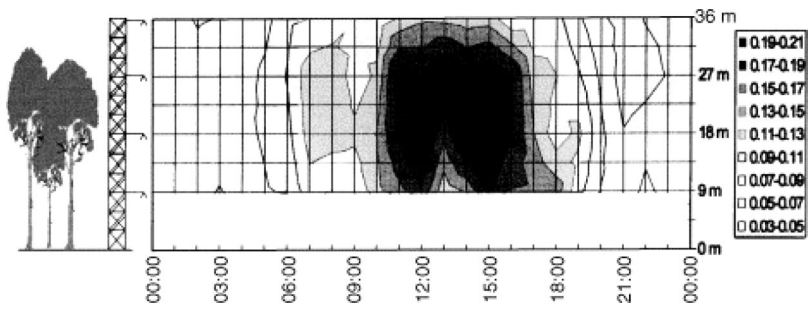

Figure 8. Contour plot of mean monoterpene concentration versus time of day (horizontal axis) and height above ground (vertical axis) from a study in a deciduous forest. Data are median values over 30 days. Concentration values are indicated in gray scale with steps of 0.02 ppbV. Reprinted with permission from ref 88. Copyright 2004 Elsevier.

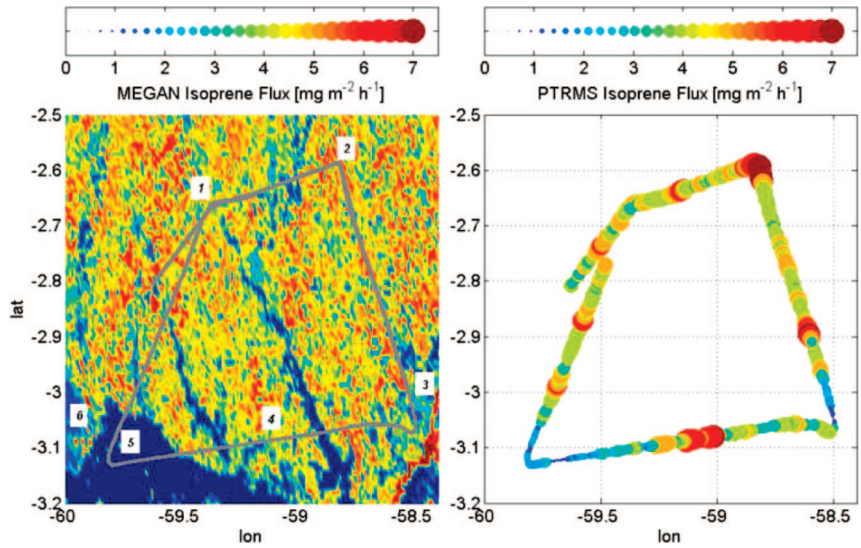

Figure 9. Comparison of predicted (MEGAN model) and measured isoprene fluxes, with the latter being derived from aircraft PTR-MS measurements. The gray line on the panel depicts the flight track. Numbers 1−6 on the left panel indicate different land cover types, namely, (1) mixed forest/plantation, (2) primary tropical forest, (3) soybean plantation, (4) mixed forest/plantation, (5) water, and (6) urban (the city of Manuas). Reprinted with permission from ref 321. Copyright 2007 American Geophysical Union.

monoterpenes, PTR-MS measurements have revealed a range of other biogenic VOCs such as hexanal, methylbutanals, pentenol, and pentenone released in late autumn from apparent leaf wounding driven by the first hard frosts.[68,70]

Measurements of carbonyl compounds such as acetaldehyde, acetone, methyl vinyl ketone, methacrolein, and isoprene at Cape Grim in Tasmania, a heavily marine-influenced site, have shown much lower concentrations than equivalent northern hemisphere measurements.[93] The authors note that the lower concentration of the carbonyl compounds and their precursor hydrocarbons may indicate a limitation on ozone production potential in the southern hemisphere when compared to the northern hemisphere.

PTR-MS measurement of biogenic VOCs has been used in combination with a range of other measurements to investigate the growth of aerosol particles in a coastal region of the eastern U.S.A.[138] The data show aerosol formation primarily during mornings when there are peaks in the amounts of of α- and β-pinene and ozone, which leads to the formation of condensable products from photochemical oxidation.

5.1.3. Anthropogenic VOCs

There are a wide range of anthropogenic VOC sources driven by combustion processes; the production, treatment, storage, and distribution of fossil fuels; and organic solvents, industrial production processes, and agriculture.[1]

Urban and suburban VOC measurements using PTR-MS have been made in a wide range of cities including Barcelona,[139] Caracas,[140] Houston,[78] Mexico City,[94,141] and Tokyo.[84,142] Measurements in Caracas and the surrounding regions showed that, even in the urban areas, the pollution levels were relatively low.[140] Seasonal measurements of VOCs in Tokyo showed higher concentrations of OVOCS in summer rather than autumn, whereas the aromatics showed little seasonal cycle.[84]

Beyond the geographical distribution, Karl et al. demonstrated the utility of PTR-MS for VOC source identification in a complex urban situation by a combination of high time resolution PTR-MS measurements, meteorological data, and multivariate source−receptor relationships.[78] Warneke et al. have used aircraft measurements downwind of Boston/New York and Los Angeles to determine emission ratios (with respect to CO) of a wide range of VOCs.[143] The data compared well to other measurements from urban areas and also to measurements of vehicle exhaust gases, indicating that a large source of VOCs in urban areas is automobile exhaust. On the other hand, the measured emission ratios did not compare well with a frequently used anthropogenic emissions database. Discrepancies of up to one order of magnitude were found for some alkanes and oxygenated VOCs.

There have been a number of roadside PTR-MS studies investigating emissions of anthropogenic VOCs from motor vehicles.[101,139,144,145] For example, Beauchamp et al. have coupled PTR-MS with traditional atmospheric composition measurements for CO, NOx, and PM_{10} particulates to assess the impact of heavy-duty vehicles on Austrian motorways.[145] In a different study by Holzinger et al., the relative enhancement in the concentrations of toluene, benzene, and acetonitrile measured during intense, short-term traffic pollution led to the estimate that <6% of the total global budget of acetonitrile comes from automobile emissions.[144] Filella et al. have investigated the weekly and seasonal patterns of VOCs in the vicinity of a highway in a semi-urban site near Barcelona and have explored possible origins of these VOCs.[139]

VOC concentrations in diesel exhaust as a function of engine load have been probed using PTR-MS. The diesel exhaust mass spectra were complex, but up to 75% of the organic ion signal could be assigned.[146]

The PTR-MS technique has been adapted for the measurement of hydrocarbon emissions from vehicles in Mexico City.[141] The instrument was mechanically reconfigured and optimized for a fast time response (<2 s). Sensitive measurements of compounds such as methanol, acetaldehyde, acetone, methyl tertiary butyl ether, benzene, and toluene within intercepted exhaust emissions were made.[94] The VOC burden in Mexico City determined from PTR-MS and other measurements was dominated by alkanes (60%), followed by aromatics (15%) and alkenes (5%). The remaining 20% was a mixture of alkynes, halogenated hydrocarbons, oxy-

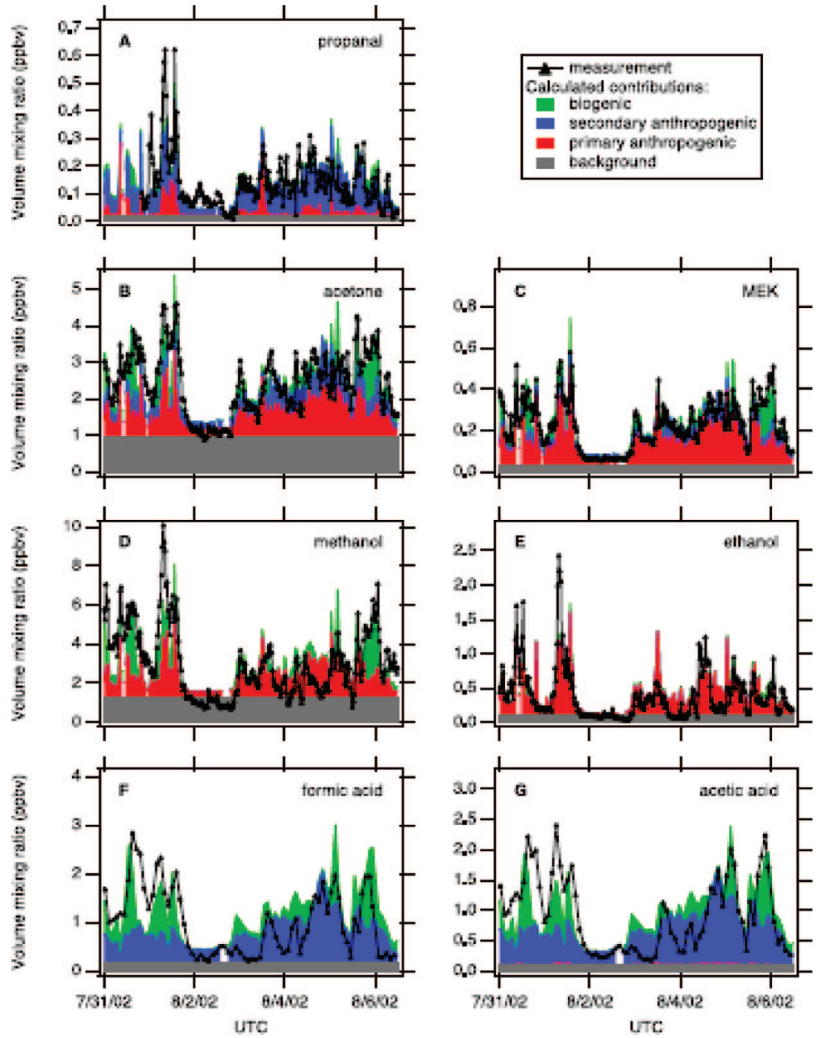

Figure 10. Source attribution (biogenic, primary/secondary anthropogenic, and background) from PTR-MS measurements of a series of VOCs in the New England Air Quality Study. Reprinted with permission from ref 152. Copyright 2005 American Geophysical Union.

genated compounds (esters, ethers, etc.), and other unidentified VOCs. However, in terms of ozone production, alkenes were the most relevant hydrocarbons. Elevated levels of toxic hydrocarbons, such as 1,3-butadiene, benzene, toluene, and xylenes, have also been observed in a comprehensive study by Velasco et al.[147]

PTR-MS has also been combined with tuneable infrared absorption spectroscopy to characterize VOC emissions from aircraft during airport operations.[148] The data showed that the hydrocarbon emission index, a measure of the amount of hydrocarbons emitted per kg of fuel burnt, was greater in idle and taxiway acceleration plumes relative to approach and takeoff plumes.[148] Direct measurements of hydrocarbon emissions from the engine exhausts of a DC-8 aircraft on the ground have also been made for various fuel types.[149,150] These real-time measurements highlighted interesting variability and transient behavior on a time scale of several seconds.

VOC emissions from dairy cows in California has been assessed by Shaw et al. using PTR-MS to determine the potential impact on photochemical ozone production production. VOCs were measured from the dry cows and their waste by PTR-MS inside a large environmental chamber (4.4 m $\times$ 2.8 m $\times$ 10.5 m).[151] The compounds with the highest fluxes when both cows and their waste were present in the chamber were methanol, acetone/propanal (isomers), dimethylsulfide, and a compound yielding a peak at *m*/*z* 109 (likely to be 4-methylphenol). The compounds with the highest fluxes from fresh waste (urine and feces) were methanol, a species giving a peak at *m*/*z* 60 (likely to be trimethylamine), and the compound responsible for the mass peak at *m*/*z* 109. The sum of reactive VOC fluxes measured when cows were present was a factor of 6−10 less than estimates historically used for regulatory purposes. In addition, ozone formation potentials of the dominant VOCs were ~10% of those of typical combustion or biogenic VOCs. The important conclusion from this work was that dairy cattle have a comparatively small impact on ozone formation per mass of VOC emitted.

Gas-phase VOC measurements have been combined with aerosol measurements of polluted and clean air masses off the northeastern U.S. coast as part of the New England Air Quality Study in 2002. The results were used to study the budget of organic carbon, separating the sources of organic carbon in an attempt to categorize them quantitatively using gas-phase indicators for primary anthropogenic emissions, the photochemical age and biogenic sources (see Figure 10).[152] As part of the same study, a comparison of the daytime and nighttime oxidation of biogenic and anthropogenic VOCs in summer was undertaken.[111] The nighttime chemistry was found to be dominant in the removal of biogenic VOCs from the air.

Fireworks provide a transient source of both gas-phase VOCs and aerosol that have been little studied. Drewnick and co-workers have recently explored this using both PTR-MS for VOC identification and aerosol mass spectrometry for particulate analysis.[153] Measurements made at a firework event during New Year festivities in Germany showed that aromatic compounds such as toluene did not show any significant contribution from the firework emissions. Other species, which are related to burning processes, showed significant increases during the firework events (e.g., methanol and acetone). In the aerosol phase, there was a significant increase in particle number density as well as in the mass concentration. The real-time PTR-MS VOC measurements showed a dip in concentration after midnight, which the authors attributed to a "champagne dip", i.e., a pause in festivities.

5.1.4. Biomass Burning

Forest fires and biomass burning are major sources of VOCs in the atmosphere.[154] Measurement and quantification of biomass burning is relatively uncertain owing to the stochastic nature of the burning events. Determination of acetonitrile concentration via PTR-MS is a powerful tool for the identification of biomass burning plumes[89,104,112,155−159] and in combination with CO measurements has been used to delineate biomass burning from fossil fuel emissions.[112,156,157] The reduced nitrogen compounds such as acetonitrile seem to be formed as a product of incomplete combustion.[154] A note of caution has been struck by Sanhueza et al., who have detected significant concentrations of acetonitrile over Venezuelan woodland savannah.[160] Much of the observed acetonitrile was attributed to release from the warm water of the Caribbean, but this was still significantly less than that observed in "typical" biomass burning plumes. There is evidence from PTR-MS measurements that the ocean is an effective sink for acetonitrile.[123,155]

Holzinger et al. have observed relatively high methanol and acetone enhancements in fire plumes over the Mediterranean and concluded that secondary production of these species must have taken place.[104] de Gouw et al. have intercepted Alaskan biomass burning plumes that had intriguing chemical signatures in terms of the ratio of biomass tracers and soluble organics, given the relative dryness of the observed plumes.[89] This was thought to be caused by cloud processing and precipitation during transport of the air mass. Salisbury et al. detected significant biomass-burning signatures from Eastern Europe flowing into the Mediterranean.[112] PTR-MS measurements of the abundance of acetonitrile relative to carbon monoxide made in the Indian Ocean in combination with an air flow trajectory analysis have shown a strong biomass burning impact in western India, mixed pollution sources in northeast India, and the dominance of fossil fuel combustion in the Middle East.[157] In the same study, the elevated abundances found for acetone and acetaldehyde were attributed to unidentified sources in both biomass-burning-impacted air masses and remote marine air.[157] Continuous monitoring of VOCs in the air by PTR-MS at Mauna Loa (Hawaii) in the remote Pacific has identified evidence of long-range transport of biomass burning plumes from Southeast Asia and the Indian subcontinent in the spring of 2001.[156] A combination of aircraft-based PTR-MS measurements off the Pacific coast of the U.S. along with air back-trajectory analysis has helped to detect sources of pollution transported from Japan, Korea, China, and S.E. Asia.[158] Contributions of biomass burning to the total VOC budget were determined to be low for Japan and Korea, higher for China, and the highest for Southeast Asia. PTR-MS measurements of biomass tracers at Chebogue point in Nova Scotia were used to track and quantify biomass-burning emissions from Alaska and the Yukon Territory in 2004.[159]

An investigation known as the Tropical Forest and Fire Emissions Experiment (TROFFEE) used laboratory measurements followed by airborne and ground-based field campaigns during the 2004 Amazon dry season to quantify the emissions from pristine tropical forest and several plantations, as well as the emissions, fuel consumption, and fire ecology of tropical deforestation fires.[128] PTR-MS in conjunction with Fourier transform infrared (FT-IR) spectroscopy was used as part of both airborne campaign and laboratory experiments to quantify a range of nonmethane hydrocarbons emitted and to derive biomass-burning emission factors.[95,128] The PTR-MS measurements led to the quantification of emission factors for a wide range of VOCs from a large number of fires,[128] showing higher concentrations of OVOCs than previously included in chemical-transport models.[95]

PTR-MS has also been used to assess the trace gas and particle emissions from a number of laboratory-based biomass burning studies.[95,161,162] For example, the data in one study, in which a variety of plant matter from different global locations was burned in the laboratory, identified a series of previously unquantified oxygenated compounds emitted from the fires, including phenol, acetol, glycoaldehyde, and furan.[161] In a follow-up study, a comparison of the quantitative performance of open-path FT-IR spectroscopy and PTR-MS has shown good agreement for the quantification of methanol, phenol, and acetol ($CH_2OHC(O)CH_3$) and for the combinations of furan/isoprene (isobaric) and acetic acid/glycolaldehyde (isomers), although worse agreement was found for propylene and the acetone/methylvinylether (isomers) combination.[162]

5.1.5. Application of PTR-MS to Laboratory Studies of Atmospheric Chemistry

Many of the laboratory applications of PTR-MS have focused on the measurement of reaction products that are difficult to observe and quantify by other techniques, particularly from the atmospherically significant terpene oxidation systems.[163−165] Wisthaler et al. measured acetone and pinonaldehyde yields from the reaction of OH with α- and β-pinene in air in the presence of NOx.[165] They noted good agreement with the yields derived from other mass spectrometric or gas-chromatographic methods but less so with optical spectroscopic methods. Zhao et al. have measured the yields of C_4 and C_5 hydroxycarbonyls arising from the OH-initiated oxidation of isoprene using PTR-MS.[163] The results showed that these hydroxycarbonyl compounds accounted for most of the previously unquantified carbon, enabling isoprene carbon closure, i.e., full apportionment of carbon product yields.

PTR-MS has been used to investigate the atmospheric chemistry of C_3-C_6 cycloalkanecarbaldehydes, which are second-generation oxidation products of monoterpene oxidation.[164] In this work, PTR-MS was combined with FT-IR spectroscopy, the latter technique being used to detect small molecules such as CO and CO_2, whereas the former was used to identify a range of organic products including nitroperoxycarbonyl cycloalkanes, cycloketones, cycloalkyl

nitrates, and a number of other multifunctional compounds containing carbonyl, hydroxy, and nitrooxy functional groups. Fragmentation was found to be a major problem at "normal" *E/N* values of >100 Td, and so more gentle conditions of 80 Td were used in the drift tube, which led to $H_3O^+(H_2O)$ being more abundant than H_3O^+. It is clear from this study that PTR-MS allows quantitative detection of volatile organic reaction products that cannot easily be achieved by other chemical ionization methods (e.g., API-MS) or other analytical techniques. However, as also noted elsewhere, PTR-MS is not a truly species-specific method for analysis when isobaric interferences occur, and thus, unambiguous compound identification can be a challenge.

PTR-MS has been used on the EUPHORE atmospheric simulation chamber to provide experimental confirmation of the dicarbonylic mechanism in the photo-oxidation of toluene and benzene.[166] The particular benefit of PTR-MS in this context is its relatively high time resolution, which provides data that can be tested against a Master Chemical Mechanism model. Differences in their mass spectral fragmentation patterns also allowed PTR-MS to distinguish between *cis*- and *trans*-butenedial, two of the products of the photo-oxidation process.

One new application in the laboratory arena is by Hanson et al., who have demonstrated the use of a laminar flow system coupled to PTR-MS for the detection of a range of peroxy radicals.[167] This is the first time that PTR-MS has been applied to the detection of free radical intermediates, with methyl, ethyl, and small cyclic peroxy radicals being successfully found. Under the high-pressure conditions employed, the dominant proton donors were hydrated hydronium cluster ions, rather than bare H_3O^+. Particularly powerful was the ability to map the formation of product distributions in organic reaction systems involving peroxy radicals.

There has been a recent resurgence in the use of laboratory chamber studies, particularly to elucidate the chemical routes for the formation of secondary organic aerosols (SOAs).[168] In general, PTR-MS has been used to follow the complex organic gas-phase VOC composition in these aerosol-forming systems.[169−172] For example, Baltensperger et al. investigated aerosol formation from the trimethylbenzene−propene−NOx−water vapor system (see Figure 11), classifying the VOCs by their temporal profile class and identifying oligimerization as a key SOA formation mechanism.[169,173] Lee et al. have investigated the photooxidation of isoprene, eight monoterpenes, three oxygenated monoterpenes, and four sesquiterpenes at the Caltech Indoor Chamber Facility under atmospherically relevant hydrocarbon/NOx ratios, monitoring the time evolution and yields of SOAs and gas-phase oxidation products using PTR-MS.[170,174] In these experiments, several oxidation products were calibrated by PTR-MS, including formaldehyde, acetaldehyde, formic acid, acetone, acetic acid, nopinone, and methacrolein/methyl vinyl ketone; other oxidation products were inferred from known fragmentation patterns, such as pinonaldehyde. Numerous unidentified products were formed, and the evolution of first- and second-generation products was clearly observed. Ng et al. have extended the analysis of these data to look at the role of first- and second-generation oxidation products in the formation of SOAs (see Figure 12).[171] Chamber experiments have also been carried out to monitor the gas-phase VOCs produced by the ozonolysis of a series of terpenes.[174] Presto et al. have developed a method using PTR-MS VOC

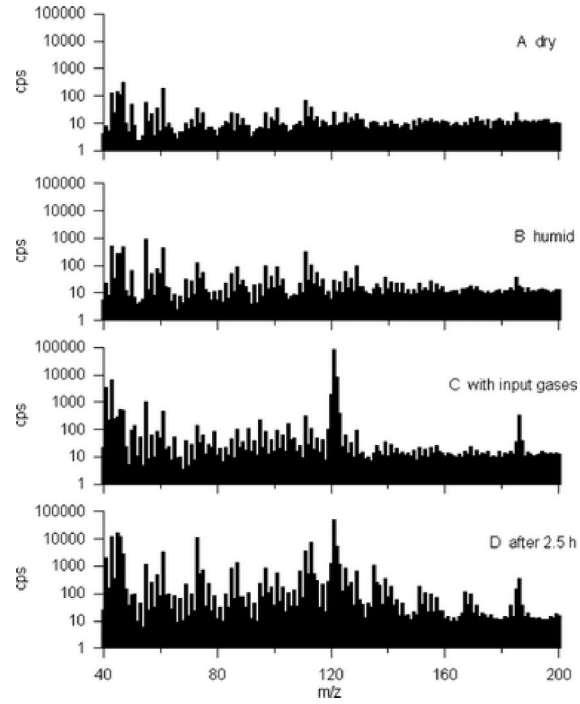

Figure 11. Series of PTR-MS spectra from an aerosol chamber experiment. The spectra show (A) the dry clean air, (B) the humidified clean air, (C) the reactant mixture (nominally 1200 ppbV 1,3,5,-trimethylbenzene, 320 ppbV NO, 320 ppbV NO_2, and 300 ppbV propene at 50% relative humidity), and (D) the mixture 2.5 h after artificial irradiation. Reprinted with permission from ref 165. Copyright 2005 Royal Society of Chemistry.

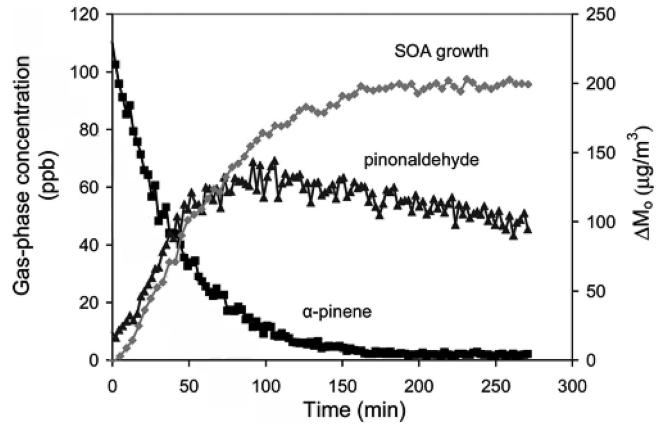

Figure 12. Time evolution of α-pinene and pinonaldehyde from α-pinene photo-oxidation as measured by PTR-MS in a reaction-chamber experiment. Also shown is the corresponding secondary organic aerosol (SOA) growth curve, as measured by aerosol mass spectrometry. Reprinted with permission from ref 171. Copyright 2006 American Chemical Society.

measurements coupled to particle measurements to measure SOA production at low total organic mass concentration ($<10\ \mu g\ m^{-3}$).[172] From that methodology, the authors show that extrapolations of current partitioning models to conditions of low organic mass concentration significantly underestimate SOA production under dark, low-NOx conditions. In contrast, SOA production under illuminated, higher NOx conditions typical of polluted regional air masses was found to be overestimated.[172]

Liggio et al. have used a combination of PTR-MS to measure the gas-phase and aerosol mass spectrometry to measure the aerosol phase to investigate the direct polymerization of isoprene and α-pinene on acidic aerosols.[175] PTR-

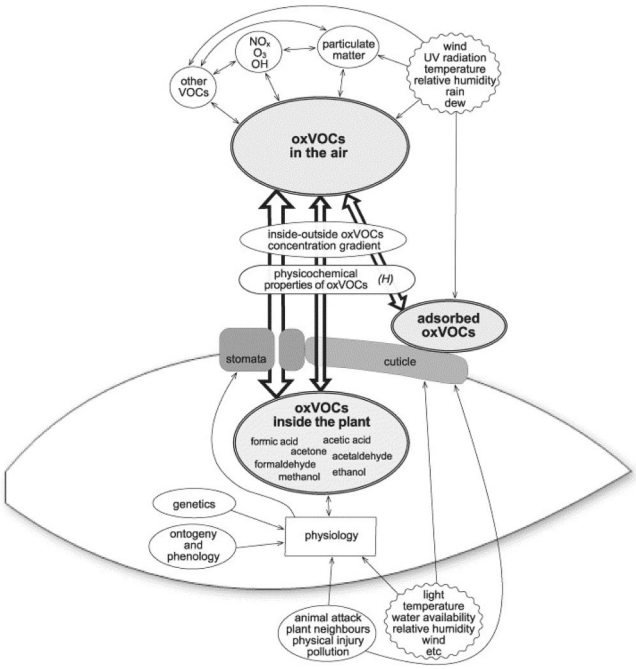

Figure 13. Schematic diagram showing the factors driving the emission and uptake of short-chain VOCs in a plant. Reprinted with permission from ref 190. Copyright 2007 Elsevier.

MS has also been combined with aerosol measurements to determine the temperature dependence of the aerosol formation yields in the α-pinene + ozone system.[176]

PTR-MS measurements of acetaldehyde, which can be formed as a primary carbonyl product or may be derived from a Criegee intermediate, have been used to investigate product yields in ozone + alkene reaction systems.[177] The yields determined for propene and (*E*)-butene ozonolysis with CO as a scavenger agree with the values reported in the literature within the experimental uncertainties.

5.2. Plant Studies

Many VOCs are emitted into the atmosphere by the leaves of plants. These VOCs can represent up to 10% of the carbon fixed by plants. In terms of emission, isoprene and monoterpenes are quantitatively the largest,[108] exerting profound influence on atmospheric chemistry, as already discussed in section 5.1. The biogenic VOCs seem to play multiple roles in plant physiology, such as providing protection against high temperatures,[178] high irradiation,[179] and oxidation stress.[180] In addition, they act as herbivore deterrents,[181] as attractants of pollinators and the enemies of herbivores,[182,183] as antimicrobials,[181] as plant−plant communication cues,[184] and as plant "safety valves".[185] Plants also release VOCs after wounding or stress.[186−189] Many of the emitted compounds are OVOCs, and the factors that drive the emission and/or uptake of these VOCs are illustrated in Figure 13. Seco et al. have recently reviewed the current knowledge of emissions of OVOCs by plants and the factors that control them.[190]

The practical approaches to the analysis of plant volatiles have been discussed by Tholl et al. and are summarized in Figure 14.[191] To provide a foundation for the study of VOCs emitted by plants, Maleknia et al. investigated representative members of various classes of compounds known to be emitted from plants, including alcohols, several carbonyl-containing compounds, and terpenes.[192] This study of reference compounds pointed out a number of problems with PTR-MS when applied as the sole analytical technique, including the occurrence of significant ion fragmentation and the formation of fragments from proton-bound dimer and trimer ions. This is yet another illustration of the fact that PTR-MS does not always deliver product signals in terms of simple protonated products, RH^+, and thus additional analytical techniques can sometimes be valuable in compound identification.

5.2.1. Local Emissions

Biogenic emissions over large scales have already been dealt with earlier in this review. Though clearly linked to regional and global distributions of biogenic VOCs, the focus here is on the VOC atmosphere in the immediate vicinity of specific plants as probed by PTR-MS.

In conjunction with a dynamic enclosure system, PTR-MS has been used to investigate the emission of VOCs from Sitka spruce.[130] The study showed that, while compounds such as isoprene were well-represented by temperature and solar radiation emission models (e.g., see ref 108), the OVOC emissions were not well-described by such models. Hayward et al. have looked at the same tree species and found larger isoprene emissions than previously reported as well as an interesting anticorrelation between isoprene and acetaldehyde during sudden light−dark transitions.[193] Fluxes of biogenic compounds in the immediate vicinity of the tree match those measured by PTR-MS over a much larger regional scale.[194]

The VOCs released from *Muscodor albus,* an endophytic fungus that produces compounds that both inhibit and kill other microorganisms, have been measured using both GC-MS for reliable compound identification and PTR-MS for the real-time emission profiles with varying physical conditions and from soil experiments.[195] Ethanolic fermentation within lichens, under oxygen-deprived conditions, has been shown by PTR-MS to emit acetaldehyde and ethanol.[196] Plant roots release about 5−20% of all photosynthetically fixed carbon and, as a result, create a carbon-rich environment for numerous rhizosphere organisms, including plant pathogens and symbiotic microbes whose exudates can emit VOCs. In conjunction with GC, PTR-MS has shown that the roots of *Arabidopsis* emit VOCs that are simple metabolites, such as ethanol, acetaldehyde, acetic acid, ethyl acetate, 2-butanone, 2,3-butanedione, acetone, and the monoterpene, 1,8-cineole.[197]

PTR-MS has been used in concert with other analysis techniques to elucidate the molecular role of pink pigmented facultative methylotrophs, a form of surface bacteria on plants during seedling growth.[198] The ability of methylotrophic bacteria to promote seedling growth and germination of a number of important crop plants was tested. In addition, the levels of methanol produced by the leaves and the consumption of methanol by the methylobacteria were determined using PTR-MS.

Mesocosm experiments in the tropical rain forest model ecosystem of Biosphere 2, an artificial closed biological system, have been used to assess measured isoprene emissions during mild water stress as well as the relationship with light and temperature.[199,200] The authors found that gross isoprene production was not significantly affected by mild water stress because the isoprene emitters were mainly distributed among the large, canopy layer trees with deep roots in the lower soil profile where water content decreased much less than in the top 30 cm.[199] Experiments showed

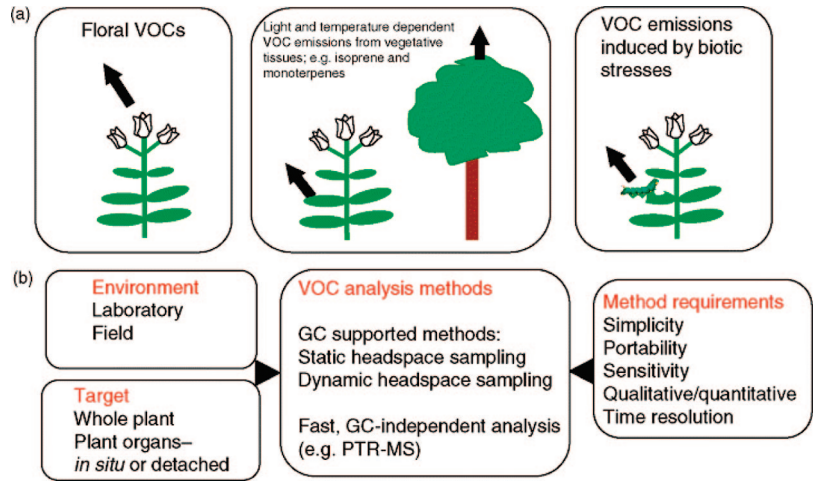

Figure 14. Strategies for plant volatile analysis: (a) typical sources of plant VOC emissions and (b) practical considerations. Reprinted with permission from ref 191. Copyright 2006 Blackwell.

that soil uptake of atmospheric isoprene in the mesocosm is likely to be modest but will be significant in a global isoprene budget.[200] Penuelas et al. have employed PTR-MS to show that the fumigation of holm oak (*Quercus ilex*) with methyl salicylate increases monoterpene emissions.[201]

5.2.2. Plant Physiology

Isotope-labeling experiments, particularly using $^{13}CO_2$, have been used to trace the biosynthesis pathways of isoprene formation.[202−205] For example, by measuring the amount of ^{13}C labeled isoprene produced, Kreuzwieser et al. showed that xylem-transported glucose or its degradation products can potentially be used as additional precursors for isoprene biosynthesis and that this carbon source becomes more important under conditions of limited photosynthesis.[202] Acetaldehyde has been shown to be a rapid "burst" product during light−dark transitions of tree leaves. ^{13}C labeling experiments suggested that this resulted from a pyruvate overflow mechanism controlled by cytosolic pyruvate levels and pyruvate decarboxylase activity.[204] More recently, ^{13}C labeled experiments have been used to probe different carbon pools within young poplar leaves, showing that isoprene comes from a combination of CO_2 biosynthesis, xylem-transported carbon, and internal stores such as starch.[205]

PTR-MS has been used to investigate the transient release of OVOCs during light−dark transitions in gray *poplar* leaves.[206] A prompt release of acetaldehyde and other OVOCs was found. In the temporal patterns after light−dark transitions, hexenal was emitted first, followed by acetaldehyde and other C_6 VOCs. Under anoxic (oxygen-free) conditions, acetaldehyde was the only compound released after switching off the light. This indicated that hexenal and the other C_6 VOCs were released from the lipoxygenase reaction taking place during light−dark transitions under aerobic conditions. Further experiments with enzyme inhibitors that artificially increased cytosolic pyruvate demonstrated that the acetaldehyde burst after a light−dark transition could not be explained by the suggested pyruvate-overflow mechanism.[206]

Jasmonic acid (JA) is a signaling compound with a key role in both stress and development in plants and can elicit the emission of VOCs. In laboratory experiments, JA was sprayed on the leaves of the Mediterranean tree species *Quercus ilex* and the uptake of VOCs was measured using PTR-MS (and GC-MS) after a dark−light transition.[207] It was found that monoterpene emissions were enhanced (20−30%) after JA spraying, and it also increased methyl salicylate emissions (more than two-fold) 1 h after treatment, although after 24 h this effect had disappeared. Formaldehyde foliar uptake decreased significantly 24 h after JA treatment. Chamber measurements of *Quercus ilex* emissions showed that, when the roots were flooded with water, there was a massive increase in ethanol and acetaldehyde production.[208] Bursts of acetaldehyde with lower ethanol emission were also found under fast light/dark changes.

Dimethylallyl diphosphate (DMADP) and geranyl diphosphate (GDP), respectively, are the immediate precursors of the isoprene and monoterpenes emitted by leaves.[209] PTR-MS measurements of evolved isoprene after acid hydrolysis of DMADP and similar measurements of linalool and several furans after acid hydrolysis of GDP were used to assess the roles of the various plant storage pools of these compounds in the emission of isoprenoids. The results showed that the pool size of the compounds does not limit the emission of isoprenoids. Rather, it indicates that the flux of volatile isoprenoids effectively controls the size of their pools of precursors. PTR-MS measurements of isoprene emissions from gray *poplar* leaves have shown that they couple to circadian rhythms.[210]

5.2.3. Plant Damage

Wounds in vegetation can lead to the release of VOCs.[186] Figure 15 shows a chemical scheme for the formation of hexanal and hexenal-family VOCs in leaves following wounding. It has been suggested that these compounds have antibiotic properties and inhibit the invasion of bacteria and other microorganisms into damaged tissues.[211]

Natural emissions from wounding may be driven by plant attack from herbivores, and there are a number of potential herbivore-deterrent or predator-attractant roles for the emitted compounds.[181] For example, it has been shown using PTR-MS that *euphydryas aurinia* caterpillars feeding on *succisa pratensis* leaves induce large emissions of methanol, as well as a range of terpenoids.[187] Von Dahl et al. have looked at the biochemistry following the attack of *Manduca sexta* larvae on *nicotiana attenuata* plants, showing that both methanol and (*E*)-2-hexenal were observed by PTR-MS.[212] Twenty-four hours after herbivore feeding, there was sustained methanol emission from the plants and the methanol level was substantially greater than that of (*E*)-2-hexenal.

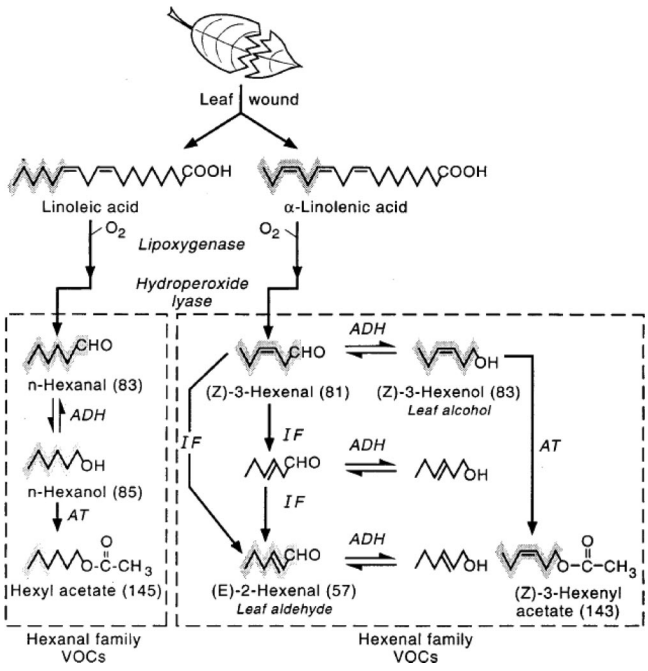

Figure 15. Scheme for the formation of hexanal and hexenal family VOCs in leaves following wounding. The origins of the six-carbon skeletons from unsaturated acids are indicated (hatched gray). For most of these C_6 VOCs, the unique or major positive ions seen in PTR-MS are shown in parentheses. Abbreviations are as follows: ADH = alcohol dehydrogenase; AT = acetyl transferase; and IF = isomerization factor. Reprinted with permission from ref 186. Copyright 1999 American Geophysical Union.

The authors demonstrate that the enzymatic demethylation of pectin is the likely source of the methanol.[212] An analogous plant-damage study has investigated the emissions from Mediteranean shrubbery produced by feeding horses and found significant enhancement of hexanals, acetic acid, and acetone from the plants following the feeding process.[213]

The quick response of PTR-MS has proved valuable in following rapidly changing VOC emissions following mechanical wounding. For example, Fall et al. were able to quantify the emission of (*Z*)-3-hexenal within 1−2 s of wounding of aspen leaves and then monitor its disappearance.[186] Similarly, the appearance of metabolites, including (*E*)-2-hexenal, hexenols, and hexenyl acetates, could also be profiled, as shown in Figure 16. The role of oxygen in the formation of the various products was also investigated, showing that there are no large pools of the hexenyl compounds in leaves.

The harvesting of various crops has been shown to lead to the emission of a range of OVOCs.[71,136,214,215] Karl et al. have shown, using PTR-MS and eddy covariance, significant fluxes of methanol, acetaldehyde, acetone, pentenols, 2-methylbutanal, hexenals, hexanal, and hexenols from hay harvesting.[71,214] As mentioned previously (section 5.1), similar fluxes have been observed from alfalfa harvesting.[136] Following the grass-harvesting process in more detail with PTR-MS has shown that, after the initial burst of VOCs following wounding, there are enhanced emissions of a wide range of compounds including methanol, acetone, acetaldehyde, butanone, and possibly formaldehyde during the drying period.[216]

The C_6 wound compounds, including (*Z*)-3-hexenal, (*E*)-2-hexenal, hexanal, hexenol, and hexanal, have been observed using PTR-MS immediately following lawn mowing.[217] Interestingly, peak levels of these biogenic VOCs were in the same concentration range (20−60 ppbV) as those originating from combustion engines of lawn mowers. Emissions of acetone and other VOCs resulted from rainfall on the lawn clippings. Atmospheric studies (see earlier) have revealed a range of biogenic OVOCs, such as hexanal, methylbutanals, pentenol, and pentenone, released in late autumn from apparent leaf wounding driven by the first hard frosts.[68,70]

Grasses, rice, and sorghum have been analyzed for release of VOCs in simulated leaf-drying/senescence experiments.[218] Upon drying under laboratory conditions, emission came primarily from leaves and not from stems. VOC release from paddy rice varieties was much greater than from sorghum, and major VOCs identified by combined GC-MS/PTR-MS included methanol, acetaldehyde, acetone, *n*-pentenal, methyl propanal, hexanol, hexanal, *(Z)*-3-hexenal, and (*E*)-2-hexenal. Online detection of VOCs using an ion trap PTR-MS gave results comparable to those obtained with standard PTR-MS, but use of an ion trap combined with collision-induced dissociation of trapped ions allowed unambiguous determination of the ratios of *cis*- and *trans*-hexenals during the different phases of drying.

VOCs produced within the octadecanoid (sum of (*E*)-2-hexanal, 1-hexanol, isomers hexanal and (*E*)-3-hexenol, and (*Z*)-3-hexenylacetate) pathway (see Figure 15) have been measured from tobacco plants subjected to exposure to ozone.[219] A delay in emission was directly related to ozone flux density into the plants. Approximately one C_6 product was emitted per five O_3 molecules taken up by the plant. The various methods of measuring and quantifying the impact of ozone on forests have been reviewed by Palitzsch et al.[220] In other studies, the emission of VOCs from a lumber kiln used for drying has been assessed using PTR-MS,[221] while Warnecke et al. have looked at the emissions from dead plant matter and have estimated that the decay of 1 g of dry matter could produce 0.1 mg of acetone and 3−5 mg of methanol.[222]

5.2.4. Soil Emissions

Asensio and co-workers have attempted to quantify the rate of exchange of VOCs between soil and the atmosphere and how they are influenced by soil moisture, temperature, and the presence of plant roots.[223] Focusing on a Mediterranean forest, the soils were found to be a sink rather than a source of VOCs in both soil moisture and temperature treatments. Most compounds observed by PTR-MS were oxygenated VOCs like alcohols, aldehydes, and ketones. Acetic acid and ethyl acetate were also observed. The approach has been extended to determine annual and seasonal fluxes of VOCs by means of manipulation experiments, where some plots were subjected to artificial drought.[224] High soil temperatures in summer increased VOC exchange rates, whereas the drought treatment tended to increase the emission rates of several VOCs. Provisional indications are that the effect of temperature on VOC emission rates is dependent on the compound type.

5.3. Food Science

One of the main applications of PTR-MS to date has been in the field of food science. The emission of organic gases from food, whether through decay or through digestion, is important in areas such as flavor perception and in food quality control. The potential utility of PTR-MS as a food

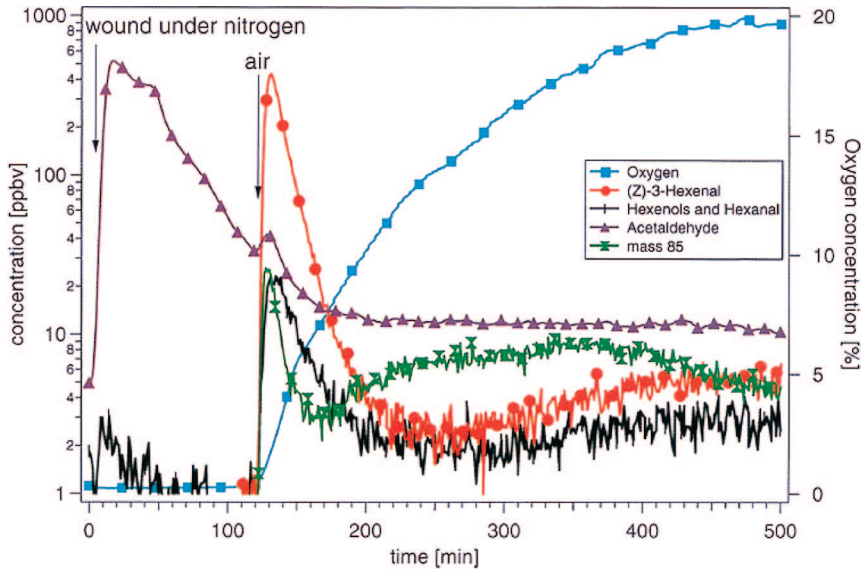

Figure 16. PTR-MS demonstration of the requirement for oxygen in the formation of hexanal and hexenal during leaf wounding. A single aspen leaf in a sealed bag was wounded at $t = 0$ in an atmosphere of nitrogen and once again at $t = 120$ min, at which point a flow of air was added. Reprinted with permission from ref 186. Copyright 1999 American Geophysical Union.

science tool was recognized almost at its inception by its pioneers, the team led by Werner Lindinger in Innsbruck. Jumping to the present date, there are now a number of research groups, including food science specialists, actively at work in this field. In this section, the exploitation of PTR-MS in food science is described. The bulk of the applications lie in flavor studies and in the assessment of food quality, but a small number of other applications in food science are also included for completeness.

5.3.1. Flavor Release and Perception

The importance of mass spectrometric techniques in flavor studies has long been recognized. When foods are consumed, flavor compounds are released from the food matrix and are transported to receptors in the mouth and nose. The release of VOCs into the nasal cavity, generating a characteristic aroma, plays a key role in the perception of flavor. The release of VOCs can be influenced by a wide variety of factors, such as saliva content, the mastication process, food fat content, and food texture. Consequently, a better understanding of the concept of flavor perception and how it is affected by the food matrix and the consumption process requires the investigation of VOC emission from foods.

The first PTR-MS study of VOC emission from foods dates back to the earliest days of PTR-MS work. This initial investigation focused on the digestion of raw garlic.[225] The breath of the individual who ate the garlic was monitored over a period of 30 h by periodic collection of breath samples in Tedlar bags, which were then subjected to PTR-MS analysis. Several organosulfur compounds derived from garlic consumption were detected in the breath samples, including allyl methyl sulfide, diallyl sulfide, and 2-propenthiol. Particularly interesting was an enhanced level of acetone (~5 ppmV) in the breath many hours after the garlic was ingested. This was tentatively linked to the enhanced metabolism of fatty components in the bloodstream following garlic consumption, showing that the identification of particular VOC components in human breath can point toward specific metabolic processes during food digestion.

In a similar vein, the same research group explored the emission of methanol in human breath following the consumption of fruit.[226,227] It was shown that, by eating several apples and oranges per day, the quantity of breath methanol approximately doubles when compared with that found under normal metabolic conditions. The production of excess methanol was attributed to the presence of pectin in the fruit, which is partly decomposed by bacteria in the colon and which is reabsorbed into the bloodstream. The methanol is then transported to the lungs and is released into the breath as a volatile waste product. The significance of this finding for human health is that the production of excessive quantities of methanol in the bloodstream could contribute toward nonalcoholic liver cirrhosis.

Coffee forms a particularly interesting target for PTR-MS investigation because of the variety and complexity of the aroma. The Lindinger group were the first to apply PTR-MS to coffee headspace analysis,[7] and subsequent work by the same group has explored this in much greater detail. The first detailed study of the headspace of coffee by PTR-MS was reported in 2003.[228] Figure 17 shows the mass spectrum derived from a particular coffee brew, illustrating the complex array of detectable VOCs in the coffee headspace. Analysis of PTR-MS spectra such as that shown in Figure 17 is a particularly challenging problem because of both the large number of volatile compounds and the potential for isobaric interferences. Some degree of ion fragmentation is also likely to contribute to the complexity of the mass spectrum. To tackle this problem, proton-transfer measurements using H_3O^+ alone were insufficient. Instead, additional information was generated by switching from H_3O^+ to NH_4^+ to change the proton affinity, by using collision-induced dissociation for energy-dependent ion fragmentation, as well as by using time-dependent measurement of air−liquid partitioning (linked to the determination of Henry's law constant, as discussed later in section 5.5; see also ref 229). With this comprehensive and painstaking approach, 64 distinct compounds could be identified in the headspace above a liquid Colombian coffee, which is an impressive achievement for PTR-MS. The ability to identify and monitor such a wide range of compounds at the 1 ppbV level and with a time resolution in the region of 1 s opens up real possibilities for new time-resolved studies.[230] One such

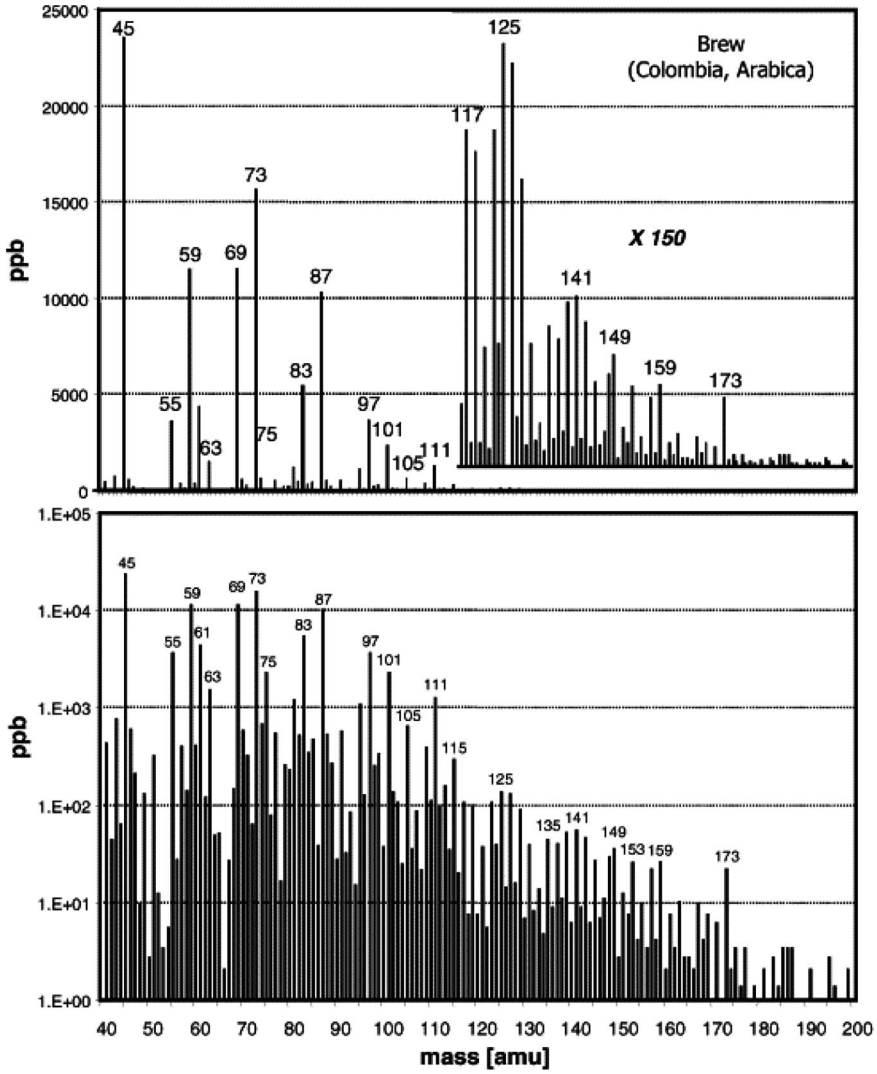

Figure 17. PTR-MS spectrum obtained from the headspace above a coffee brew maintained at 40 °C. The bottom is the same as the top spectrum except the vertical scale is logarithmic. Reprinted with permission from ref 228. Copyright 2003 Elsevier.

example is the real-time monitoring of the volatile emissions during coffee roasting, where the time profiles of specific compounds were monitored during the roasting phase at a variety of roasting temperatures.[231] More recently, the kinetics of VOC release from coffees has been subjected to a detailed investigation that combines PTR-MS analysis with sophisticated diffusion models to learn more about the mechanism of flavor release.[232]

An important facet in the study of aromas is to recognize how the release of VOCs during eating differs from the headspace emission of odor compounds from the uneaten foodstuff. The first group to explore this using PTR-MS was that of Mayr et al.[233] who compared the VOC composition in the nose during mastication of banana with that produced from a banana sample entrained in a flow of air. Nasal air was sampled during eating through a simple inlet line composed of two glass tubes fitted into the nostrils. Both ripe and unripe bananas were considered. Ripe bananas produce a much broader and more intense array of volatile esters than unripe bananas, as well as producing higher yields of compounds such as hexanal. Significant differences were found between the headspace and nosespace measurements for both ripe and unripe bananas, showing that mastication has an important impact on the aroma profile.

The important role of mastication has been further demonstrated in many additional PTR-MS studies. These can be broadly divided into work using human volunteers, as in the banana study above, and those that make use of an artificial (model) mouth. In model mouth studies, artificial saliva is normally employed and consists of water, several salts, mucin (a protein found in saliva), and α-amylase (a major digestive enzyme).[234] The model mouth may be as simple as a glass flask containing the above ingredients, and chewing can be simulated by a plunger whose compression rate can be externally controlled to simulate fast or slow chewing. The advantage of carrying out some investigations with a model mouth is that it provides a well-defined and more simplified environment than a real mouth, and therefore, controlled changes can easily be made to the "eating" conditions. An early combination of a model mouth study with PTR-MS analysis focused on the flavor compounds released from red bell peppers.[235] Introduction of artificial saliva into the model mouth was found to reduce the headspace concentrations of several volatile compounds, including 2-methylpropanal, 2/3-methylbutanal, and hexanal. Comparison of the model mouth findings with in-nose measurements from a human volunteer yielded good agreement between the two environments.

Subsequent work by van Ruth and co-workers has seen the model mouth applied to other flavor-related phenomena. One such study investigated the effect of both saliva addition and mastication rate on pectin-containing gels,[236] while in a subsequent study the influence of gel strength on aroma release was explored.[237] In the latter, an artificial flavor mixture composed of 11 different compounds, mainly alcohols, aldehydes, and ketones, was added to three different gels: gelatin, starch, and pectin. The flavor release was found to be correlated with the stiffness of the gel, where the stiffest gel, gelatin, gave the lowest emission rate as determined by PTR-MS. However, gel stiffness was not the only factor affecting flavor release, as shown by comparison of starch and pectin, which have similar rigidities but showed different compound-release profiles. This was shown to be linked to matrix−volatile interactions and, in particular, the hydrophobicities of the two gels. The importance of the mastication rate was also demonstrated in a model mouth study of flavor release from sunflower oil.[238] The release of artificial flavor compounds was followed in real time by PTR-MS, and an increase in mastication rate was found to bring about an increase in the proportion of the more hydrophilic compounds (such as 2-butanone) released into the air relative to more hydrophobic compounds (such as 2-heptanone).

Another area of food science where PTR-MS has the potential to make important contributions is in the study of flavor perception. This involves attempts to correlate aroma compounds emitted from foodstuffs with the flavor characteristics perceived by human beings. The concentrations of flavor compounds can be measured objectively by PTR-MS and other techniques, but the identification of flavor characteristics is far more subjective. Although untrained individuals can be used to describe flavors, it is more usual and more acceptable to employ a trained panel of sensory judges. Prior training is important to ensure that the judges work from the same set of flavor descriptors, e.g., sour, sweet, pungent, grassy, etc. In this way, the sensory evaluation from the panel of judges takes on a much greater statistical significance. To date, flavor perception studies utilizing PTR-MS have tended to focus on a few specific groups of foodstuffs, notably vegetables and dairy products.

Flavor perception work on vegetables using PTR-MS has included studies of red peppers,[239] red kidney beans, and soybeans.[240,241] Dairy products, such as cheese, whey, and custard, have been subjected to a far greater number of PTR-MS studies. The first cheese flavor study was carried out by Gasperi et al., in which seven different varieties of mozzarella were subjected to headspace measurements.[242] A principal-component analysis of the mass spectral data provided a degree of discrimination between the different cheese types that was comparable to the discrimination achieved by the sensory panel through identification of characteristic flavor attributes. A later study, focusing on the hard Italian cheeses Grand Padano, Parmigiano Reggiano, and Grana Trentino, reached a similar conclusion.[243] A more sophisticated statistical study of 20 different varieties of Grand Padano has also been carried out.[244] This combined a quantitative descriptive analysis of the flavor attributes by a panel of eight judges with partial least-squares analysis of the mass spectral data. Good correlation of several mass spectral features could be attributed to specific flavor attributes, although a complete identification of all significant compounds was not achieved.

Flavor studies of wheys, yogurts, and custards by PTR-MS can be divided into several different categories. Some of the work has tried to link flavor compounds to specific sensory characteristics using simple headspace analysis, as with the cheese studies described above. The work of Gallardo-Escamilla et al. on liquid and fermented wheys falls into this category.[245,246] Other workers have addressed the issue of sample rigidity, in a similar manner to the case of gels mentioned earlier, but with the additional link being made to flavor emphasis through input from a sensory evaluation panel. Some of this work has included in vivo PTR-MS measurements via nosespace extraction, such as the studies on wheys by Mestres et al.[247,248] and on custards by Aprea et al. and van Ruth et al.[249,250] Nosespace measurements have also played an important part in the study of yogurt composition on aroma release[251] and the elucidation of fat content on the release of aroma compounds from different types of milks.[252]

In other flavor-related studies, PTR-MS has been used to characterize the VOCs emitted from powdered infant foods,[253] in a sensory study of flavored gelatin and pectin gels,[254] to assess the impact of hydrocolloids on the aroma of fermented whey,[255] and to compare the relative effects of water-in-oil emulsions versus microemulsions on the release of volatile aroma compounds.[256] It has also been used to draw a link between sensory data and genetic factors.[257] This last study investigated the emission of various esters from strawberries, with esters being the group of compounds largely responsible for their sweet smell. These esters are produced by esterification of alcohols by the enzyme alcohol acyl transferase (AAT). By detecting the esters in the headspace above strawberries by PTR-MS, a correlation was found between the expression of an AAT gene, total AAT activity, and the presence of esters.

One of the challenges for PTR-MS in flavor analysis is to be able to successfully identify the full range of active compounds. Not only is there the possibility of isobaric interferences, but fragmentation can complicate the analysis when a series of similar compounds are explored. This is a significant issue in flavor studies, where a variety of compound types, such as aldehydes, ketones, alcohols, and esters, might contribute to the flavor profile. Comparisons with the extensive work on the reactions between H_3O^+ and various classes of organic compounds from SIFT-MS is a useful guide but is not definitive because of the higher collision energies encountered in PTR-MS. To reconcile this matter, Buhr and co-workers have carried out a study of the fragmentation behavior of a range of alcohols, aldehydes, ketones, and esters under typical drift tube operating conditions.[258] The dependence of the fragmentation patterns on the functional group holds out some promise for distinguishing isobaric compounds with different functional groups, with Buhr et al.[258] emphasizing the ability to distinguish some alcohols from isobaric esters. However, unless one is dealing with a particularly simple flavor mixture, the likelihood of successfully using fragmentation patterns to distinguish isobaric species is small. Aprea et al. have carried out a more detailed study of the fragmentation behavior of esters, which includes ion product ratios as a function of E/N.[259]

5.3.2. Food Quality

The assessment of food quality was another application of PTR-MS recognized early on by the founders of the technique. The initial suggestion was that PTR-MS may have value in providing an automated means of assessing the spoilage of meat products. Everyone is familiar with the increas-

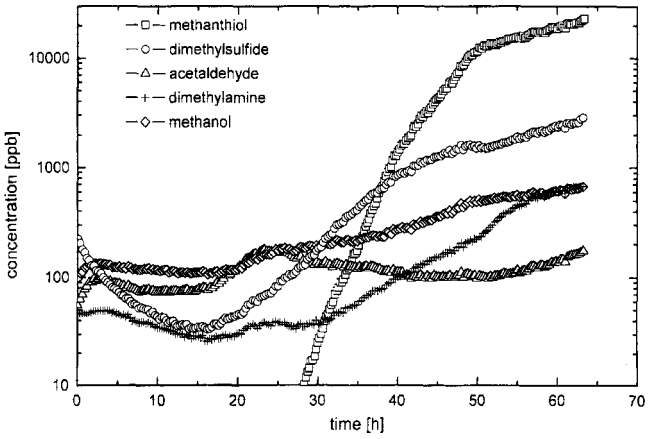

Figure 18. Concentration versus time profiles for several organic compounds emitted from beef kept at room temperature. Reprinted with permission from ref 7. Copyright 1998 Elsevier.

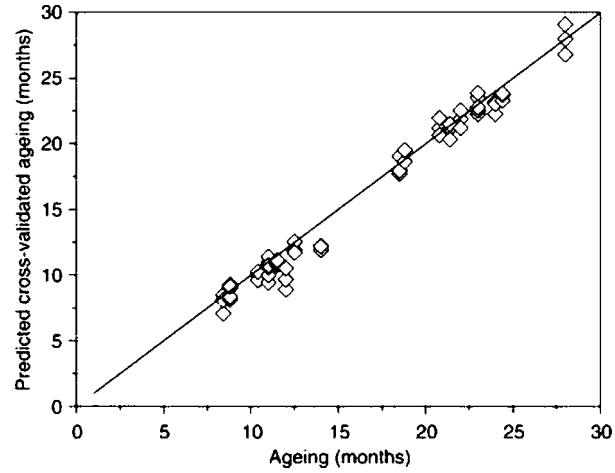

Figure 19. Predicted cross-validated estimation of cheese ages derived from PTR-MS emission data versus actual ages. Reprinted with permission from ref 265. Copyright 2007 Elsevier.

ingly unpleasant odor from meat as it undergoes decay. This change in odor is likely to be reflected by a change in VOC emissions from the meat, and therefore, PTR-MS is potentially well-suited to assessing the extent of decay by detecting the relevant VOCs. The normal means of assessing the quality of meat is through bacteriological tests, but these can take several days to complete. On the other hand, if VOC emissions can be used for the same purpose, then a rapid and noninvasive test becomes available.

The early work by the Lindinger group identified a number of potential markers for meat spoilage.[7,8] Particularly significant was the production of organosulfur compounds as the meat decays. This is illustrated in Figure 18, which shows time profiles for some selected compounds emitted from beef kept at room temperature. The sudden production of methanethiol after little more than 1 day is especially noticeable, and a sharp rise in its concentration ensues thereafter. The preliminary conclusion from this early work was that the meat is still safe to consume providing the methanethiol concentration remains below that of dimethyl sulfide.

More recent work on meat spoilage using PTR-MS has looked in more detail at the decay process. Mayr et al. have investigated the effect of packaging, both air and vacuum packaging, on the decay of beef and pork.[260,261] The VOCs acting as decay markers were found to differ depending on the packaging conditions. For air-packaged beef and pork, a peak at *m*/*z* 63, which was assigned to protonated dimethyl sulfide, was found to be the most clear-cut marker of decay. On the other hand, ethanol was the most significant marker for vacuum-packed meats. This difference between air and vacuum packaging reflects the different bacterial activities under aerobic and anaerobic conditions. Under aerobic conditions, the primary bacterial agent is thought to be *pseudomonas*, whereas under vacuum conditions, it is mostly lactic acid bacteria that are active. A plot of the marker VOC concentrations from PTR-MS versus bacterial counts (determined separately by standard bacterial counting methods) gave a linear relationship, suggesting that PTR-MS headspace measurements could provide a rapid and quantitative assessment of meat spoilage.

In a follow-up study to the meat spoilage work by Mayr et al., Jaksch et al. have investigated the effect of ozone treatment for reducing the bacterial content of meat.[262] By monitoring dimethyl sulfide (DMS), ozone-treated meat samples were found to yield greatly reduced DMS emissions when compared with untreated samples. However, these findings were confusing because separate microbial counting measurements showed no reduction in bacterial numbers. This discrepancy was attributed to physiological disruption of the bacterial activity by the ozone, resulting in reduced DMS emission, but the effect was not large enough to cause cell death. This strongly suggests that ozone treatment at the dose levels employed by Jaksch et al. would be insufficient to meet safety requirements, and therefore, some caution is warranted in using VOC emissions in assessing bacterial levels in meat products.

PTR-MS also has potential for assessing aging and spoilage effects in other food products. For example, Aprea et al. have explored the oxidative degradation of virgin olive oils in order to try to obtain an automated means of distinguishing between healthy and defective oils.[263] To assist in this assessment, a panel of sensory judges was employed to provide descriptors of the oil flavors. Oxidation over time and/or through thermal treatment led to an increase in volatiles, such as hexanal, which in turn were found to confer a rancid flavor. By multivariate analysis of the mass spectral data, complete discrimination between normal and rancid olive oils proved possible. Another aspect of thermal treatment is the possible production of furan and methylfuran, which are potential carcinogens. Although furan can be identified in many foods at very low levels, there has been some concern by the U.S. Food and Drug Administration about increased levels in thermally processed foods, such as certain canned and jarred products. Märk et al. have carried out an investigation of simplified chemical systems that might model the production of furan in real foods.[264] Both ascorbic acid and linolenic acid were subjected to heat treatment, and PTR-MS measurements showed the presence of significant quantities of both furan and methylfuran in the headspace of these compounds under dry roasting conditions.

Aside from determining harmful or unpleasant effects of foods, PTR-MS headspace measurements can also be used to assess food ripening. A demonstration of this was provided by Aprea et al., who focused on a number of varieties of Trentingrana cheese.[265] Ripening was shown to correlate strongly with the production of various esters, and through a combination of the PTR-MS data with a partial least-squares analysis, a systematic means of distinguishing ripe from young cheeses was found. This excellent correlation is shown in Figure 19.

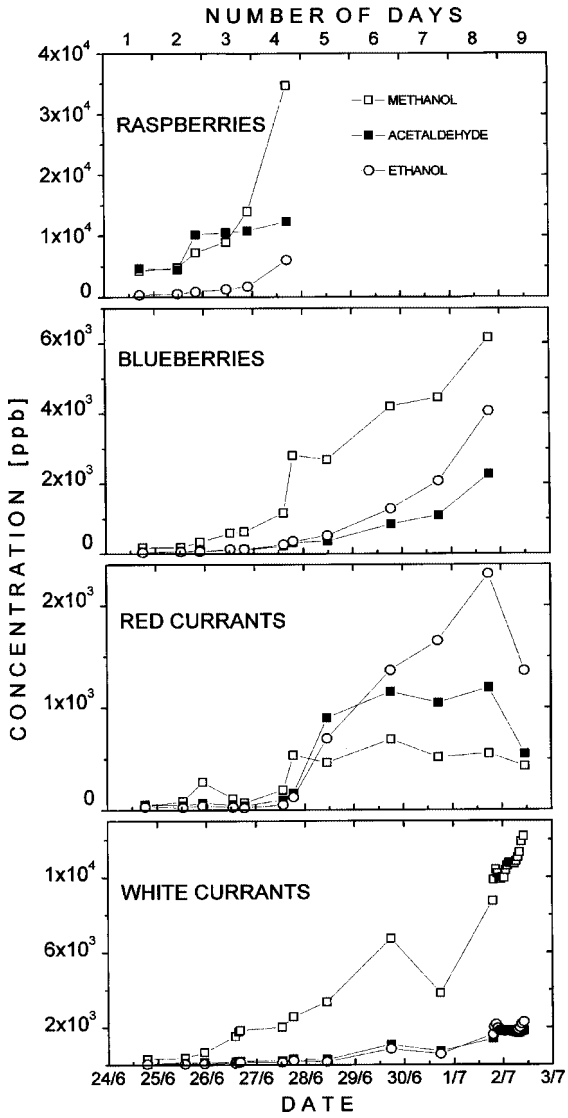

Figure 20. Evolution of methanol, acetaldehyde, and ethanol emissions during aging for four different berries measured from their headspace with the PTR-MS technique. Reprinted with permission from ref 266. Copyright 1999 Elsevier.

The ripening of fruits has also been investigated by PTR-MS.[266] Postharvest VOC emissions from strawberries, blackberries, raspberries, blueberries, white currants, and red currants were measured as a function of time (see Figure 20). The time-dependence of the VOCs was found to vary from one berry type to another, but some common features were observed. In particular, all berries showed a gradually increasing emission of methanol with age, which could potentially be used to assess how ripe, or indeed how overripe, is a particular fruit sample.

In addition to providing markers of food decay and food ripening, the volatile composition above foods is a potential signature of specific varieties of certain food types. This aspect of PTR-MS is only beginning to be explored and has, therefore, seen just a few initial investigations. For example, it has been shown that PTR-MS headspace measurements can distinguish between different types of orange juice, namely, untreated, flash-pasteurized, juice-pasteurized, and high-pressure treated juices.[267] Similarly, PTR-MS has been shown to provide an automated and objective assessment of the quality of herb extracts.[262] The emissions from truffles are responsible for their rich aroma but also offer potential for quality control. Aprea et al. have combined PTR-MS headspace analysis with a corresponding GC-MS study to identify the compounds emitted from white truffles.[268] In line with earlier GC-MS studies, a number of sulfur-containing compounds, including dimethyl sulfide, dimethyl disulfide, and bis(methylthio)methane, were found to be important constituents of the vapor. The comparison between GC-MS and PTR-MS showed that the latter technique was capable of identifying all of the major compounds reliably through characteristic mass peaks and is clearly better suited to dynamic VOC measurements than GC-MS.

The combination of PTR-MS with multivariate statistical analysis has recently been shown to have potential for distinguishing different types of strawberries.[269,270] The mass spectral fingerprints from strawberries harvested from three different years and from different locations were found to be sufficient to distinguish the different cultivars. This fast and nondestructive means of identification may have important applications in quality control and may also assist breeders in making informed fruit selections for selective breeding programs.

Wine discrimination presents another important potential application of PTR-MS, especially given the huge commercial market in wines and the potential for fake products at the fine wine end of the market. However, standard PTR-MS poses problems in this application, since the high ethanol content in the vapor can seriously deplete the amount of H_3O^+ in the drift tube, making it difficult to see other vapor constituents. A solution to this has been found by Boscaini et al.,[271] who added a stream of ethanol in nitrogen carrier gas into the analyte line in order to fully convert the H_3O^+ into protonated ethanol and protonated ethanol cluster ions in the upstream part of the drift tube, i.e.,

$$H_3O^+ + C_2H_5OH \rightarrow C_2H_5OH_2^+ + H_2O \qquad \text{(R8)}$$

$$C_2H_5OH_2^+ + C_2H_5OH + M \rightarrow C_2H_5OH_2^+(C_2H_5OH) + M \qquad \text{(R9)}$$

The two main product ions of this conversion, $C_2H_5OH_2^+$ and $C_2H_5OH_2^+(C_2H_5OH)$, now act as the proton donors and are unaffected by fluctuations in the ethanol content of the wine because of the large excess of ethanol carried in the nitrogen stream. A preliminary test using two different red wines and two different white wines was carried out in the study by Boscaini et al. No attempt was made to assign the many mass peaks observed in the PTR-MS spectra, but these unassigned peaks were used in a principal-component analysis to show that the spectra were sufficient to provide a clear discrimination between the four types of wine.

Disadvantages of using protonated ethanol for wine characterization include a lower reactivity with VOCs (when compared to H_3O^+) and a tendency for ligand-switching reactions, with the latter leading to mixed protonated VOC−ethanol clusters. Furthermore, since ethanol has a significantly higher proton affinity than H_2O (see Table 1), its protonated form will be able to transfer its proton to a smaller subset of compounds than H_3O^+.

The same research team has recently proposed an alternative approach in which the headspace of a wine is heavily diluted (by a factor of ~40 times) in nitrogen so that H_3O^+ can be used in place of protonated ethanol for the proton-transfer reactions.[272] The high degree of dilution is necessary to minimize effects from reactions of protonated ethanol, as well as to minimize the impact of variable alcohol contents

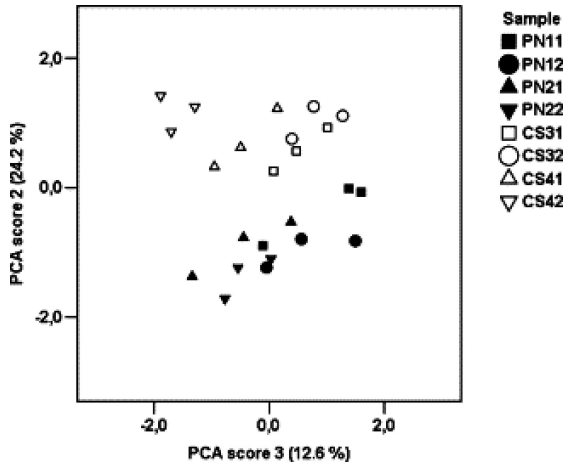

Figure 21. Principal component analysis of PTR-MS data from headspace measurements above a selection of pinot noir (PN) and cabernet sauvignon (CS) wines. The second and third principal components provide a clear distinction between wines from the two grape varieties. Reprinted with permission from ref 272. Copyright 2007 Elsevier.

in different wines. This procedure was tested on eight different wine samples based on two grape varieties, pinot noir and cabernet sauvignon. Using a simple principal-component analysis, the mass spectral features were found to be sufficient to distinguish between wines from the two grape varieties, as illustrated in Figure 21. Although more extensive testing is required, most likely in combination with a more sophisticated statistical analysis, it seems that PTR-MS headspace measurements hold promise as a rapid means of wine identification and/or quality control.

5.3.3. Other Applications of PTR-MS in Food Science

Other areas of food science where PTR-MS has been employed include the study of fermentation processes in apples.[273] The antioxidative effects of red grape seeds and red grape peel on lipid oxidation in sunflower oils have also been investigated by PTR-MS through measurement of volatile oxidation products, such as propanol and hexanal.[274] Zini and co-workers have used the VOCs emitted from ripe apples to draw a link to their genetic constitution.[275] Analysis using quantitative trait loci was able to link specific peaks in the mass spectrum to particular regions of the genome.

High-temperature processing of carbohydrate-rich foods, such as French fries, potato chips, and crispbread, can lead to the formation of acrylamide. Acrylamide is a potentially carcinogenic compound that can be formed through a Maillard-type reaction between an amino acid and a reducing sugar. To investigate the possible formation of acrylamide, Pollien et al. employed PTR-MS to detect the release of acrylamide vapor from a Maillard model system consisting of asparagine and either glucose or fructose.[276] The formation of acrylamide was found to increase with temperature and favored fructose over glucose. In a follow-up study, the kinetics of acrylamide formation was followed in model Maillard systems, and it was shown that the choice of ingredients, their physical state, the reaction temperature, and the reaction time all affect the formation of acrylamide during the cooking process.[277]

5.4. Medical Applications

PTR-MS has been tested for a number of potential medical applications, including breath analysis,[278−281] urine analysis,[282] in vivo human skin studies,[283] and occupational health exposure in medical environments.[279,284−286] Many of these applications are considered in more detail below.

5.4.1. Breath Composition

Breath is a mixture of nitrogen, oxygen, carbon dioxide, water vapor, inert gases, and a small fraction of VOCs in the ppmV to pptV range. VOCs can be produced anywhere in the body and are transported via the bloodstream to the lungs, where they are exhaled in breath. On the basis that VOCs in breath are representative of VOCs in the blood and, therefore, processes occurring in the body, analysis of exhaled breath may become a noninvasive diagnostic for use in clinical practice (see next section).[287−289]

It was Linus Pauling and co-workers who made the first detailed analysis of VOCs in human breath.[290] Breath constituents were first trapped at low temperature and then released through heating for analysis by GC-MS. This investigation revealed about 250 different VOCs in an average breath sample. It has since been shown that breath VOC composition may vary widely from person to person, in both the type of VOCs present and in the concentration of a specific VOC.[291]

Early experiments by Lindinger et al. demonstrated the use of PTR-MS in monitoring breath VOCs down to the pptV level.[7,8,17] This work provided the foundation for subsequent application of PTR-MS to studies of human breath.

Warneke et al. have measured the concentration of propanol on the breath of 46 healthy volunteers, finding an average concentration of 150 ppbV.[292] Moser et al. have investigated breath samples from 344 people to ascertain typical concentrations for many trace compounds in breath.[293] Interestingly, it was found that there were no significant correlations of age, blood pressure, or body mass index with any mass peak seen in the PTR-MS spectra. In contrast, Lechner et al. measured the volatiles on the breath of 126 volunteers, finding that isoprene was elevated in the exhaled air of male subjects.[294] Furthermore, subjects in the 19−29 years old age group exhaled significantly lower levels of isoprene than older adults. The latter result is in agreement with earlier work with children.[295]

5.4.2. Breath Analysis for Medical Diagnosis

In one of the earliest studies of human breath by PTR-MS, the concentration and time-dependence of ethanol and methanol was measured on the breath of volunteers after either eating fruit or ingesting "hard liquor".[226] The authors of this work speculated that, in the long term, the measurement of methanol might be used to assess forms of hepatic disease. Since this and other early studies of human breath by PTR-MS, the prospects for using the composition of breath as an indicator of the disease state of an individual have been increasingly explored, and we summarize here the investigations carried out to date.

Breath isoprene has been shown to be related to blood cholesterol levels.[296] During lipid-lowering therapy, the breath isoprene reduced and was shown to correlate with cholesterol (32%) and LDL concentrations (35%) in blood over a period of 15 days.[297] However, exercise raises isoprene

levels significantly, highlighting one of the difficulties of reliable patient sampling.[296] Breath isoprene has been found to be enhanced in end-stage renal disease patients following dialysis.[298]

Patients with lung cancer and hemato-oncologic disorders have been reported to show distinct patterns of exhaled VOCs. On the basis of PTR-MS breath measurements, Rieder et al. suggested that a peak at $m/z = 108$, which was attributed to *ortho*-toluidine, is a possible marker for cancer.[297] However, subsequent clinical studies by Amann and co-workers suggested that m/z 108 is not a reliable biomarker for lung carcinoma.[280] Recently, Wehinger et al. measured exhaled breath samples of primary lung cancer patients and analyzed them against a number of healthy controls.[299] It was found that the product ions at $m/z = 31$ and 43 (tentatively attributed to protonated formaldehyde and a fragment of protonated isopropanol, respectively) were found at significantly higher concentrations in the breath gas of the primary lung cancer patients when compared to the healthy controls. This suggests that there may be some scope for diagnosing lung cancer by PTR-MS breath analysis, although such suggestions are a long way from a practical means of diagnosis and require much further work.

Carbohydrate malabsorption is a condition in which patients are unable to absorb or digest certain carbohydrates owing to the lack of one or more intestinal enzymes or transport systems. As the carbohydrates remain in the intestinal lumen, this leads to fluid retention, causing diarrhea and abdominal distention. Bacterial sugar fermentation in the gut leads to gaseous and acidic stools. Routine diagnosis is carried out by measuring the hydrogen content in the breath after oral administration of the sugar that is suspected not to be absorbed. However, breath analysis by PTR-MS following administration of a sugar showed elevation of ethanethiol/dimethylsulfide (protonated signal at $m/z = 63$), which may provide an alternative marker of carbohydrate malabsorption.[280]

Helicobacter pylori infection is one of the most common chronic bacterial infections worldwide, causing chronic gastritis and increasing the risk of peptic ulcer disease and gastric cancer. Breath analysis of patients with confirmed *H. pylori* infection shows levels of exhaled nitric acid and hydrogen cyanide that are significantly elevated relative to uninfected people.[280] The authors noted that further studies are necessary to find out whether the differences in the detected mass spectrum are specific enough to differentiate patients with *H. pylori* gastritis from healthy controls. VOCs emitted from *H. pylori* bacterial cultures have also been measured and, while HCN was detectable, HNO_3 was not.[300,301] It has, therefore, been suggested that nitric acid is a byproduct of chronic inflammation.[301]

5.4.3. Other Breath-Based Studies

Most PTR-MS studies of breath have involved direct (online) sampling, but there has also been work using off-line sampling with Tedlar bags.[295,302] To test the integrity of Tedlar bags, PTR-MS has been used to monitor the changes in composition with time of various mixtures of methanol, acetaldehyde, acetone, isoprene, benzene, toluene, and styrene.[302] It was found that characteristic ions at m/z 88 and 95 arise from the bag material. The pollutant at m/z 88 was ascribed to *N*,*N*-dimethylacetamide, a solvent used in the production of Tedlar film. Gas composition losses during filling were found to range from 5 to 47%, depending on the compound. Once stored, the half-lives of methanol, acetaldehyde, acetone, isoprene, benzene, toluene, and styrene were estimated between 5 and 13 days. Losses from breath samples (52 h after filling) were found to be <10%.[302]

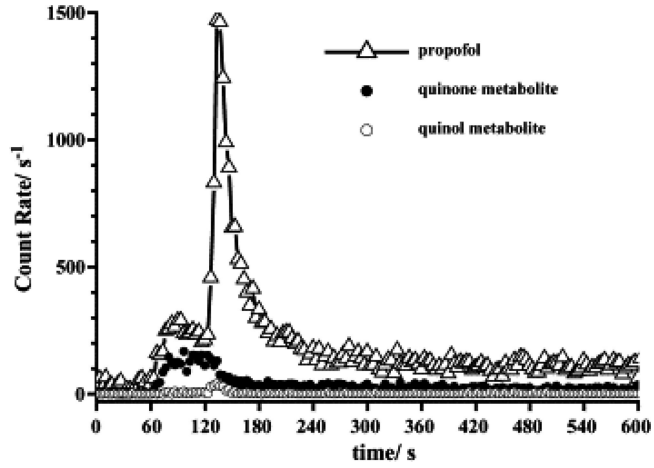

Figure 22. Real-time PTR-MS measurements of propofol and metabolite trace gas measurements for the first 10 min of breath sampling from a patient undergoing surgery. Reprinted with permission from ref 303. Copyright 2004 Elsevier.

PTR-MS has been used for real-time breath monitoring of the intravenous anesthetic agent propofol and its volatile metabolites on patients undergoing surgery.[303,304] As shown in Figure 22, propofol and its two metabolites were easily detected in the breath of the patient.

In a related area, PTR-MS has been used to investigate occupational health exposure in medical environments.[279,284−286] In particular, exposure to sevoflurane, a commonly used halogenated anesthetic, was explored in a surgical postanesthetic care unit,[284] in an operating theater,[286] and in the breath of operating room personnel.[285] The authors suggest that PTR-MS could be used as an intelligent sensor to control the ventilation system and thereby reduce exposure of personnel to lower levels of this anesthetic.[284] An overview of the occupational exposure to volatile agents in medical environments has been given by Lirk et al.[279]

Off-line breath analysis has been performed on patients suffering from propionic acidaemia.[305] The data showed enhancement of peaks at m/z 73 and 115. The peak at 115 was confirmed by GC-MS to be due to 3-heptanone, a product of valeryl-CoA biosynthesis.

In some of the earliest PTR-MS studies of breath, it was shown that benzene and acetonitrile are present in greater concentrations in the breath of smokers than in nonsmokers.[7,17,306] After smoking, the concentration of benzene in the breath of smokers rapidly decreases, declining to values similar to those of nonsmokers within 1 h. In contrast, the concentration of acetonitrile in the breath of smokers takes nearly one week to decrease to that of nonsmokers after smoking has ceased. Lirk et al. have expanded this early work to look at the certainty to which a smoker can be detected using acetonitrile on the breath as a marker.[307] The same marker measured by PTR-MS has been used to assess the impact of passive smoking, finding that staying for a working day (8 h) in a smoke-laden environment is equivalent to smoking 1−2 cigarettes.[308] SIFT-MS work has shown that the acetonitrile from smoking is equilibrated among the bodily fluids (blood, total body water, and urine) and that excretion occurs via both exhaled breath and urine.[309]

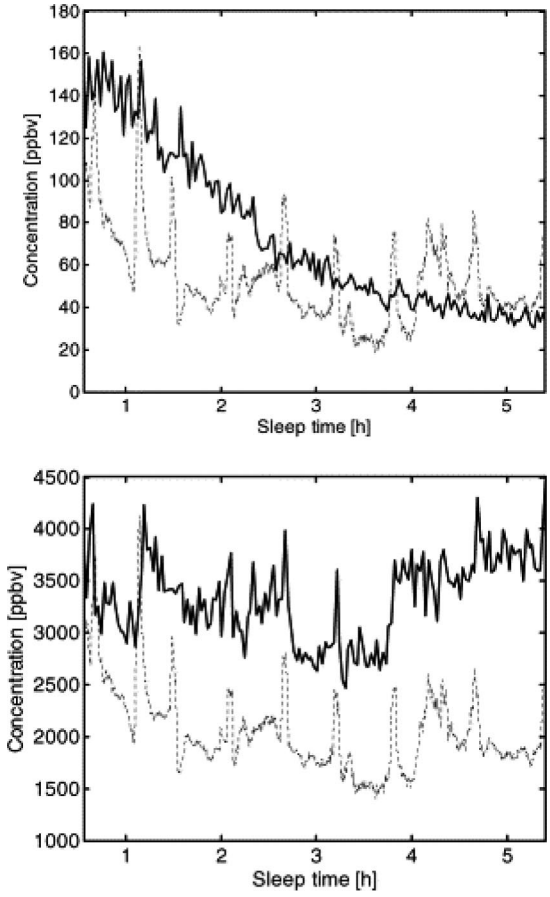

Figure 23. PTR-MS measurements of exhaled air composition from a person during sleep. The upper panel shows the concentration of acetaldehyde (solid line) and heart rate (dashed line) as a function of time. The lower panel shows comparable data for acetone. Reprinted with permission from ref 280. Copyright 2004 Elsevier.

The VOCs in the breath of people sleeping has been studied by PTR-MS.[280,295,310] The various stages of the sleep cycle are represented by the time profiles of the detected VOCs, as shown in Figure 23. For example, acetaldehyde is an oxidation product of ethanol, and its concentration decreases during sleep, while acetone, a degradation product of acetyl-CoA when fat breakdown predominates, exhibits a more complicated pattern with a minimum during the middle of the sleep period. The increase in acetone levels during the second half of the sleep period may indicate increasing hunger.[280]

5.4.4. Other Medical Applications

PTR-MS has seen a number of other medical applications that do not involve breath measurements. For example, it has been used to assess the concentration of acetonitrile in the urine of habitual cigarette smokers and in nonsmokers as a quantitative marker of recent smoking behavior.[282] The results showed a significant enhancement of acetonitrile concentration in the urine of the heavy smokers.

PTR-MS has been applied to both headspace screening of fluid obtained from the gut during colonoscopy and in breath analysis with a view to diagnosing gastrointestinal diseases.[311] Patients with inflammatory bowel disease showed enhanced peaks at *m*/*z* 57 and 83 in the fluid samples and *m*/*z* 31 and 77 from the breath for those with inflammatory bowel syndrome over the control group, making these possible indicators of gastrointestinal disease.

PTR-MS has also been used to study in vivo lipid peroxidation in human skin by the action of ultraviolet light. The VOCs emitted from the skin of 16 healthy volunteers was monitored before, during, and after UV irradiation. Five VOCs were found to reflect the damage caused by UV-radiation. The two major compounds were identified as acetaldehyde and propanal using a combination of Tenax-based gas chromatographic preseparation with PTR-MS, while other volatiles (with characteristic ions at, among others, *m*/*z* 73 and 87) could not be identified.[283]

Critchley et al. have shown that it is possible to use PTR-MS headspace measurements to discriminate between pure blood agar cultures of *Pseudomonas aeruginosa* and *Streptococcus milleri* via PTR-MS.[303] More recently, Lechner et al. have measured the head space emissions of *Escherichia coli*, *Klebsiella*, *Citrobacter*, *Pseudomonas aeruginosa*, *Staphylococcus aureus*, and *Helicobacter pylori*[300,301] and claim that the resultant spectra show significant differences.[300] If verified, this suggests a rapid means for identifying the bacterial content of biological cultures.

5.5. Other Applications

PTR-MS has seen applications in fields other than those described above. For example, a combination of in situ XPS with PTR-MS has been used to investigate the epoxidation of ethylene on silver.[312] The data showed a correlation between the abundance of electrophilic oxygen and the yield of ethylene oxide in the gas phase, indicating that this form of surface oxygen species was responsible for the oxidation of ethylene to ethylene oxide.

PTR-MS has been used to assess organic gas-phase pollutants and the performance of different forms of air purification systems used in simulated aircraft cabins.[313,314] The concentration of most organic pollutants present in aircraft cabin air was efficiently reduced by all forms of the air purifier units. However, it was shown that photocatalytic units incompletely oxidized ethanol released by the wet wipes commonly supplied with airline meals and could lead to unacceptably high levels of acetaldehyde and formaldehyde through subsequent chemistry.[313]

The forensic analysis of fire debris is crucial in establishing the cause of many fires. The standard procedure involves off-line sampling in which traces of vapors of any added accelerants are collected on activated charcoal strips for subsequent laboratory analysis (typically by GC-MS). Whyte et al. have shown that PTR-MS has potential as a rapid on-scene technique for detecting the presence of fire accelerants.[315] A variety of common building and household materials were exposed to four common arson accelerants, namely, diesel, paraffin, petrol, and white spirit. These were then set on fire, and after the fire was extinguished, PTR-MS headspace analysis was applied. Even after extensive periods of storage for the burnt material, it proved possible to identify the accelerant through the characteristic mass spectra in combination with a principal-component analysis.

Malodorous emissions and potentially pathogenic microorganisms that develop during domestic organic waste collection are not only a nuisance but may also pose health risks.[316] PTR-MS has been used to assess the relationship between specific microorganisms and the emission of VOCs in domestic organic waste.[317] Over a 16 day period, 60 different bacterial species and 20 fungal species were

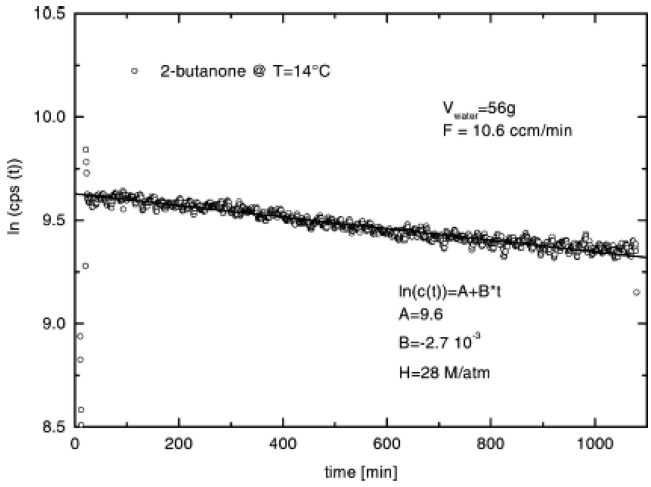

Figure 24. Illustration of data for the determination of the Henry's law coefficient for 2-butanone using PTR-MS measurements coupled to dynamic stripping coils. The notation cps refers to counts per seconds, which are normalized such that the value corresponds to the actual ln(concentration) in the gas flow. Reprinted with permission from ref 318. Copyright 2003 Elsevier.

identified. The main VOCs tentatively identified by PTR-MS were butyric acid, dimethylsulfide, isoprene, and butanone.

PTR-MS has been coupled to dynamic stripping cells in order to experimentally determine Henry's law coefficients (HLCs) for a range of VOCs in aqueous solution.[318] The technique works by bubbling clean air into the bottom of the cells, which then travels upward through the liquid at a rate determined by the flow rate of the incoming gas. The dissolved substance establishes an equilibrium concentration in the gas bubbles and when the top of the liquid layer is reached it is driven out of the system and onward to a PTR-MS instrument for detection. By this means, the amount of substance dissolved in the liquid is gradually reduced, and this is reflected in the partial pressure of that substance in the liquid, which in turn is linked to Henry's law. A comparison with other techniques for determining HLCs showed the PTR-MS approach to be simple, fast, and less prone to artifacts. Figure 24 shows a typical plot of concentration of gas versus time used to determine the HLC.

The identification and quantification of the chemical warfare agents mustard gas and sarin has been shown to be possible by PTR-MS.[319] This preliminary study has shown that PTR-MS is highly sensitive to these species and may have potential for detecting a wider range of chemical warfare agents.

6. Conclusions and Outlook

PTR-MS is emerging as a powerful tool in the armory of trace gas analysis techniques. Its fast response, high detection sensitivity, strength in quantitative determination, and focus particularly on trace organic gases is finding many niche applications. Already in its relatively short lifetime it has demonstrated great versatility, with trial studies and applications found in fields as diverse as atmospheric chemistry, food science, botany, medicine, and process monitoring. Such a diverse range of applications so soon after the inception of the technique owes much to the provision of a commercial supplier of PTR-MS instruments, Ionicon Analytik, early on in the development cycle. Without this parallel commercial development, PTR-MS might still be a rather specialized technique restricted to relatively few laboratories.

So what are the prospects for PTR-MS in the future? There is little doubt that increasing awareness of the capabilities of the technique will lead to a further expansion in the number of users and in the diversity of areas in scientific research and in commerce to which it is applied. Alongside this widening of participation, new instrumental developments in the coming years are likely to provide enhanced capabilities. The type of mass analyzer is one area that has seen considerable recent activity. Although still dominated by quadrupole filters, PTR-MS systems are now available in several laboratories that contain time-of-flight or ion trap analyzers. These alternatives to quadrupoles offer important advantages but do not yet deliver comparable detection sensitivities for individual compounds, although the gap is steadily being narrowed. New approaches, such as high-duty-cycle time-of-flight analyzers based on rapidly modulated ion beams, are also likely. The combination of new instrumentation and a wider user community means that these are exciting times for PTR-MS and much promising research lies ahead.

7. Acknowledgments

The authors would like to acknowledge here the contributions of a number of members of our research group to our work in PTR-MS, including Kevin Wyche, Chris Whyte, Rebecca Cordell, Kerry Willis, Milan Patel, and Timo Carr. Ann Crane is thanked for assistance with the production of some of the figures. The authors are also grateful for helpful comments from the referees during the production of this review.

8. References

(1) Hewitt, C. N. *Reactive Hydrocarbons in the Atmosphere*; Academic Press: San Diego, CA, 1999.
(2) Hester, R. *Volatile Organic Compounds in the Atmosphere*; Royal Society of Chemistry: London, 1995.
(3) *Chemical Ionization Mass Spectrometry*; Harrison, A., Ed.; CRC Press: Boca Raton, FL, 1992.
(4) Huey, L. G. *Mass Spectrom. Rev.* **2007**, *26*, 166.
(5) Viggiano, A. A. *Mass Spectrom. Rev.* **1993**, *12*, 115.
(6) Hansel, A.; Jordan, A.; Warneke, C.; Holzinger, R.; Wisthaler, A.; Lindinger, W. *Plasma Sources Sci. Technol.* **1999**, *8*, 332.
(7) Lindinger, W.; Hansel, A.; Jordan, A. *Int. J. Mass Spectrom. Ion Process.* **1998**, *173*, 191.
(8) Lindinger, W.; Hansel, A.; Jordan, A. *Chem. Soc. Rev.* **1998**, *27*, 347.
(9) Hewitt, C. N.; Hayward, S.; Tani, A. *J. Environ. Monit.* **2003**, *5*, 1.
(10) de Gouw, J. A.; Warneke, C. *Mass Spectrom. Rev.* **2007**, *26*, 223.
(11) Fehsenfeld, F. C.; Ferguson, E. E.; Schmeltkopf, A. L. *J. Chem. Phys.* **1966**, *44*, 3022.
(12) Ferguson, E. E.; Fehsenfeld, F.; Schmeltkopf, A. L. *Adv. At. Mol. Phys.* **1969**, *5*, 1.
(13) Adams, N. G.; Smith, D. *Int. J. Mass Spectrom. Ion Phys.* **1976**, *21*, 349.
(14) Smith, D.; Španěl, P. *Mass Spectrom. Rev.* **2005**, *24*, 661.
(15) Španěl, P.; Pavlik, M.; Smith, D. *Int. J. Mass Spectrom. Ion Process.* **1995**, *145*, 177.
(16) Lagg, A.; Taucher, J.; Hansel, A.; Lindinger, W. *Int. J. Mass Spectrom. Ion Process.* **1994**, *134*, 55.
(17) Hansel, A.; Jordan, A.; Holzinger, R.; Prazeller, P.; Vogel, W.; Lindinger, W. *Int. J. Mass Spectrom. Ion Process.* **1995**, *149/150*, 609.
(18) Hunter, E.; Lias, S. *J. Phys. Chem. Ref. Data* **1998**, *27*, 413.
(19) Španěl, P.; Smith, D. *Int. J. Mass Spectrom. Ion Process.* **1997**, *167/168*, 375.
(20) Španěl, P.; Ji, Y.; Smith, D. *Int. J. Mass Spectrom. Ion Process.* **1997**, *165/166*, 25.
(21) Španěl, P.; Smith, D. *Int. J. Mass Spectrom. Ion Process.* **1998**, *172*, 137.
(22) Arnold, S. T.; Viggiano, A. A.; Morris, R. A. *J. Phys. Chem. A* **1998**, *102*, 8881.
(23) Španěl, P.; Smith, D. *Int. J. Mass Spectrom.* **1998**, *181*, 1.

(24) Bohme, D. K. In *Interactions between Ions and Molecules*; Ausloos, P., Ed.; Plenum Press: New York, 1975.
(25) Ikezoe, Y.; Matsoka, S.; Takebe, M.; Viggiano, A. *Gas Phase Reaction Rate Constants Through 1986*; Maurzen Company Ltd.: Tokyo, 1987.
(26) Arnold, S. T.; Thomas, J. M.; Viggiano, A. *Int. J. Mass Spectrom.* **1998**, *179/180*, 243.
(27) Midey, A. J.; Arnold, S. T.; Viggiano, A. A. *J. Phys. Chem.* **2000**, *104*, 2706.
(28) Midey, A. J.; Williams, S.; Arnold, S. T.; Viggiano, A. A. *J. Phys. Chem. A* **2002**, *106*, 11726.
(29) Schoon, N.; Amelynck, C.; Vereecken, L.; Coeckelberghs, E.; Arijs, E. *Int. J. Mass Spectrom.* **2004**, *239*, 7.
(30) Michel, E.; Schoon, N.; Amelynck, C.; Gumbaud, C.; Catoire, V.; Arijs, E. *Int. J. Mass Spectrom.* **2005**, *244*, 50.
(31) Amelynck, C.; Schoon, N.; Kuppens, T.; Bultinck, P.; Arijs, E. *Int. J. Mass Spectrom.* **2005**, *247*, 1.
(32) Anicich, V. G. JPL Publication 03-19.
(33) Langevin, M. *Ann. Chim. Phys.* **1905**, *5*, 245.
(34) Moran, T. F.; Hamill, W. H. *J. Chem. Phys.* **1963**, *39*, 1413.
(35) Su, T.; Bowers, M. T. *J. Chem. Phys.* **1973**, *58*, 3027.
(36) Su, T.; Bowers, M. T. *J. Am. Chem. Soc.* **1973**, *95*, 1370.
(37) Su, T.; Bowers, M. T. *Int. J. Mass Spectrom. Ion Phys.* **1973**, *12*, 347.
(38) Mackay, G. I.; Betowski, L. D.; Payzant, J. D.; Schiff, H. I.; Bohme, D. K. *J. Chem. Phys.* **1976**, *80*, 2919.
(39) Su, T.; Chesnavich, W. J. *J. Chem. Phys.* **1982**, *76*, 5183.
(40) Su, T. *J. Chem. Phys.* **1994**, *100*, 4703.
(41) Bhowmik, K.; Su, T. *J. Chem. Phys.* **1986**, *84*, 1432.
(42) Turulski, J.; Su, T.; Niedzielski, J.; Pezler, B. *Int. J. Mass Spectrom.* **2002**, *216*, 115.
(43) Zhao, J.; Zhang, R. *Atmos. Environ.* **2004**, *38*, 2177.
(44) McFarland, M.; Albritten, D. L.; Fehsenfeld, F. C.; Ferguson, E. E.; Schmeltekopf, A. L. *J. Chem. Phys.* **1973**, *59*, 6620.
(45) Wannier, G. H. *Phys. Rev.* **1951**, *83*, 281.
(46) Wannier, G. H. *Bell Syst. Tech. J.* **1953**, *32*, 170.
(47) Goebbert, D.; Wenthold, P. *Eur. J. Mass Spectrom.* **2004**, *10*, 837.
(48) Bohme, D. K.; Mackay, G. I.; Tanner, S. D. *J. Am. Chem. Soc.* **1979**, *101*, 3724.
(49) Midey, A. J.; Williams, S.; Arnold, S. T.; Viggiano, A. A. *J. Phys. Chem. A* **2002**, *106*, 11726.
(50) Munson, M.; Field, F. *J. Am. Chem. Soc.* **1966**, *88*, 2621.
(51) Blake, R. S.; Wyche, K. P.; Ellis, A. M.; Monks, P. S. *Int. J. Mass Spectrom.* **2006**, *254*, 85.
(52) Blake, R. S. Ph.D. Thesis, University of Leicester, Leicester, U.K., 2005.
(53) Dupeyrat, G.; Rowe, B. R.; Fahey, D. W.; Albritton, D. L. *Int. J. Mass Spectrom. Ion Phys.* **1982**, *44*, 1.
(54) de Gouw, J. A.; Goldan, P. D.; Warneke, C.; Kuster, W. C.; Roberts, J. M.; Marchewka, M.; Bertman, S. B.; Pszenny, A. A. P.; Keene, W. C. *J. Geophys. Res.* **2003**, *108*, D4682.
(55) Inomata, S.; Tanimoto, H.; Aoki, N.; Hirokawa, J.; Sadanaga, Y. *Rapid Commun. Mass Spectrom.* **2006**, *20*, 1025.
(56) Hanson, D. R.; Greenberg, J.; Henry, B. E.; Kosciuch, E. *Int. J. Mass Spectrom.* **2003**, *223*, 507.
(57) Wyche, K. P.; Blake, R. S.; Willis, K. A.; Monks, P. S.; Ellis, A. M. *Rapid Commun. Mass Spectrom.* **2005**, *19*, 3356.
(58) Norman, M.; Hansel, A.; Wisthaler, A. *Int. J. Mass Spectrom.* **2007**, *265*, 382.
(59) Prazeller, P.; Palmer, P. T.; Boscaini, E.; Jobson, T.; Alexander, M. *Rapid Commun. Mass Spectrom.* **2003**, *17*, 1593.
(60) Warneke, C.; de Gouw, J. A.; Lovejoy, E. R.; Murphy, P. C.; Kuster, W. C.; Fall, R. *J. Am. Soc. Mass Spectrom.* **2005**, *16*, 1316.
(61) Warneke, C.; Rosen, S.; Lovejoy, E. R.; de Gouw, J. A.; Fall, R. *Rapid Commun. Mass Spectrom.* **2004**, *18*, 133.
(62) Steeghs, M. M. L.; Sikkens, C.; Crespo, E.; Cristescu, S. M.; Harren, F. J. M. *Int. J. Mass Spectrom.* **2007**, *262*, 16.
(63) Steeghs, M. M. L.; Crespo, E.; Harren, F. J. M. *Int. J. Mass Spectrom.* **2007**, *263*, 204.
(64) Blake, R. S.; Whyte, C.; Hughes, C. O.; Ellis, A. M.; Monks, P. S. *Anal. Chem.* **2004**, *76*, 3841.
(65) Wyche, K. P.; Blake, R. S.; Ellis, A. M.; Monks, P. S.; Brauers, T.; Koppmann, R.; Apel, E. C. *Atmos. Chem. Phys.* **2007**, *7*, 609.
(66) Ennis, C. J.; Reynolds, J. C.; Keely, B. J.; Carpenter, L. J. *Int. J. Mass Spectrom.* **2005**, *247*, 72.
(67) Tanimoto, H.; Aoki, N.; Inomata, S.; Hirokawa, J.; Sadanaga, Y. *Int. J. Mass Spectrom.* **2007**, *263*, 1.
(68) Fall, R.; Karl, T.; Jordan, A.; Lindinger, W. *Atmos. Environ.* **2001**, *35*, 3905.
(69) de Gouw, J.; Warneke, C.; Karl, T.; Eerdekens, G.; van der Veen, C.; Fall, R. *Int. J. Mass Spectrom.* **2003**, *223*−*224*, 365.
(70) Karl, T.; Fall, R.; Crutzen, P. J.; Jordan, A.; Lindinger, W. *Geophys. Res. Lett.* **2001**, *28*, 507.
(71) Karl, T.; Guenther, A.; Lindinger, C.; Jordan, A.; Fall, R.; Lindinger, W. *J. Geophys. Res.* **2001**, *106*, D24157.
(72) Lindinger, C.; Pollien, P.; Ali, S.; Yeretzian, C.; Blank, I.; Märk, T. *Anal. Chem.* **2005**, *77*, 4117.
(73) Alexander, M.; Boscaini, E.; Lindinger, W.; Märk, T. D. *Int. J. Mass Spectrom.* **2003**, *223*−*224*, 763.
(74) Boscaini, E.; Alexander, M. L.; Prazeller, P.; Märk, T. D. *Int. J. Mass Spectrom.* **2004**, *239*, 179.
(75) Keck, L.; Oeh, U.; Hoeschen, C. *Int. J. Mass Spectrom.* **2007**, *264*, 92.
(76) Warneke, C.; van der Veen, C.; Luxembourg, S.; de Gouw, J. A.; Kok, A. *Int. J. Mass Spectrom.* **2001**, *207*, 167.
(77) Hansel, A.; Singer, W.; Wisthaler, A.; Schwarzmann, M.; Lindinger, W. *Int. J. Mass Spectrom. Ion Process.* **1997**, *167/168*, 697.
(78) Karl, T.; Jobson, T.; Kuster, W. C.; Williams, E.; Stutz, J.; Shetter, R.; Hall, S. R.; Goldan, P.; Fehsenfeld, F.; Lindinger, W. *J. Geophys. Res.* **2003**, *108*, D4508.
(79) Monks, P. S. *Chem. Soc. Rev.* **2005**, 2.
(80) Hansel, A.; Jordan, A.; Warneke, C.; Holzinger, R.; Lindinger, W. *Rapid Commun. Mass Spectrom.* **1998**, *12*, 871.
(81) Hayward, S.; Hewitt, C. N.; Sartin, J. H.; Owen, S. M. *Environ. Sci. Technol.* **2002**, *36*, 1554.
(82) Steinbacher, M.; Dommen, J.; Ammann, C.; Spirig, C.; Neftel, A.; Prevot, A. S. H. *Int. J. Mass Spectrom.* **2004**, *239*, 117.
(83) Warneke, C.; de Gouw, J. A.; Kuster, W. C.; Goldan, P. D.; Fall, R. *Environ. Sci. Technol.* **2003**, *37*, 2494.
(84) Kato, S.; Miyakawa, Y.; Kaneko, T.; Kajii, Y. *Int. J. Mass Spectrom.* **2004**, *235*, 103.
(85) Kuster, W. C.; Jobson, B. T.; Karl, T.; Riemer, D.; Apel, E.; Goldan, P. D.; Fehsenfeld, F. C. *Environ. Sci. Technol.* **2004**, *38*, 221.
(86) Warneke, C.; Kato, S.; de Gouw, J. A.; Goldan, P. D.; Kuster, W. C.; Shao, M.; Lovejoy, E. R.; Fall, R.; Fehsenfeld, F. C. *Environ. Sci. Technol.* **2005**, *39*, 5390.
(87) de Gouw, J.; Warneke, C.; Holzinger, R.; Kluepfel, T.; Williams, J. *Int. J. Mass Spectrom.* **2004**, *239*, 129.
(88) Ammann, C.; Spirig, C.; Neftel, A.; Steinbacher, M.; Komenda, M.; Schaub, A. *Int. J. Mass Spectrom.* **200**, *238*, 87.
(89) de Gouw, J. A.; Warneke, C.; Stohl, A.; Wollny, A. G.; Brock, C. A.; Cooper, O. R.; Holloway, J. S.; Trainer, M.; Fehsenfeld, F. C.; Atlas, E. L.; Donnelly, S. G.; Stroud, V.; Lueb, A. *J. Geophys. Res.* **2006**, *111*, D10303.
(90) Sprung, D.; Jost, C.; Reiner, T.; Hansel, A.; Wisthaler, A. *J. Geophys. Res.* **2001**, *106*, D28511.
(91) Lee, A.; Schade, G. W.; Holzinger, R.; Goldstein, A. H. *Atmos. Chem. Phys.* **2005**, *5*, 505.
(92) Inomata, S.; Tanimoto, H.; Kameyama, S.; Tsunogai, U.; Irie, H.; Kanaya, Y.; Wang, Z. *Atmos. Chem. Phys. Discuss.* **2007**, *7*, 12845.
(93) Galbally, I. E.; Lawson, S. J.; Weeks, I. A.; Bentley, S. T.; Gillett, R. W.; Meyer, M.; Golstein, A. H. *Environ. Chem. (CSIRO)* **2007**, *4*, 178.
(94) Rogers, T. M.; Grimsrud, E. P.; Herndon, S. C.; Jayne, J. T.; Kolb, C. E.; Allwine, E.; Westberg, H.; Lamb, B. K.; Zavala, M.; Molina, L. T.; Molina, M. J.; Knighton, W. B. *Int. J. Mass Spectrom.* **2006**, *252*, 26.
(95) Karl, T. G.; Christian, T. J.; Yokelson, R. J.; Artaxo, P.; Hao, W. M.; Guenther, A. *Atmos. Chem. Phys.* **2007**, *7*, 5883.
(96) Brenninkmeijer, C.; Crutzen, P. J.; Boumard, F.; Dauer, T.; Dix, B.; Ebinghaus, R.; Filippi, D.; Fischer, H.; Franke, H.; Friess, U.; Heintzenberg, J.; Helleis, F.; Hermann, M.; Kock, H.; Koeppel, C.; Lelieveld, J.; Leuenberger, M.; Martinsson, B.; Miemczyk, S.; Moret, H.; Nguyen, H.; Nyfeler, P.; Oram, D.; O'Sulllivan, D.; Penkett, S.; Platt, U.; Pupek, M.; Ramonet, M.; Randa, B.; Reichelt, M.; Rhee, T.; Rohwer, J.; Rosenfeld, K.; Scharffe, D.; Schlager, H.; Schumann, U.; Slemr, F.; Sprung, D.; Stock, P.; Thaler, R.; Valentino, F.; van Velthoven, P.; Waibel, A.; Wandel, A.; Waschitschek, K.; Wiedensohler, A.; Xueref-Remy, I.; Zahn, A.; Zech, U., Ziereis *Atmos. Chem. Phys.* **2007**, *7*, 4953.
(97) Roberts, J. M. In *Composition and Climate of the Atmosphere*; Singh, H. B., Ed.; Van Nostrand Reinhold: New York, 1995.
(98) Hansel, A.; Wisthaler, A. *Geophys. Res. Lett.* **2000**, *27*, 895.
(99) Aoki, N.; Inomata, S.; Tanimoto, H. *Int. J. Mass Spectrom.* **2007**, *263*, 12.
(100) Singh, H. B.; Kanakidou, M.; Crutzen, P. J.; Jacob, D. J. *Nature* **1995**, *378*, 50.
(101) Holzinger, R.; Jordan, A.; Hansel, A.; Lindinger, W. *Atmos. Environ.* **2001**, *35*, 2525.
(102) Holzinger, R.; Lee, A.; Paw, U. K. T.; Goldstein, A. H. *Atmos. Chem. Phys.* **2005**, 5.
(103) Poschl, U.; Williams, J.; Hoor, P.; Fischer, H.; Crutzen, P. J.; Warneke, C.; Holzinger, R.; Hansel, A.; Jordan, A.; Lindinger, W.; Scheeren, H. A.; Peters, W.; Lelieveld, J. *J. Atmos. Chem.* **2001**, *38*, 115.

(104) Holzinger, R.; Williams, J.; Salisbury, G.; Kluepfel, T.; de Reus, M.; Traub, M.; Crutzen, P. J.; Lelieveld, J. *Atmos. Chem. Phys.* **2005**, *5*, 39.
(105) Northway, M. J.; de Gouw, J. A.; Fahey, D. W.; Gao, R. S.; Warneke, C.; Roberts, J. M.; Flocke, F. *Atmos. Environ.* **2004**, *38*, 6017.
(106) Knighton, W. B.; Herndon, S. C.; Shorter, J. H.; Miake-Lye, R. C.; Zahniser, M. S.; Akiyama, K.; Shimono, A.; Kitasaka, K.; Shimajiri, H.; Sugihara, K. *J. Air Waste Manage. Assoc.* **2007**, *57*, 1370.
(107) Guenther, A.; Karl, T.; Harley, P.; Wiedinmyer, C.; Palmer, P. I.; Geron, C. *Atmos. Chem. Phys.* **2006**, *6*, 3181.
(108) Guenther, A.; Hewitt, C. N.; Erickson, D.; Fall, R.; Geron, C.; Graedel, T.; Harley, P.; Klinger, L.; Lerdau, M.; Mckay, W.; Pierce, T.; Scoles, B.; Steinbrecher, R.; Tallamraju, R.; Taylor, J.; Zimmerman, P. *J. Geophys. Res.* **1995**, *100*, D8873.
(109) Tani, A.; Hayward, S.; Hansel, A.; Hewitt, C. N. *Int. J. Mass Spectrom.* **2004**, *239*, 161.
(110) Tani, A.; Hayward, S.; Hewitt, C. N. *Int. J. Mass Spectrom.* **2003**, *223*−*224*, 561.
(111) Warneke, C.; de Gouw, J. A.; Goldan, P.; Kuster, W.; Williams, E.; Lerner, B.; Jaboubek, R.; Brown, S.; Stark, H.; Aldener, M.; Ravishankara, A.; Roberts, D. D.; Marchewka, M.; Bertman, S.; Sueper, D.; McKeen, S.; Meagher, J.; Fehsenfeld, F. *J. Geophys. Res.* **2004**, *109*, D10309.
(112) Salisbury, G.; Williams, J.; Holzinger, R.; Gros, V.; Mihalopoulos, N.; Vrekoussis, M.; Sarda-esteve, R.; Berresheim, H.; von Kuhlmann, R.; Lawrence, M.; Lelieveld, J. *Atmos. Chem. Phys.* **2003**, *3*, 925.
(113) Karl, T.; Potosnak, M.; Guenther, A.; Clark, D.; Walker, J.; Herrick, J. D.; Geron, C. *J. Geophys. Res.* **2004**, *109*, D18306.
(114) Crutzen, P. J.; Williams, J.; Poschl, U.; Hoor, P.; Fischer, H.; Warneke, C.; Holzinger, R.; Hansel, A.; Lindinger, W.; Scheeren, B.; Lelieveld, J. *Atmos. Environ.* **2000**, *34*, 1161.
(115) Williams, J.; Poschl, U.; Crutzen, P. J.; Hansel, A.; Holzinger, R.; Warneke, C.; Lindinger, W.; Lelieveld, J. *J. Atmos. Chem.* **2001**, *38*, 133.
(116) Warneke, C.; Holzinger, R.; Hansel, A.; Jordan, A.; Lindinger, W.; Poschl, U.; Williams, J.; Hoor, P.; Fischer, H.; Crutzen, P. J.; Scheeren, H. A.; Lelieveld, J. *J. Atmos. Chem.* **2001**, *38*, 167.
(117) Holzinger, R.; Sanhueza, E.; von Kuhlmann, R.; Kleiss, B.; Donoso, L.; Crutzen, P. J. *Global Biogeochem. Cycles* **2002**, *16*, 1074.
(118) Mueller, K.; Haferkorn, S.; Grabmer, W.; Wisthaler, A.; Hansel, A.; Kreuzwieser, J.; Cojocariu, C.; Rennenberg, H.; Herrmann, H. *Atmos. Environ.* **2006**, *40*, S81.
(119) Rinne, J.; Ruuskanen, T. M.; Reissell, A.; Taipale, R.; Hakola, H.; Kulmala, M. *Boreal Environ. Res.* **2005**, *10*, 425.
(120) Jobson, B. T.; McKeen, S. A.; Parrish, D. D.; Fehsenfeld, F. C.; Blake, D. R.; Goldstein, A. H.; Schauffler, S. M.; Elkins, J. C. *J. Geophys. Res.* **1999**, *104*, D16091.
(121) Williams, J.; Fischer, H.; Harris, G. W.; Crutzen, P. J.; Hoor, P.; Hansel, A.; Holzinger, R.; Warneke, C.; Lindinger, W.; Scheeren, B.; Lelieveld, J. *J. Geophys. Res.* **2000**, *105*, D20473.
(122) Karl, T.; Crutzen, P. J.; Mandl, M.; Staudinger, M.; Guenther, A.; Jordan, A.; Fall, R.; Lindinger, W. *Atmos. Environ.* **2001**, *35*, 5287.
(123) Warneke, C.; de Gouw, J. A. *Atmos. Environ.* **2001**, *35*, 5923.
(124) Rinne, H. J. I.; Guenther, A.; Warneke, C.; de Gouw, J. A.; Luxembourg, S. L. *Geophys. Res. Lett.* **2001**, *28*, 3139.
(125) Spirig, C.; Neftel, A.; Ammann, C.; Dommen, J.; Grabmer, W.; Thielmann, A.; Schaub, A.; Beauchamp, J.; Wisthaler, A.; Hansel, A. *Atmos. Chem. Phys.* **2005**, *5*, 465.
(126) Karl, T.; Guenther, A. *Int. J. Mass Spectrom.* **2004**, *239*, 77.
(127) Karl, T. G.; Spirig, C.; Rinne, J.; Stroud, C.; Prevost, P.; Greenberg, J.; Fall, R.; Guenther, A. *Atmos. Chem. Phys.* **2002**, *2*, 279.
(128) Yokelson, R. J.; Karl, T.; Artaxo, P.; Blake, D. R.; Christian, T. J.; Griffith, D. W. T.; Guenther, A.; Hao, W. M. *Atmos. Chem. Phys.* **2007**, *7*, 5175.
(129) Graus, M.; Hansel, A.; Wisthaler, A.; Lindinger, C.; Forkel, R.; Hauff, K.; Klauer, M.; Pfichner, A.; Rappenglueck, B.; Steigner, D.; Steinbrecher, R. *Atmos. Environ.* **2006**, *40*, S43.
(130) Grabmer, W.; Kreuzwieser, J.; Wisthaler, A.; Cojocariu, C.; Graus, M.; Rennenberg, H.; Steigner, D.; Steinbrecher, R.; Hansel, A. *Atmos. Environ.* **2006**, *40*, S128.
(131) Ammann, C.; Brunner, A.; Spirig, C.; Neftel, A. *Atmos. Chem. Phys.* **2006**, *6*, 4643.
(132) Rinne, J.; Taipale, R.; Markkanen, T.; Ruuskanen, T. M.; Hellen, H.; Kajos, M. K.; Vesala, T.; Kulmala, M. *Atmos. Chem. Phys.* **2007**, *7*, 3361.
(133) Ruuskanen, T. M.; Kolari, P.; Back, J.; Kulmala, M.; Rinne, J.; Hakola, H.; Taipale, R.; Raivonen, M.; Altimir, N.; Hari, P. *Boreal Environ. Res.* **2005**, *10*, 553.
(134) Holzinger, R.; Lee, A.; McKay, M.; Goldstein, A. H. *Atmos. Chem. Phys.* **2006**, *6*, 1267.
(135) Schade, G. W.; Custer, T. G. *Atmos. Environ.* **2004**, *38*, 6105.
(136) Warneke, C.; Luxembourg, S. L.; de Gouw, J. A.; Rinne, H. J. I.; Guenther, A. B.; Fall, R. *J. Geophys. Res.* **2002**, *107*, D4067.
(137) Sinha, V.; Williams, J.; Meyerhofer, M.; Riebesell, U.; Paulino, A.; Larsen, A. *Atmos. Chem. Phys.* **2007**, *7*, 739.
(138) Russell, L. M.; Mensah, A. A.; Fischer, E. V.; Sive, B. C.; Vamer, R. K.; Keene, W. C.; Stutz, J.; Pszenny, A. A. P. *J. Geophys. Res.* **2007**, *112*, D10S21.
(139) Filella, I.; Penuelas, J. *Atmos. Environ.* **2006**, *40*, 7752.
(140) Holzinger, R.; Kleiss, B.; Donoso, L.; Sanhueza, E. *Atmos. Environ.* **2001**, *35*, 4917.
(141) Molina, L. T.; Kolb, C. E.; de Foy, B.; Lamb, B. K.; Brune, W. H.; Jimenez, J. L.; Ramos-Villegas, R.; Sarmiento, J.; Paramo-Figueroa, V. H.; Cardenas, B.; Gutierrez-Avedoy, V.; Molina, M. J. *Atmos. Chem. Phys.* **2007**, *7*, 2447.
(142) Miyakawa, Y.; Kato, S.; Kajii, Y. *Taiki Kankyo Gakkaishi* **2005**, *40*, 209.
(143) Warneke, C.; McKeen, S. A.; de Gouw, J. A.; Goldan, P. D.; Kuster, W. C.; Holloway, J. S.; Williams, E. J.; Lerner, B. M.; Parrish, D. D.; Trainer, M.; Fehsenfeld, F. C.; Kato, S.; Atlas, E. L.; Baker, A.; Blake, D. R. *J. Geophys. Res* **2007**, *112*, D10S47.
(144) Holzinger, R.; Jordan, A.; Hansel, A.; Lindinger, W. *J. Atmos. Chem.* **2001**, *38*, 187.
(145) Beauchamp, J.; Wisthaler, A.; Grabmer, W.; Neuner, C.; Weber, A.; Hansel, A. *Atmos. Environ.* **2004**, *38*, 2511.
(146) Jobson, B. T.; Alexander, M. L.; Maupin, G. D.; Muntean, G. G. *Int. J. Mass Spectrom.* **2005**, *245*, 78.
(147) Velasco, E.; Lamb, B.; Westberg, H.; Allwine, E.; Sosa, G.; Arriaga-Colina, J.; Jobson, T.; Alexander, M.; Prazeller, P.; Knighton, W.; Rogers, T.; Grutter, M.; Herndon, S.; Kolb, C.; Zavala, M.; De Foy, B.; Volkamer, R.; Molina, L.; Molina, M. *Atmos. Chem. Phys.* **2007**, *7*, 329.
(148) Herndon, S. C.; Rogers, T.; Dunlea, E. J.; Jayne, J. T.; Miake-Lye, R.; Knighton, B. *Environ. Sci. Technol.* **2006**, *40*, 4406.
(149) Knighton, W. B.; Rogers, T. M.; Anderson, B. E.; Herndon, S. C.; Yelvington, R. C.; Miake-Lye, J. *J. Propul. Power* **2007**, *23*, 949.
(150) Yelvington, P. E.; Herndon, S. C.; Wormhoudt, J. C.; Jayne, J. T.; Miake-Lye, R. C.; Knighton, W. B.; Wey, C. *J. Propul. Power* **2007**, *23*, 912.
(151) Shaw, S. L.; Mitloehner, F. M.; Jackson, W.; DePeters, E. J.; Fadel, J. G.; Robinson, P. H.; Holzinger, R.; Goldstein, A. H. *Environ. Sci. Technol.* **2007**, *41*, 1310.
(152) de Gouw, J. A.; Middlebrook, A. M.; Warneke, C.; Goldan, P. D.; Kuster, W. C.; Roberts, J. M.; Fehsenfeld, F. C.; Worsnop, D. R.; Canagaratna, M. R.; Pszenny, A. A. P.; Keene, W. C.; Marchewka, M.; Bertman, S. B.; Bates, T. S. *J. Geophys. Res.* **2005**, *110*, D16305.
(153) Drewnick, F.; Hings, S. S.; Curtius, J.; Eerdekens, G.; Williams, J. *Atmos. Environ.* **2006**, *40*, 4316.
(154) Lobert, J. M.; Scharffe, D. H.; Hao, W. M.; Crutzen, P. J. *Nature* **1990**, *346*, 552.
(155) de Gouw, J. A.; Warneke, C.; Parrish, D.; Holloway, J.; Trainer, M.; Fehsenfeld, F. *J. Geophys. Res.* **2003**, *108*, D4329.
(156) Karl, T.; Hansel, A.; Mark, T.; Lindinger, W.; Hoffmann, D. *Int. J. Mass Spectrom.* **2003**, *223*−*224*, 527.
(157) Wisthaler, A.; Hansel, A.; Dickerson, R. R.; Crutzen, P. J. *J. Geophys. Res.* **2002**, *107*, D8024.
(158) de Gouw, J. A.; Cooper, O. R.; Warneke, C.; Hudson, P. K.; Fehsenfeld, F. C.; Holloway, J. S.; Huebler, G.; Nicks, D. K.; Nowak, J. B.; Parrish, D. D.; Ryerson, T. B.; Atlas, E. L.; Donnelly, S. G.; Schauffler, S. M.; Stroud, V.; Johnson, K.; Carmichael, G. R.; Streets, D. G. *J. Geophys. Res.* **2004**, *109*, D23S20.
(159) Duck, T. J.; Firanski, B. J.; Millet, D. B.; Goldstein, A. H.; Allan, J.; Holzinger, R.; Worsnop, D. R.; White, A. B.; Stohl, A.; Dickinson, C. S.; van Donkelaar, A. *J. Geophys. Res.* **2007**, *112*, D10S44.
(160) Sanhueza, E.; Holzinger, R.; Kleiss, B.; Donoso, L.; Crutzen, P. J. *Atmos. Chem. Phys.* **2004**, *4*, 275.
(161) Christian, T. J.; Kleiss, B.; Yokelson, R. J.; Holzinger, R.; Crutzen, P. J.; Hao, W. M.; Saharjo, B. H.; Ward, D. E. *J. Geophys. Res.* **2003**, *108*, D4719.
(162) Christian, T. J.; Kleiss, B.; Yokelson, R. J.; Holzinger, R.; Crutzen, P. J.; Hao, W. M.; Shirai, T.; Blake, D. R. *J. Geophys. Res.* **2004**, *109*, D02311.
(163) Zhao, J.; Zhang, R.; Fortner, E. C.; North, S. W. *J. Am. Chem. Soc.* **2004**, *126*, 2686.
(164) D'Anna, B.; Wisthaler, A.; Andreasen, O.; Hansel, A.; Hjorth, J.; Jensen, N. R.; Nielsen, C. J.; Stenstrom, Y.; Viidanoja, J. *J. Phys. Chem. A* **2005**, *109*, 5104.
(165) Wisthaler, A.; Jensen, N. R.; Winterhalter, R.; Lindinger, W.; Hjorth, J. *Atmos. Environ.* **2001**, *35*, 6181.
(166) Gomez Alvarez, E.; Viidanoja, J.; Munoz, A.; Wirtz, K.; Hjorth, J. *Environ. Sci. Technol.* **2007**, *41*, 8362.
(167) Hanson, D. R.; Orlando, J.; Noziere, B.; Kosciuch, E. *Int. J. Mass Spectrom.* **2004**, *239*, 147.
(168) Paulsen, D.; Dommen, J.; Kalberer, M.; Prevot, A.; Sax, M.; Steinbacher, M.; Weingartner, E.; Baltensperger, U. *Environ. Sci. Technol.* **2005**, *39*, 2668.

(169) Baltensperger, U.; Kalberer, M.; Dommen, J.; Paulsen, D.; Alfarra, M. R.; Coe, H.; Fisseha, R.; Gascho, A.; Gysel, M.; Nyeki, S.; Sax, M.; Steinbacher, M.; Prevot, A. S. H.; Sjogren, S.; Weingartner, E.; Zenobi, R. *Faraday Discuss.* **2005**, *130*, 265.
(170) Lee, A.; Goldstein, A.; Kroll, J.; Ng, N.; Varutbangkul, V.; Flagan, R. C.; Seinfeld, J. H. *J. Geophys. Res.* **2006**, *111*, D17305.
(171) Ng, N. L.; Kroll, J. H.; Keywood, M. D.; Bahreini, R.; Varutbangkul, V.; Flagan, R. C.; Seinfeld, J. H.; Lee, A.; Goldstein, A. H. *Environ. Sci. Technol.* **2006**, *40*, 2283.
(172) Presto, A. A.; Donahue, N. M. *Environ. Sci. Technol.* **2006**, *40*, 3536.
(173) Kalberer, M.; Paulsen, D.; Sax, M.; Steinbacher, M.; Dommen, J.; Prevot, A. S. H.; Fisseha, R.; Weingartner, E.; Frankevich, V.; Zenobi, R.; Baltensperger, U. *Science* **2004**, *303*, 1659.
(174) Lee, A.; Goldstein, A.; Keywood, M.; Gao, S.; Varutbangkul, V.; Bahreini, R.; Ng, N.; Flagan, R.; Seinfeld, J. *J. Geophys. Res.* **2006**, *111*, D07302.
(175) Liggio, J.; Li, S.-M.; Brook, J.; Mihele, C. *Geophys. Res. Lett.* **2007**, *34*, L05814.
(176) Pathak, R. K.; Stanier, C. O.; Donahue, N. M.; Pandis, S. N. *J. Geophys. Res.* **2007**, *112*, D03201.
(177) Wegener, R.; Brauers, T.; Koppmann, R.; Rodriguez Bares, S.; Rohrer, F.; Tillman, R.; Wahner, A.; Hansel, A.; Wisthaler, A. *J. Geophys. Res.* **2007**, *112*, D13301.
(178) Singsaas, E. L.; Sharkey, T. D. *Plant Cell Environ.* **1998**, *21*, 1181.
(179) Penuelas, J.; Munne-Bosch, S. *Trends Plant Sci.* **2005**, *10*, 166.
(180) Velikova, V.; Pinelli, P.; Pasqualini, S.; Reale, L.; Ferranti, F.; Loreto, F. *New Phytol.* **2005**, *166*, 419.
(181) Langenheim, J. H. *J. Chem. Ecol.* **1994**, *20*, 1223.
(182) Pichersky, E.; Gershenzon, J. *Curr. Opin. Plant Biol.* **2002**, *5*, 237.
(183) Pare, P.; Tumlinson, J. *Plant Physiol.* **1997**, *114*, 1161.
(184) Penuelas, J.; Llusia, J.; Estiarte, M. *Trends Ecol. Evol.* **1995**, *10*, 289.
(185) Rosenstiel, T. N.; Ebbets, A. L.; Khatri, W. C.; Fall, R.; Monson, R. K. *Plant Biol.* **2004**, *6*, 12.
(186) Fall, R.; Karl, T.; Hansel, A.; Jordan, A.; Lindinger, W. *J. Geophys. Res.* **1999**, *104*, D15963.
(187) Penuelas, J.; Filella, I.; Stefanescu, C.; Llusia, J. *New Phytol.* **2005**, *167*, 851.
(188) Fukui, Y.; Doskey, P. V. *J. Geophys. Res.* **1998**, *103*, D13153.
(189) Heiden, A. C.; Kobel, K.; Langebartels, C.; Schuh-Thomas, G.; Wildt, J. *J. Atmos. Chem.* **2003**, *45*, 143.
(190) Seco, R.; Penuelas, J.; Filella, I. *Atmos. Environ.* **2007**, *41*, 2477.
(191) Tholl, D.; Boland, W.; Hansel, A.; Rose, U.; Schnitzler, J.-P. *Plant J.* **2006**, *45*, 540.
(192) Maleknia, S. D.; Bell, T. L.; Adams, M. A. *Int. J. Mass Spectrom.* **2007**, *262*, 203.
(193) Hayward, S.; Tani, A.; Owen Sue, M.; Hewitt, C. N. *Tree Physiol.* **2004**, *24*, 721.
(194) Grabmer, W.; Graus, M.; Lindinger, C.; Wisthaler, A.; Rappenglueck, B.; Steinbrecher, R.; Hansel, A. *Int. J. Mass Spectrom.* **2004**, *239*, 111.
(195) Ezra, D.; Jasper, J.; Rogers, T.; Knighton, B.; Grimsrud, E.; Strobel, G. *Plant Sci.* **2004**, *166*, 1471.
(196) Wilske, B.; Holzinger, R.; Kesselmeier, J. *Symbiosis* **2001**, *31*, 95.
(197) Steeghs, M. M. L.; Bais, H. P.; de Gouw, J.; Goldan, P.; Kuster, W.; Northway, M.; Fall, R.; Vivanco, J. M. *Plant Physiol.* **2004**, *135*, 47.
(198) Abanda-Nkpwatt, D.; Muesch, M.; Tschiersch, J.; Boettner, M.; Schwab, W. *J. Exp. Bot.* **2006**, *57*, 4025.
(199) Pegoraro, E.; Rey, A.; Abrell, L.; van Haren, J.; Lin, G. *Global Change Biology* **2006**, *12*, 456.
(200) Pegoraro, E.; Abrell, L.; Van Haren, J.; Barron-Gafford, G.; Grieve, K. A.; Malhi, Y.; Murthy, R.; Lin, G. H. *Global Change Biology* **2005**, *11*, 1234.
(201) Penuelas, J.; Llusia, J.; Filella, I. *Biologia Plantarum* **2007**, *51*, 372.
(202) Kreuzwieser, J.; Graus, M.; Wisthaler, A.; Hansel, A.; Rennenberg, H.; Schnitzler, J.-P. *New Phytologist* **2002**, *156*, 171.
(203) Karl, T.; Fall, R.; Rosenstiel, T. N.; Prazeller, P.; Larsen, B.; Seufert, G.; Lindinger, W. *Planta* **2002**, *215*, 894.
(204) Karl, T.; Curtis, A. J.; Rosenstiel, T. N.; Monson, R. K.; Fall, R. *Plant Cell Environ.* **2002**, *25*, 1121.
(205) Schnitzler, J.-P.; Graus, M.; Kreuzwieser, J.; Heizman, U.; Rennenberg, H.; Wisthaler, A.; Hansel, A. *Plant Physiol.* **2004**, *135*, 152.
(206) Graus, M.; Schnitzler, J.-P.; Hansel, A.; Cojocariu, C.; Rennenberg, H.; Wisthaler, A.; Kreuzwieser, J. *Plant Physiol.* **2004**, *135*, 1967.
(207) Filella, I.; Penuelas, J.; Llusia, J. *New Phytol.* **2006**, *169*, 135.
(208) Holzinger, R.; Sandoval-Soto, L.; Rottenberger, S.; Crutzen, P. J.; Kesselmeier, J. *J. Geophys. Res.* **2000**, *105*, D20573.
(209) Nogues, I.; Brilli, F.; Loreto, F. *Plant Physiol.* **2006**, *141*, 721.
(210) Loivamaki, M.; Louis, S.; Cinege, G.; Zimmer, I.; Fishbach, R. J.; Schnitzler, J.-P. *Plant Physiol.* **2007**, *143*, 540.
(211) Croft, K. P. C.; Juttner, F.; Slusarenko, A. *J. Plant Physiol.* **1993**, *101*, 13.
(212) von Dahl, C. C.; Haevecker, M.; Schloegl, R.; Baldwin, I. T. *Plant J.* **2006**, *46*, 948.
(213) Bartolome, J.; Penuelas, J.; Filella, I.; Llusia, J.; Broncano, M. J.; Plaixats, J. *J. Environ. Monit.* **2007**, *28*, 697.
(214) Karl, T.; Guenther, A.; Jordan, A.; Fall, R.; Lindinger, W. *Atmos. Environ.* **2000**, *35*, 491.
(215) de Gouw, J. A.; Howard, C. J.; Custer, T. G.; Baker, B. M.; Fall, R. *Environ. Sci. Technol.* **2000**, *34*, 2640.
(216) de Gouw, J. A.; Howard, C.; Custer, T. G.; Fall, R. *Geophys. Res. Lett.* **1999**, *26*, 811.
(217) Karl, T.; Fall, R.; Jordan, A.; Lindinger, W. *Environ. Sci. Technol.* **2001**, *35*, 2926.
(218) Karl, T.; Harren, F.; Warneke, C.; de Gouw, J.; Grayless, C.; Fall, R. *J. Geophys. Res.* **2005**, *110*, D15302.
(219) Beauchamp, J.; Wisthaler, A.; Hansel, A.; Kleist, E.; Miebach, M.; Ninemets, U.; Schurr, U.; Wildt, J. *Plant Cell Environ.* **2005**, *28*, 1334.
(220) Palitzsch, K.; Goellner, S.; Lupa, K.; Matschullat, J.; Messal, C.; Plessow, K.; Schipek, M.; Schnabel, I.; Weller, C.; Zimmermann, F. *Umweltwiss. Schadst.−Forsch.* **2005**, *17*, 231.
(221) Fritz, B.; Lamb, B.; Westberg, H.; Folk, R.; Knighton, B.; Grimsrud, E. *For. Prod. J.* **2004**, *54*, 50.
(222) Warneke, C.; Karl, T.; Judmaier, H.; Hansel, A.; Jordan, A.; Lindinger, W.; Crutzen, P. J. *Global Biogeochem. Cycles* **1999**, *13*, 9.
(223) Asensio, D.; Penuelas, J.; Filella, I.; Llusia, J. *Plant Soil* **2007**, *291*, 249.
(224) Asensio, D.; Penuelas, J.; Llusia, J.; Ogaya, R.; Filella, I. *Soil Biol. Biochem.* **2007**, *39*, 2471.
(225) Taucher, J.; Hansel, A.; Jordan, A.; Lindinger, W. *J. Agric. Food Chem.* **1996**, *44*, 3778.
(226) Taucher, J.; Lagg, A.; Hansel, A.; Vogel, W.; Lindinger, W. *Alcohol.: Clin. Exp. Res.* **1995**, *19*, 1147.
(227) Lindinger, W.; Taucher, J.; Jordan, A.; Hansel, A.; Vogel, W. *Alcohol.: Clin. Exp. Res.* **1997**, *21*, 939.
(228) Yeretzian, C.; Jordan, A.; Lindinger, W. *Int. J. Mass Spectrom.* **2003**, *223−224*, 115.
(229) Pollien, P.; Jordan, A.; Lindinger, W.; Yeretzian, C. *Int. J. Mass Spectrom.* **2003**, *228*, 69.
(230) Yeretzian, C.; Pollien, P.; Lindinger, C.; Ali, S. *Compr. Rev. Food Sci. Food Saf.* **2004**, *3*, 152.
(231) Yeretzian, C.; Jordan, A.; Badoud, R.; Lindinger, W. *Eur. Food Res. Technol.* **2002**, *214*, 92.
(232) Mateus, M.-L.; Lindinger, C.; Gumy, J.-C.; Liardon, R. *J. Agric. Food Chem.* **2007**, *55*, 10117.
(233) Mayr, D.; Märk, T.; Lindinger, W.; Brevard, H.; Yeretzian, C. *Int. J. Mass Spectrom.* **2003**, *223−224*, 743.
(234) van Ruth, S. M.; Roozen, J. P. *Food Chem.* **2000**, *71*, 339.
(235) van Ruth, S. M.; Buhr, K. *Eur. Food Res. Technol.* **2003**, *216*, 220.
(236) Hansson, A.; Giannouli, P.; Van Ruth, S. *J. Agric. Food Chem.* **2003**, *51*, 4732.
(237) Boland, A. B.; Buhr, K.; Giannouli, P.; van Ruth, S. M. *Food Chem.* **2004**, *86*, 401.
(238) van Ruth, S. M.; Buhr, K. *Int. J. Mass Spectrom.* **2004**, *239*, 187.
(239) van Ruth, S. M.; Boscaini, E.; Mayr, D.; Pugh, J.; Posthumus, M. *Int. J. Mass Spectrom.* **2003**, *223*, 55.
(240) van Ruth, S. M.; Dings, L.; Buhr, K.; Posthumus, M. A. *Food Res. Int.* **2004**, *37*, 785.
(241) van Ruth, S. M.; Dings, L.; Aprea, E.; Odake, S. *Food Sci. Technol. Res.* **2005**, *11*, 63.
(242) Gasperi, F.; Gallerani, G.; Boschetti, A.; Biasioli, F.; Monetti, A.; Boscaini, E.; Jordan, A.; Lindinger, W.; Iannotta, S. *J. Sci. Food Agric.* **2001**, *81*, 357.
(243) Boscaini, E.; van Ruth, S.; Biasioli, F.; Gasperi, F.; Märk, T. *J. Agric. Food Chem.* **2003**, *51*, 1782.
(244) Biasioli, F.; Gasperi, F.; Aprea, E.; Endrizzi, I.; Framondino, V.; Marini, F.; Mott, D.; Märk, T. D. *Food Qual. Preference* **2006**, *17*, 63.
(245) Gallardo-Escamilla, F. J.; Kelly, A. L.; Delahunty, C. M. *J. Dairy Sci.* **2005**, *88*, 2689.
(246) Gallardo-Escamilla, F. J.; Kelly, A. L.; Delahunty, C. M. *J. Dairy Sci.* **2005**, *88*, 3745.
(247) Mestres, M.; Moran, N.; Jordan, A.; Buettner, A. *J. Agric. Food Chem.* **2005**, *53*, 403.
(248) Mestres, M.; Kieffer, R.; Buettner, A. *J. Agric. Food Chem.* **2006**, *54*, 1814.
(249) Aprea, E.; Biasioli, F.; Gasperi, F.; Märk, T. D.; van Ruth, S. *Flavour Fragrance J.* **2006**, *21*, 53.
(250) van Ruth, S. M.; de Witte, L.; Uriarte, A. R. *J. Agric. Food Chem.* **2004**, *52*, 8105.
(251) Mei, J. B.; Reineccius, G. A.; Knighton, W. B.; Grimsrud, E. P. *J. Agric. Food Chem.* **2004**, *52*, 6267.

(252) Roberts, D. D.; Pollien, P.; Antille, N.; Lindinger, C.; Yeretzian, C. *J. Agric. Food Chem.* **2003**, *51*, 3636.
(253) van Ruth, S. M.; Floris, V.; Fayoux, S. *Food Chem.* **2006**, *98*, 343.
(254) Boland, A. B.; Delahunty, C. M.; van Ruth, S. M. *Food Chem.* **2006**, *96*, 452.
(255) Gallardo-Escamilla, F. J.; Kelly, A. L.; Delahunty, C. M. *Int. Dairy J.* **2007**, *17*, 308.
(256) Landy, P.; Pollien, P.; Rytz, A.; Leser, M. E.; Sagalowicz, L.; Blank, I.; Spadone, J.-C. *J. Agric. Food Chem.* **2007**, *55*, 1915.
(257) Carbone, F.; Mourgues, F.; Biasioli, F.; Gasperi, F.; Märk, T. D.; Rosati, C.; Perrotta, G. *Mol. Breed.* **2006**, *18*, 127.
(258) Buhr, K.; van Ruth, S.; Delahunty, C. *Int. J. Mass Spectrom.* **2002**, *221*, 1.
(259) Aprea, E.; Biasioli, F.; Märk, T. D.; Gasperi, F. *Int. J. Mass Spectrom.* **2007**, *262*, 114.
(260) Mayr, D.; Margesin, R.; Klingsbichel, E.; Hartungen, E.; Jenewein, D.; Schinner, F.; Märk, T. D. *Appl. Environ. Microbiol.* **2003**, *69*, 4697.
(261) Mayr, D.; Margesin, R.; Schinner, F.; Märk, T. D. *Int. J. Mass Spectrom.* **2003**, *223*−*224*, 229.
(262) Jaksch, D.; Margesin, R.; Mikoviny, T.; Skalny, J. D.; Hartungen, E.; Schinner, F.; Mason, N. J.; Märk, T. D. *Int. J. Mass Spectrom.* **2004**, *239*, 209.
(263) Aprea, E.; Biasioli, F.; Sani, G.; Cantini, C.; Märk, T. D.; Gasperi, F. *J. Agric. Food Chem.* **2006**, *54*, 7635.
(264) Märk, J.; Pollien, P.; Lindinger, C.; Blank, I.; Märk, T. *J. Agric. Food Chem.* **2006**, *54*, 2786.
(265) Aprea, E.; Biasioli, F.; Gasperi, F.; Mott, D.; Marini, F.; Märk, T. D. *Int. Dairy J.* **2007**, *17*, 226.
(266) Boschetti, A.; Biasioli, F.; van Opbergen, M.; Warneke, C.; Jordan, A.; Holzinger, R.; Prazeller, P.; Karl, T.; Hansel, A.; Lindinger, W.; Iannotta, S. *Postharvest Biol. Technol.* **1999**, *17*, 143.
(267) Biasioli, F.; Gasperi, F.; Aprea, E.; Colato, L.; Boscaini, E.; Märk, T. D. *Int. J. Mass Spectrom.* **2003**, *223*−*224*, 343.
(268) Aprea, E.; Biasioli, F.; Carlin, S.; Versini, G.; Märk, T.; Gasperi, F. *Rapid Commun. Mass Spectrom.* **2007**, *21*, 2564.
(269) Biasioli, F.; Gasperi, F.; Aprea, E.; Mott, D.; Boscaini, E.; Mayr, D.; Märk, T. D. *J. Agric. Food Chem.* **2003**, *51*, 7227.
(270) Granitto, P.; Biasioli, F.; Aprea, E.; Mott, D.; Furlanello, C.; Märk, T. D.; Gasperi, F. *Sens. Actuators, B* **2007**, *121*, 379.
(271) Boscaini, E.; Mikoviny, T.; Wisthaler, A.; von Hartungen, E.; Märk, T. D. *Int. J. Mass Spectrom.* **2004**, *239*, 215.
(272) Spitaler, R.; Araghipour, N.; Mikoviny, T.; Wisthaler, A.; Dalla Via, J.; Märk, T. D. *Int. J. Mass Spectrom.* **2007**, *266*, 1.
(273) Boamfa, E. I.; Steeghs, M. M. L.; Cristescu, S. M.; Harren, F. J. M. *Int. J. Mass Spectrom.* **2004**, *239*, 193.
(274) Shaker, E. S. *LWT--Food Sci. Technol.* **2006**, *39*, 883.
(275) Zini, E.; Biasioli, F.; Gasperi, F.; Mott, D.; Aprea, E.; Märk, T. D.; Patocchi, A.; Gessler, C.; Komjanc, M. *Euphytica* **2005**, *145*, 269.
(276) Pollien, P.; Lindinger, C.; Yeretzian, C.; Blank, I. *Anal. Chem.* **2003**, *75*, 5488.
(277) Robert, F.; Vuataz, G.; Pollien, P.; Saucy, F.; Alonso, M.-I.; Bauwens, I.; Blank, I. *J. Agric. Food Chem.* **2004**, *52*, 6837.
(278) Miekisch, W.; Schubert, J. K. *Trends Anal. Chem.* **2006**, *25*, 665.
(279) Lirk, P.; Bodrogi, F.; Rieder, J. *Int. J. Mass Spectrom.* **2004**, *239*, 221.
(280) Amann, A.; Poupart, G.; Telser, S.; Ledochowski, M.; Schmid, A.; Mechtcheriakov, S. *Int. J. Mass Spectrom.* **2004**, *239*, 227.
(281) Amann, A.; Spanel, P.; Smith, D. *Mini-Rev. Med. Chem.* **2007**, *7*, 115.
(282) Pinggera, G.-M.; Lirk, P.; Bodogri, F.; Herwig, R.; Steckel-Berger, G.; Bartsch, G.; Rieder, J. *BJU Int.* **2005**, *95*, 306.
(283) Steeghs, M. M. L.; Moeskops, B. W. M.; van Swam, K.; Cristescu, S. M.; Scheepers, P. T. J.; Harren, F. J. M. *Int. J. Mass Spectrom.* **2006**, *253*, 58.
(284) Rieder, J.; Prazeller, P.; Boehler, M.; Lirk, P.; Lindinger, W.; Amann, A. *Anesth. Analg.* **2001**, *92*, 389.
(285) Summer, G.; Lirk, P.; Hoerauf, K.; Riccabona, U.; Bodrogi, F.; Raifer, H.; Deibl, M.; Rieder, J.; Schobersberger, W. *Anesth. Analg.* **2003**, *97*, 1070.
(286) Rieder, J.; Keller, C.; Brimacombe, J.; Gruber, G.; Lirk, P.; Summer, G.; Amann, A. *Anaesthesia* **2002**, *57*, 663.
(287) Buszewski, B.; Kesy, M.; Ligor, T.; Amann, A. *Biomed. Chromatogr.* **2007**, *21*, 553.
(288) Risby, T. H.; Solga, S. F. *Appl. Phys. B* **2006**, *85*, 421.
(289) Lechner, M.; Rieder, J. *Curr. Med. Chem.* **2007**, *14*, 987.
(290) Pauling, L.; Robinson, A.; Teranish, R.; Cary, P. *PNAS* **1971**, *68*, 2374.
(291) Phillips, M.; Herrera, J.; Krishnan, S.; Zain, M.; Greenberg, J.; Cataneo, R. N. *J. Chromatogr., B* **1999**, *729*, 75.
(292) Warneke, C.; Kuczynski, J.; Hansel, A.; Jordan, A.; Vogel, W.; Lindinger, W. *Int. J. Mass Spectrom. Ion Process.* **1996**, *154*, 61.
(293) Moser, B.; Bodrogi, F.; Eibl, G.; Lechner, M.; Rieder, J.; Lirk, P. *Respir. Physiol. Neurobiol.* **2005**, *145*, 295.
(294) Lechner, M.; Moser, B.; Niederseer, D.; Karlseder, A.; Holzknecht, B.; Fuchs, M.; Colvin, S.; Tilg, H.; Rieder, J. *Respir. Physiol. Neurobiol.* **2006**, *154*, 478.
(295) Taucher, J.; Hansel, A.; Jordan, A.; Fall, R.; Futrell, J. H.; Lindinger, W. *Rapid Commun. Mass Spectrom.* **1997**, *11*, 1230.
(296) Karl, T.; Prazeller, P.; Mayr, D.; Jordan, A.; Rieder, J.; Fall, R.; Lindinger, W. *J. Appl. Physiol.* **2001**, *91*, 762.
(297) Rieder, J.; Lirk, P.; Ebenbichler, C.; Gruber, G.; Prazeller, P.; Lindinger, W.; Amann, A. *Wien. Klin. Wochenschr.* **2001**, *113*, 181.
(298) Lirk, P.; Bodrogi, F.; Raifer, H.; Greiner, K.; Ulmer, H.; Rieder, J. *Nephrol., Dial., Transplant.* **2003**, *18*, 937.
(299) Wehinger, A.; Schmid, A.; Mechtcheriakov, S.; Ledochowski, M.; Grabmer, C.; Gastl, G. A.; Amann, A. *Int. J. Mass Spectrom.* **2007**, *265*, 49.
(300) Lechner, M.; Fille, M.; Hausdorfer, J.; Dierich, M. P.; Rieder, J. *Curr. Microbiol.* **2005**, *51*, 267.
(301) Lechner, M.; Tilg, H.; Rieder, J. *Helicobacter* **2006**, *11*, 66.
(302) Steeghs, M. M. L.; Cristescu, S. M.; Munnik, P.; Zanen, P.; Harren, F. J. M. *Physiol. Meas.* **2007**, *28*, 503.
(303) Critchley, A.; Elliott, T. S.; Harrison, G.; Mayhew, C. A.; Thompson, J. M.; Worthington, T. *Int. J. Mass Spectrom.* **2004**, *239*, 235.
(304) Harrison, G. R.; Critchley, A. D. J.; Mayhew, C. A.; Thompson, J. M. *Br. J. Anaesth.* **2003**, *91*, 797.
(305) Janovsky, U.; Scholl-Buergi, S.; Karall, D.; Beauchamp, J.; Hansel, A.; Poupart, G.; Schmid, A.; Amann, A. In *Breath Analysis for Clinical Diagnosis and Therapeutic Monitoring*; Amann, A., Smith, D., Eds.; World Scientific: Singapore, 2005.
(306) Jordan, A.; Hansel, A.; Holzinger, R.; Lindinger, W. *Int. J. Mass Spectrom. Ion Process.* **1995**, *148*, L1.
(307) Lirk, P.; Bodrogi, F.; Deibl, M.; Kaehler, C. M.; Colvin, J.; Moser, B.; Pinggera, G.; Raifer, H.; Rieder, J.; Schobersberger, W. *Wien. Klin. Wochenschr.* **2004**, *116*, 21.
(308) Prazeller, P.; Karl, T.; Jordan, A.; Holzinger, R.; Hansel, A.; Lindinger, W. *Int. J. Mass Spectrom.* **1998**, *178*, L1.
(309) Abbott, S. M.; Elder, J. B.; Spanel, P.; Smith, D. *Int. J. Mass Spectrom.* **2003**, *228*, 655.
(310) Amann, A.; Telser, S.; Hofer, L.; Schmid, A.; Hinterhuber, H. In *Breath Analysis for Clinical Diagnosis and Therapeutic Monitoring*; Amann, A., Smith, D., Eds.; World Scientific: Singapore, 2005.
(311) Lechner, M.; Colvin, H. P.; Ginzel, C.; Lirk, P.; Rieder, J.; Tilg, H. *Int. J. Mass Spectrom.* **2005**, *243*, 151.
(312) Bukhtiyarov, V. I.; Nizovskii, A. I.; Bluhm, H.; Haevecker, M.; Kleimenov, E.; Knop-Gericke, A.; Schloegl, R. *J. Catal.* **2006**, *238*, 260.
(313) Wisthaler, A.; Strom-Tejsen, P.; Fang, L.; Arnaud, T. J.; Hansel, A.; Märk, T. D.; Wyon, D. P. *Environ. Sci. Technol.* **2007**, *41*, 229.
(314) Wisthaler, A.; Tamas, G.; Wyon, D. P.; Strom-Tejsen, P.; Space, D.; Beauchamp, J.; Hansel, A.; Tilmann, M. D.; Weschler, C. J. *Environ. Sci. Technol.* **2005**, *39*, 4823.
(315) Whyte, C.; Wyche, K. P.; Kholia, M.; Ellis, A. M.; Monks, P. S. *Int. J. Mass Spectrom.* **2007**, *263*, 222.
(316) Smet, E.; Van Langenhove, H.; De Bo, I. *Atmos. Environ.* **1999**, *33*, 1295.
(317) Mayrhofer, S.; Mikoviny, T.; Waldhuber, S.; Wagner, A. O.; Innerebner, G.; Franke-Whittle, I. H.; Märk, T. D.; Hansel, A.; Insam, H. *Environ. Microbiol.* **2006**, *8*, 1960.
(318) Karl, T.; Yeretzian, C.; Jordan, A.; Lindinger, W. *Int. J. Mass Spectrom.* **2003**, *223*−*224*, 383.
(319) Cordell, R. L.; Willis, K. A.; Wyche, K. P.; Blake, R. S.; Ellis, A. M.; Monks, P. S. *Anal. Chem.* **2007**, *79*, 8359.
(320) Rinne, J.; Taipale, R.; Markkanen, T.; Ruuskanen, T.; Hellen, H.; Kajos, M.; Vesala, T.; Kulmala, M. *Atmos. Chem. Phys. Discuss.* **2007**, *7*, 2357.
(321) Karl, T.; Guenther, A.; Yokelson, R. J.; Greenberg, J.; Potosnak, M.; Blake, D. R.; Artaxo, P. *J. Geophys. Res.* **2007**, *112*, D18302.

CR800364Q